

number of daily observations oscillated by one. This occurs when the device start time and sampling frequency results in the last observation of the day being very close to midnight. For example, depending on the start time, a monitoring device set at a 1.6-hr sampling frequency will have 15 daily observations on one day, then have 14 daily observations on the next day. When days with daily fragments were encountered the daily observation was left in the data set, however, the temperature values were set to missing. Without the *maximum minus one* provision, every other day (the day with 14 observations) would have had all the temperature values set to missing. The data set with daily fragments removed (set to missing) is henceforth referred to as the *defragmented weekly data set*.

Additional temporal refinement was applied to the defragmented weekly data set for statistical analyses. Many multivariate analyses and modeling in this regional assessment were based on the highest daily maximum (XY1DX), the highest seven-day moving averages of both the daily average (XYA7DA) and the daily maximum (XYA7DX) for the year. Limiting the temporal window of the temperature data to June 1 through September 30 for all sites and all years helped ensure that stream temperatures across a consistent time frame were used in summary statistics. However, even with this precaution it became apparent that the “highest” value for a particular site may not necessarily have been captured if data were missing during the time the “true” highest stream temperatures occurred. Thus, the defragmented weekly data set converted daily and seven-day moving average temperature values to missing values for days with incomplete observations. It was deemed critical to refine the temporal window to the time period when the highest stream temperature metrics were most likely to occur. This time frame was determined from the defragmented weekly data set by calculating the mean and median day of year in which the highest seven-day moving average occurred.

To briefly summarize, there were 1090 spatially unique study sites monitored between 1990 and 1998 inclusive. The mean day of the year the XYA7DA and XYA7DX occurred was determined by running a series of queries. The mean value for the day of

occurrence was 215, which corresponds to August 4. This calendar date may vary by one day, depending on whether or not a given year was a leap year. A 15-day period on either side of day 215 was used as the temporal window (day of year between 201 and 230 or approximately July 21 through August 19). Additionally, sites having five or more days within this period with missing values were removed from further analyses. This criterion represents about 85% of the days within the desired time frame required to have non-missing observations. This missing data criterion is the same as that used by the National Weather Service for inclusion of air temperature monitoring data in their data summaries. Of the 1090 study sites, 1034 sites had data within the 30-day window, with 1014 sites having data that met all criteria. The most data-rich year, that is existence of data for both stream temperature and many of the site-specific attributes, was 1998 – there were 518 sites for this year. This year was used predominantly throughout the report to explore relationships between stream temperature and various landscape and site-specific variables.

Temporal, Spatial, and Physical Stratification

The temporal delimiters placed on the data to remove errors in statistical analyses were discussed above. Certain spatial and physical criteria were also imposed on the data used in stream temperature analyses to render the data comparable within and between years. Table 2.3 lists the criteria used in data standardization. Figure 2.2 shows the spatial distribution of sites for each year and all years combined (1990-1998) that met the criteria shown in Table 2.3. As can be noted from the spatial displays in Figure 2.2, the spatial distribution of sites was not uniform across all years. The lack of uniformity in spatial coverage was taken into consideration when relationships between stream temperature and certain landscape- and site-level attributes were examined

The spatial qualifiers that were applied to the data ensured that data used in the regional assessment were gathered from the appropriate areas of interest. A spatial hierarchy was used to post-stratify the data by these areas of interest. The focus of this temperature assessment was on anadromous fish,

FSP Regional Stream Temperature Assessment Report

Table 2.3. Criteria Used to Standardize Stream Temperature Data Within and Between Years.

<u>Criterion</u>	<u>Value</u>	<u>Description</u>
Stream class	= 1	Class 1, fish-bearing streams
	= 5	Stream class not specified
	= ‘ ’	Stream class missing
Site type	= water air	Water or air temperature. Relative humidity data were excluded from analyses.
Temporal	≥ 21 July	Date was greater than or equal to 21 July for each year
	≤ 19 Aug	Date was less than or equal to 19 August for each year
Spatial	Only sites that fell within the boundaries of the California portion of the Southern Oregon Northern Coastal California and Central California evolutionarily significant units	

namely coho salmon. Thus, the largest spatial boundary applied to the geographic distribution of sampling points was the combined SONCC and CC evolutionarily significant units for coho salmon (*O. kisutch*) (Figure 1.1). If in the assessment, status and trends in stream temperatures pertinent to coho salmon within one of the ESUs were of interest, the coho ESU boundary for that ESU was used to poststratify sampling points by this area of interest. Likewise, if relationships between stream temperature and certain landscape- and site-specific variables were explored by ecoprovinces (USDA,

1997), the spatial boundaries of these ecoprovinces were used to aggregate data by this area of interest.

Measurement Techniques and Data Processing

The measurement techniques used by the various data contributors and the Forest Science Project’s methods of data processing are presented in Appendix A.

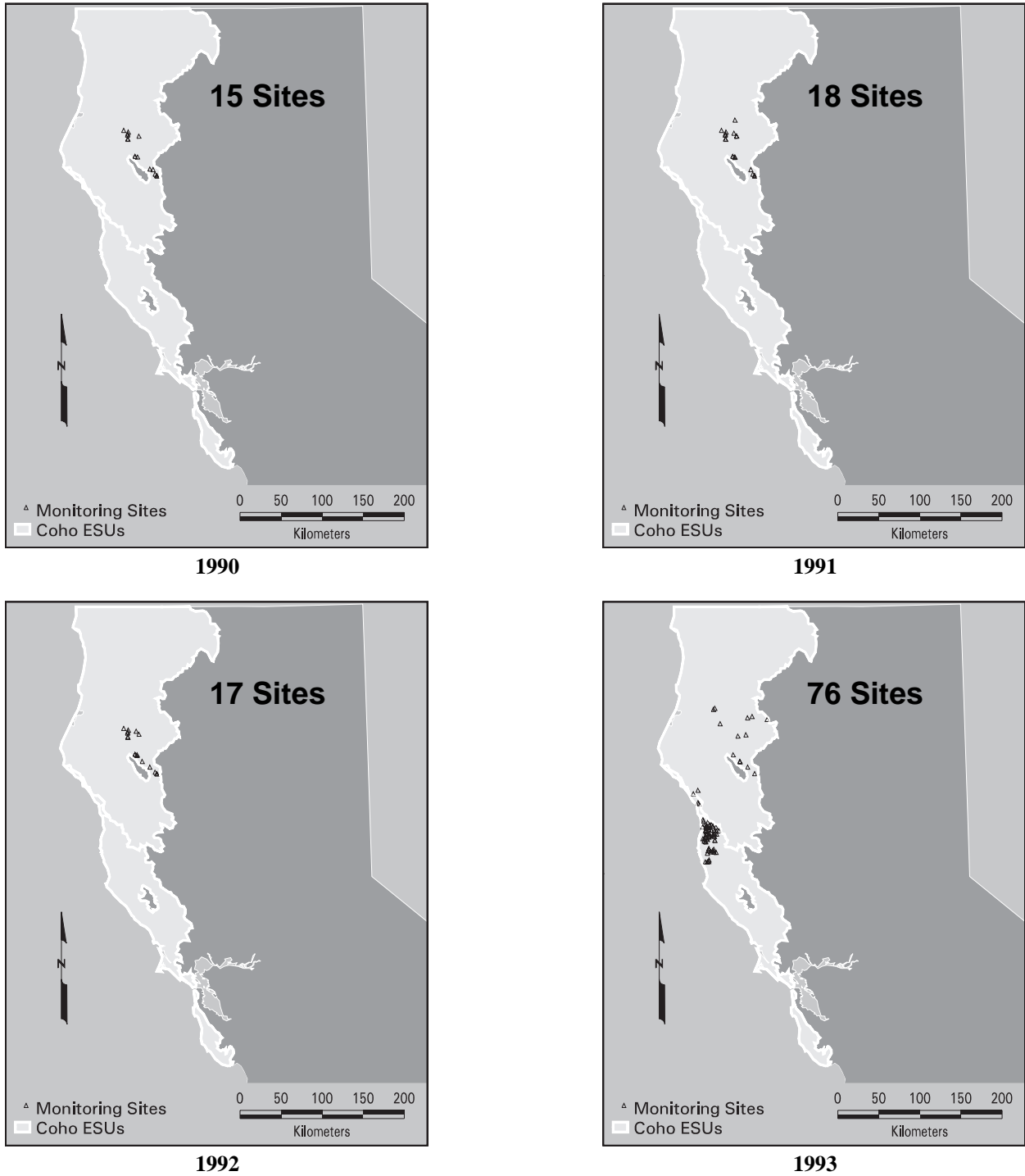
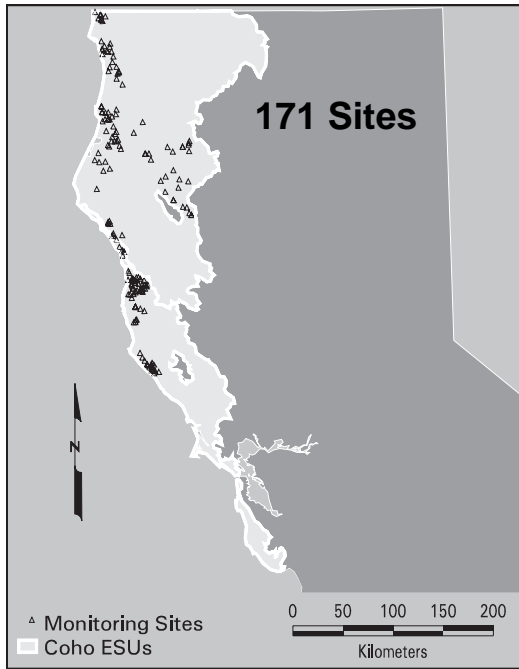
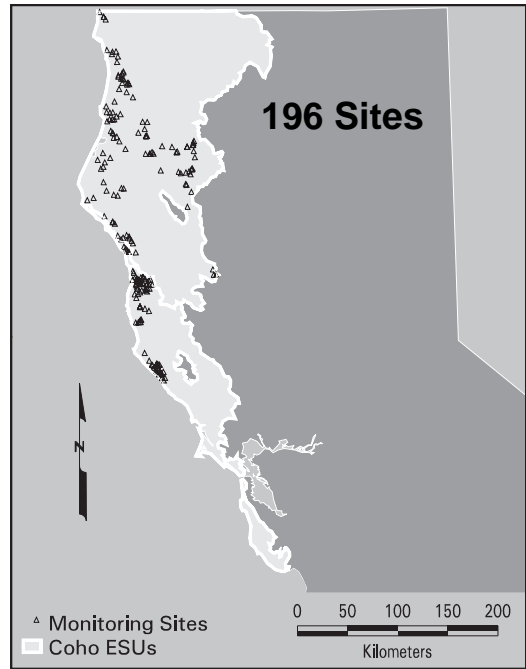


Figure 2.2. Location of stream temperature monitoring sites used in the Regional Stream Temperature Assessment.

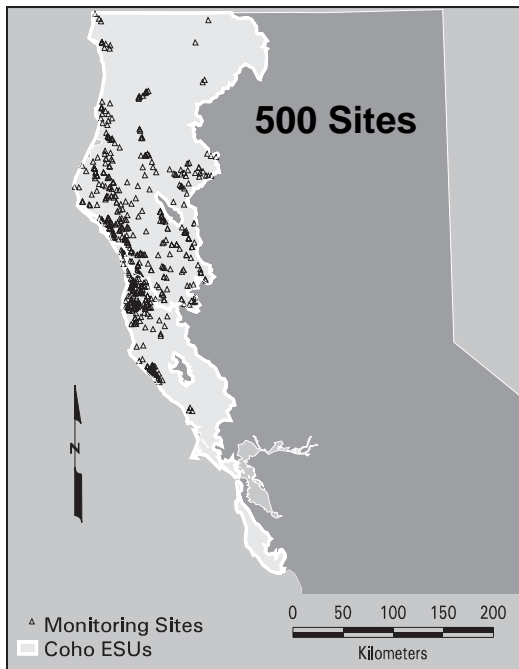
FSP Regional Stream Temperature Assessment Report



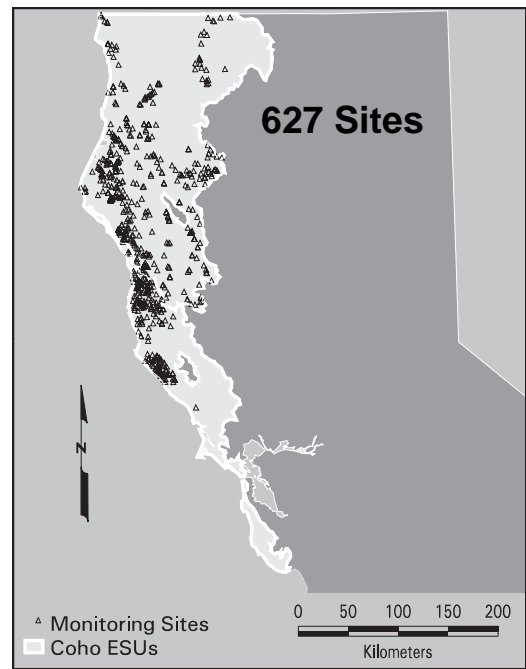
1994



1995

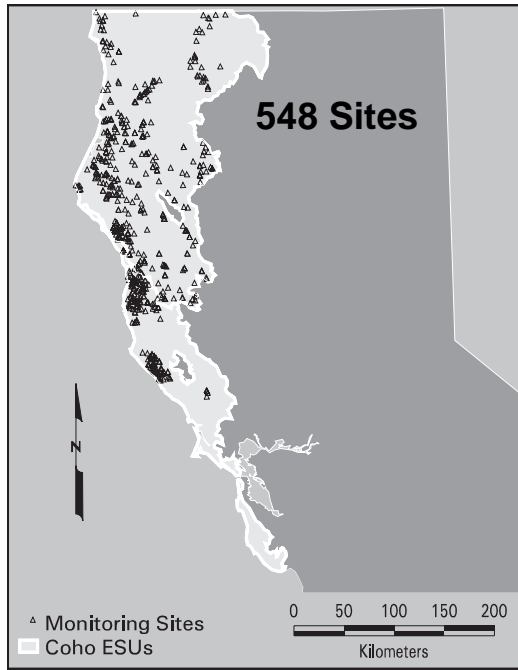


1996

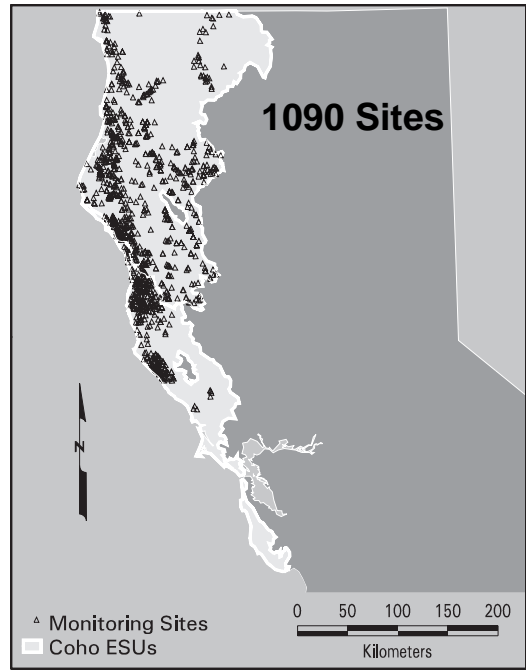


1997

Figure 2.2. (continued)



1998



All Sites, All Years (1990-1998)

Figure 2.2. (continued)

Chapter 3

SUMMARY OF THE STATISTICAL ATTRIBUTES OF REGIONAL STREAM TEMPERATURES

Introduction

Summary statistics were calculated for data sets containing individual observations (henceforth referred to as the *hourly data set*) and data sets containing the daily minimum, average, and maximum, and seven-day moving averages (henceforth referred to as the *weekly data set*). The defragmented weekly data set was used to produce summary statistics, to avoid the inherent errors if days with missing observations were used to calculate summary statistics. The PROC UNIVARIATE procedure in SAS was used to generate summary statistics (SAS, 1985).

Hourly Summary Statistics

Summary statistics were generated from the hourly data set containing the individual observations (e.g., hourly observations, 1.5-hr intervals, etc., depending on the sampling frequency of each device). The summary statistics of hourly data are presented in detail in Appendix B. The temporal window for which summary statistics were calculated was June 1 through September 30 of each year.

Daily and Weekly Stream Temperature Metrics Summary Statistics

Summary statistics were generated by year for the defragmented weekly data set for the following stream temperature metrics:

- daily minimum
- daily mean
- daily maximum
- seven-day moving average of the daily minimum
- seven-day moving average of the daily mean
- seven-day moving average of the daily maximum

Sidebar #1

Interpreting Summary Statistics

A cautionary note is offered to the reader. Hourly and weekly summary statistics are only applicable to the sites monitored in a single year. The number of sites and their geographic distribution increased from 1990 to 1998. The sites are by no means consistent across all nine years. Therefore, inferences should not be made from yearly summary statistics as to whether stream temperatures showed increasing or decreasing trends across years.

FSP Regional Stream Temperature Assessment Report

The summary statistics for the daily stream temperature metrics are presented in Appendix B for years 1990 through 1998. A cautionary note is provided in Sidebar #1 that should be read before examining and interpreting yearly summary statistics.

The summary statistics for the weekly (seven-day moving average) temperature metrics are also presented in Appendix B for years 1990 through 1998. The highest seven-day moving average of the daily mean is often referred to as the **Maximum Weekly Average Temperature** or **MWAT** (Ferraro et al., 1978). Some state and federal agencies in California and other states have been referring to the highest seven-day moving average of the daily maximum as the MWAT value. The summary statistics for the seven-day moving average of the daily maximum are presented in Appendix B, Table B-10 through B-19.

Cumulative Distributions of Regional Stream Temperatures

The cumulative distribution function (CDF) graphical technique was used by the FSP as one method of presenting regional stream temperature analytical results. This introduction describes how to interpret a CDF graph. The effort to learn how to interpret the output from this graphical technique is modest, and the reward is substantial; many monitoring programs around the world use this simple, powerful, and informative graphical technique for presenting data summaries.

A CDF is better than a tabular summary for presenting an objective view of FSP data. Specifically, optimal or suboptimal stream temperature has not unequivocally or universally been defined. The use of a CDF permits readers to choose a reference or threshold value for a stream temperature or ecological indicator, and see what proportion of the sampled population is estimated to fall below or above the value for that measurement or indicator. Tabular summaries stratify the data according to a reference value defined by the data analyst, but the reader is unable to see how an interpretation could change if a different reference value was chosen (FHM, 1994). If needed, a tabular summary can be prepared for any particular reference

value. Until such time as biologically meaningful thermal threshold values are widely accepted, the CDF graphical presentation is an effective means of disseminating information.

The examination of the cumulative distribution of temperatures across the region is an effective means of gaining an understanding of the thermal regimes across the region. Before this information is presented, a discussion of how to interpret a cumulative distribution function graph is appropriate.

How to Interpret a CDF

Each CDF is identified by the variable X (a measurement or indicator, on the horizontal axis) and by the subset of spatial entities (e.g., sites, streams, watersheds, etc.) in the population that the graph represents. For example, X could be the highest seven-day moving average of the daily mean stream temperature and the subset of the population could be those sites on Class I streams that fall within a FSP assessment area of interest. To find the estimated proportion of the population that falls below some reference value, say for example the MWAT threshold, use the following procedure (Figure 3.1).

1. Find the desired reference value (X) on the horizontal axis.
2. Draw a line perpendicular from the chosen X value to meet the solid line that is plotted on the CDF.
3. Draw a line from this intersection to the left to perpendicularly meet the vertical axis.
4. Read the estimated proportion where the line meets the vertical axis.
5. The proportion is the fraction of the population that is estimated to have a value of X that is less than the reference value.

In the example, a reference value of 18.3°C in step 1 leads to the interpretation that about 95% of the sites, streams, watersheds, or other unit of the population have an X value less than 18.3°C. Different reference values (in step 1) will yield different cumulative proportion estimates (in step 4). By experimenting with reference values, the reader can see how data interpretations change with changes in the reference value. For example, a different

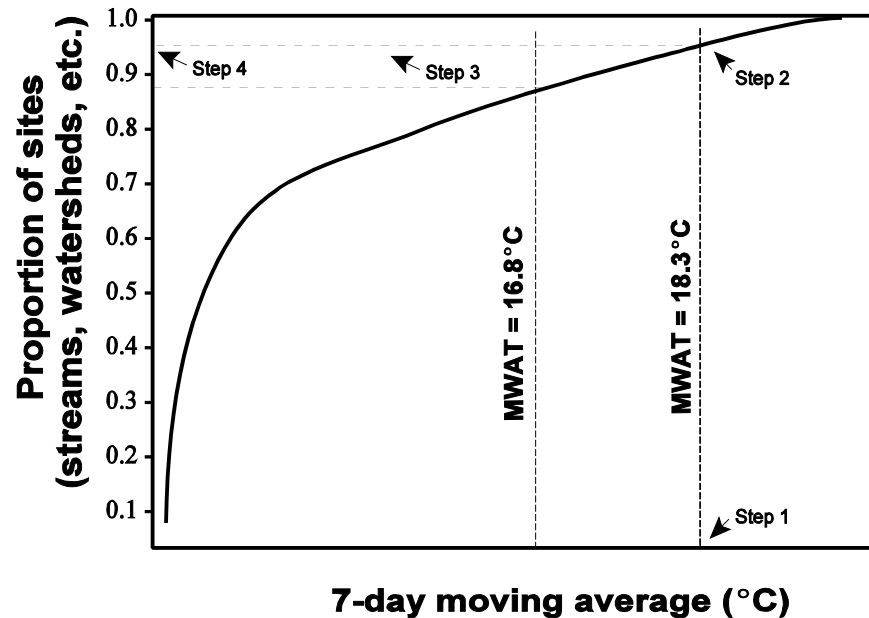


Figure 3.1. Hypothetical cumulative distribution function graph.

reference value of 16.8°C in step 1 leads to the interpretation that about 88% of the population is below the MWAT threshold.

There are some important considerations to keep in mind when using the above procedure. First, this graphical technique is suitable for obtaining **rough estimates**, but precise computation requires the use of the data base and appropriate algorithms. Algorithms were applied to the data base in this report to calculate the precise cumulative proportion at the reference value. Second, the CDF cannot be used (strictly) to get estimates of the proportion of the population **greater** than some value of X . Instead, a new chart of $1-f(X)$ must be prepared, again using the data base and appropriate algorithms. If the cumulative distribution function (CDF) were the true, continuous, cumulative distribution function of the population resource, it would be acceptable to take $1-f(X)$ as the probability of being larger than value X . But in survey sampling, one does not have the continuous population CDF. Instead, one has an approximation which has gaps and jumps that reflect

the variability seen in the sample. A jump in the CDF may be due to large sample weights, or to a large number of sample values in that vicinity. In particular, an X value near one of these jumps becomes sensitive to the presentation of the CDF. Near one of these jumps in the CDF the estimate of the exceedance probability may not be well-estimated by one minus the estimated proportion less than or equal to X . For this reason, it is recommended that exceedance probabilities be calculated from the descending CDF (Diaz-Ramos et al., 1996).

In summary, the CDF technique is a flexible format for presenting an overview of data. It gives any reader or analyst the ability to choose their own threshold and determine what fraction of the population is estimated to be above or below that criterion. The CDF does not change the data in any way, it simply presents it in a non-tabular fashion. Despite the simplicity of the approach, some readers will never be comfortable with the CDF technique. For these readers, only the possibility of making one's own interpretation will be lost; it is always possible to

FSP Regional Stream Temperature Assessment Report

accept or reject the interpretations that other scientists will make when they assign thresholds and present the data in a tabular format.

Sidebar #2 ***Reference Values and CDFs***

The reference values presented on the various CDF graphs in Appendix B are for reference purposes only. Until such time as agreed upon threshold or exposure values are developed for Northern California, reference values should be used as such, reference values.

CDFs of Seven-Day Moving Averages and Daily Maximum Stream Temperatures

The highest seven-day moving average of both the daily mean (XYA7DA) and the daily maximum (XYA7DX), and the highest daily maximum temperature (XY1DX) for each site for each year was used in cumulative distribution analyses. The highest seven-day moving averages were compared to two reference values of 16.8°C and 18.3°C. These two values have been commonly used to evaluate chronic thermal stress metrics such as seven-day moving averages (Armour, 1991; Becker and Genoway,

1979). The highest daily maximum temperature was compared to the upper lethal incipient temperature (26°C) for juvenile coho salmon and a two-degree safety margin temperature (24°C) (Coutant, 1972). The highest daily maximum temperature is an acute thermal stress metric and thus should be compared to an acute thermal threshold. CDF graphs for the three temperature metrics can be found in Appendix B. The highest seven-day moving average of the daily average is often referred to as the Maximum Weekly Average Temperature or MWAT. This value is compared to MWAT thresholds for various species and life stages to determine potential chronic exposure to elevated stream temperatures. Oregon, Washington, and Idaho have adopted the seven-day moving average of the daily maximum as the metric for evaluation of stream temperature in their states. There is debate in California as to whether the highest seven-day moving average of the daily mean or the seven-day moving average of the daily maximum should be used to assess potential chronic stress. Therefore, both metrics are presented in this report.

The precise cumulative proportion above and below two reference values, 16.8°C and 18.3°C, was calculated mathematically (not visually estimated from the graph) and are presented with their accompanying CDF graphs in Appendix B.

The CDF graphs and data tables are applicable to the year in which the data were gathered. It must be kept in mind that comparisons across years are not appropriate because different sites were sampled in each year (See Sidebar #1).

Chapter 4

REGIONAL TRENDS IN AIR TEMPERATURE

Introduction

Air temperature is known to have a significant influence on stream temperatures. In conjunction with solar radiation it is an important source of heat input into aquatic systems (Hostetler, 1991; Sullivan et al., 1990; Stoneman and Jones, 1996). Most stream temperature models based on the physics of heat transfer use air temperature as a driver to predict temporal change in stream temperature (Bartholow, 1989; Sullivan et al., 1990). The difference between air and water temperature determines the rate of energy exchange for several heat transfer processes included in the energy balance equations of these models. The location at which air temperature should be monitored varies depending on which energy balance equation requires the data. For example, the back radiation equation requires input of air temperature data collected well above the stream (sky temperature) (Adams and Sullivan, 1990). The convection equation considers air temperature collected just above the stream surface. The evaporation rate is often calculated using air temperature data collected at about two meters above the stream surface.

Local air temperature is an important parameter influencing the *daily mean stream temperature* at equilibrium (Edinger et al., 1968; Adams and Sullivan, 1990). The daily mean stream temperature under equilibrium conditions is generally near the daily mean air temperature (Adams and Sullivan, 1990). Unfortunately, not many stream temperature data contributors submitted local air temperature data collected near their stream temperature sites. To

determine the effects of air temperatures on mean stream temperature, acquisition of *local* air temperatures is particularly important. If one uses remote or approximate air temperature data, then one can only hope for remote or approximate stream temperature predictions (Sullivan et al., 1990). Alternatively, if one wants to account for daily maximum stream temperatures, information on solar insolation is also necessary. The amount of solar heat input would most likely be obtained from estimates of effective canopy and topographic shading.

To understand how water temperatures vary regionally, an understanding of regional trends in air temperature is required. This chapter examines the variation in air temperatures across Northern California using data from National Oceanic and Atmospheric Administration (NOAA) weather stations and modeled air temperatures obtained from Oregon State University. We show that air temperature, an important variable in determining water temperature, varies greatly across the area of interest. Using air monitoring station data, air temperature was found to be strongly related to distance from coast (marine influence) for the Coastal Steppe Province and elevation (adiabatic influence) for the Sierran Steppe - Mixed Forest - Coniferous Forest Province. An advanced climate analysis procedure was used to estimate long-term air temperatures regimes across the ecoprovinces and basins of Northern California. Yearly air temperatures were compared to the 30-yr long-term averages for each ecoprovince. Finally, yearly average air temperature was used to estimate groundwater temperatures across the area of interest.

FSP Regional Stream Temperature Assessment Report

Air temperature discussed in this chapter is considered to be macroair temperature, and not stream-side air temperature (microair). Macroair temperature represents above-ground temperatures like those reported on the evening news.

Air Temperature Data Acquisition and Analysis

Air Monitoring Station Data

Air temperature data were downloaded from two Internet sources: Western Regional Climate Center (WRCC; web address: <http://www.wrcc.dri.edu/climsum.html>) and University of California Statewide Integrated Pest Management Project (UCIPM; web address: <http://axp.ipm.ucdavis.edu/WEATHER/retrieveavgs.html>). The downloaded data for all 25 WRCC air temperature data sets were from stations operated by NOAA. The downloaded data for the 47 UCIPM air temperature data sets were from three different sources; data providers were listed as automatic, touchtone, and climate stations. The automatic stations are part of the California Irrigation Management Information System (CIMIS) Network operated by California Department of Water Resources. The touchtone stations are volunteers that record observations daily and transmit them to the UCIPM computer. The climate stations are maintained by NOAA. There were 11 downloaded data sets for the automatic stations, 3 sets for touchtone stations, and 33 sets for climate stations. Although water temperature data from FSP data contributors were for years 1990 through 1998, air temperature data were acquired for the entire period of record at each air station. The historical air temperature data were later used in Chapter 11 to interpret historical trends in water temperature.

The air temperature data obtained from WRCC only included monthly averages for the minimum, maximum, and daily average. Daily data were not available. UCIPM provided only daily minimum and maximum air temperatures. Daily averages were not available. There are two commonly used methods for calculating daily average air temperatures. One method is the *true average* of the hourly (or some other sampling rate) readings for a 24-hour period.

The other method is performed by adding the daily maximum and daily minimum air temperatures and dividing the sum by two, henceforth referred to as the *maximum-minimum average*. The method used by WRCC in their monthly summary reports is that of the maximum-minimum averaging technique. Since we did not have the ability to calculate a *true average* for each month in the study period, the *maximum-minimum average* was calculated for each day, and subsequently the daily maximum, minimum, and maximum-minimum averages were averaged by month and year. If a particular site had more than five days with missing daily maximum and/or minimum values (and hence a missing value for the calculated daily max-min average), the monthly average was set to null. Application of this procedure was similar to the way in which water temperature summary statistics were calculated (see Chapter 3). Potential errors are introduced into monthly averaging procedures if partial monthly records are included. The criterion that FSP used for the number of records that were permitted to be missing in a monthly average air temperature, i.e., 85% data completeness criterion, is used by NOAA and the WRCC in their data summaries.

After thorough examination of the integrity of the data, e.g., completeness of the record, level of temporal aggregation across all sites, etc., 72 sites were found to exhibit sufficient consistency across the nine years of the stream temperature assessment period (1990 through 1998) allowing for their inclusion in the regional assessment. Figure 4.1 shows the location of the 72 sites used in the analyses.

PRISM Air Temperature Data

In addition to the data acquired from the aforementioned 72 sites, regional air temperature data were acquired from Oregon State University (OSU) Climate Analysis Service and the Oregon Climate Service at OSU. These data were developed using PRISM (Parameter-elevation Regressions on Independent Slopes Model). PRISM is a climate analysis system that uses point data, a digital elevation model (DEM), and other spatial datasets to generate gridded estimates of annual, monthly and

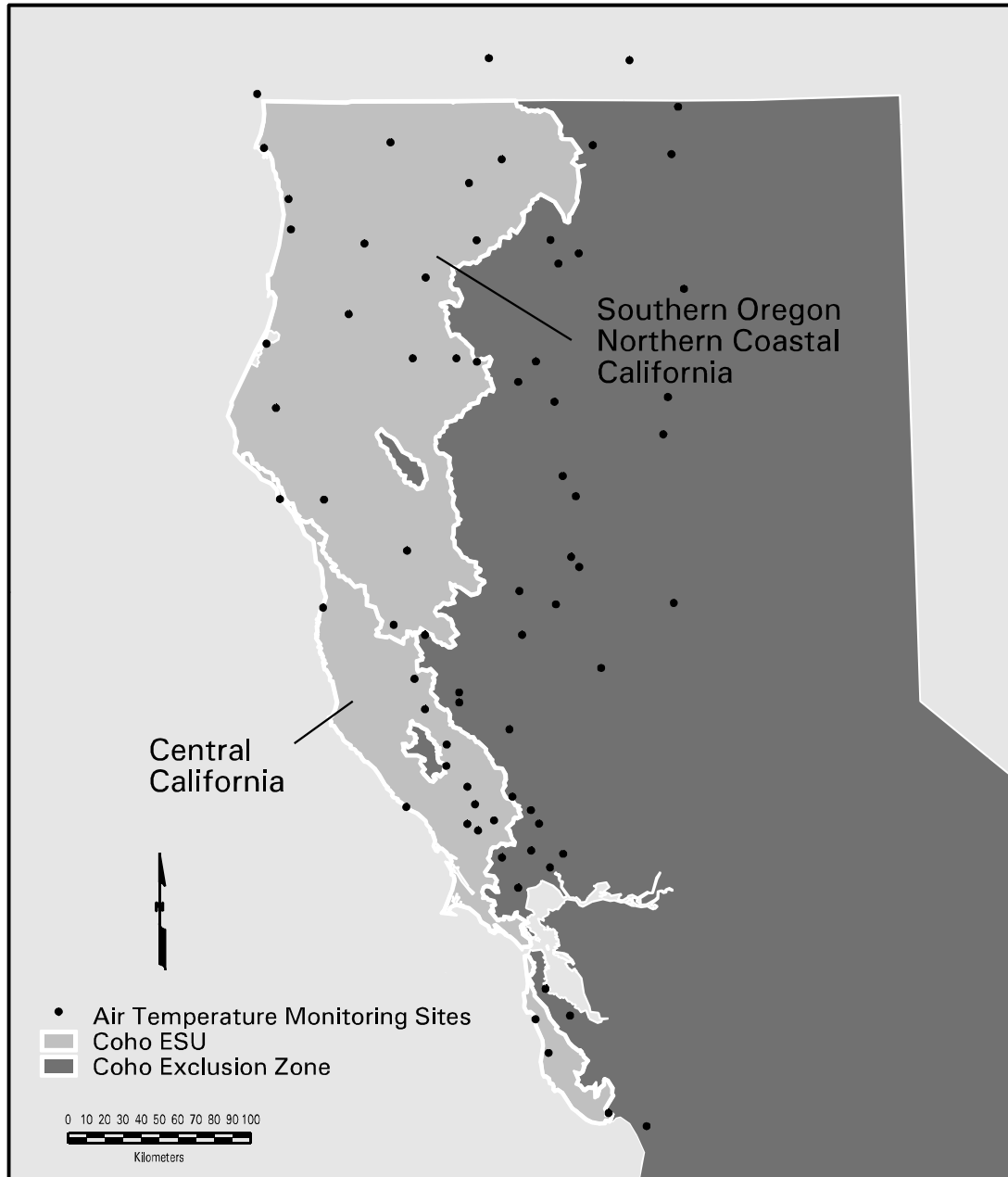


Figure 4.1. Location of air temperature monitoring sites used in the Forest Science Project’s regional stream temperature assessment.

FSP Regional Stream Temperature Assessment Report

event-based climatic parameters (Daly et al., 1994). Originally developed in 1991 for precipitation estimation, PRISM has been generalized and applied successfully to temperature, snowfall, growing degree-days, and weather generator parameters, among others (Johnson et al., 1997, Taylor et al., 1997). It has been used extensively to map precipitation and minimum and maximum air temperature over the United States, Canada, and other countries (Kittel et al., 1997; Parzybok et al., 1997).

The acquired PRISM air temperature data has been reduced to 30-yr long-term monthly averages at 4-km grid resolution. The monthly averages for the maximum and minimum were available, from which the monthly average was calculated by adding the maximum and minimum and dividing by two. Most of the data from the 72 sites mentioned above were most likely utilized in PRISM model development.

The PRISM system determines climate at grid cells by calculating linear relationships between the climate element in question (e.g., air temperature) and elevation. The slope of these linear regression lines changes locally with elevation, as dictated by the available point climate data. With a separate regression function each grid cell estimate is determined using data from many nearby climate stations. Each station in the multiple regression is weighted based on five factors: distance, elevation, vertical layer, topographic facet, and coastal proximity. In short, the closer a given station is to a target grid cell in distance and elevation, and the more similar that station is in its climatology to the cell (given by the other three factors), the higher the weight the station will have on the final, predicted value for that grid cell. A technique within PRISM determines the lowest possible prediction error for the map as a whole (all cells). PRISM typically is configured to predict values approximately every 4 km horizontally.

PRISM has been compared to kriging, detrended kriging, and cokriging in the Willamette River Basin, Oregon (Daly et al., 1994). In a jackknife cross-validation exercise, PRISM exhibited lower overall bias and mean absolute error. PRISM was also applied to northern Oregon and to the entire western

United States. Detrended kriging and cokriging could not be used in these regions because there was no overall relationship between elevation and precipitation. PRISM's cross-validation bias and absolute error in northern Oregon increased a small to moderate amount compared to those in the Willamette River Basin; errors in the western United States showed little further increase. PRISM has since been applied to the entire United States with excellent results, even in regions where orographic processes do not dominate precipitation patterns.

By relying on many localized, facet-specific air/elevation relationships rather than a single domain-wide relationship, PRISM continually adjusts its frame of reference to accommodate local and regional changes in orographic regime with minimal loss of predictive capability.

The PRISM data does not provide the temporal resolution needed for predicting stream temperatures. However, the spatial resolution was ideal for developing a regional picture of air temperature regimes across Northern California.

The following evaluation of how air temperature varies with elevation and distance from the coast relied on the finer temporal resolution of the data from the 72 air temperature sites.

Air Temperature as a Function of Elevation and Distance from Coast

A decrease in air temperature at higher elevations is well documented and known to be driven by adiabatic cooling processes. Adiabatic cooling deals with the cooling of parcels of air as they rise, or are forced upward, through the atmosphere. An example would be the cooling of an air parcel as it rises over a mountain range.

In Figure 4.2-A the monthly average air temperatures for all sites for which 1998 August monthly average values were available (66 sites) were plotted against elevation. The expected decrease in air temperature with increasing elevation was not discernable across the full range in elevation values (Figure 4.2-A). A slight negative slope (-0.0001) can be discerned from

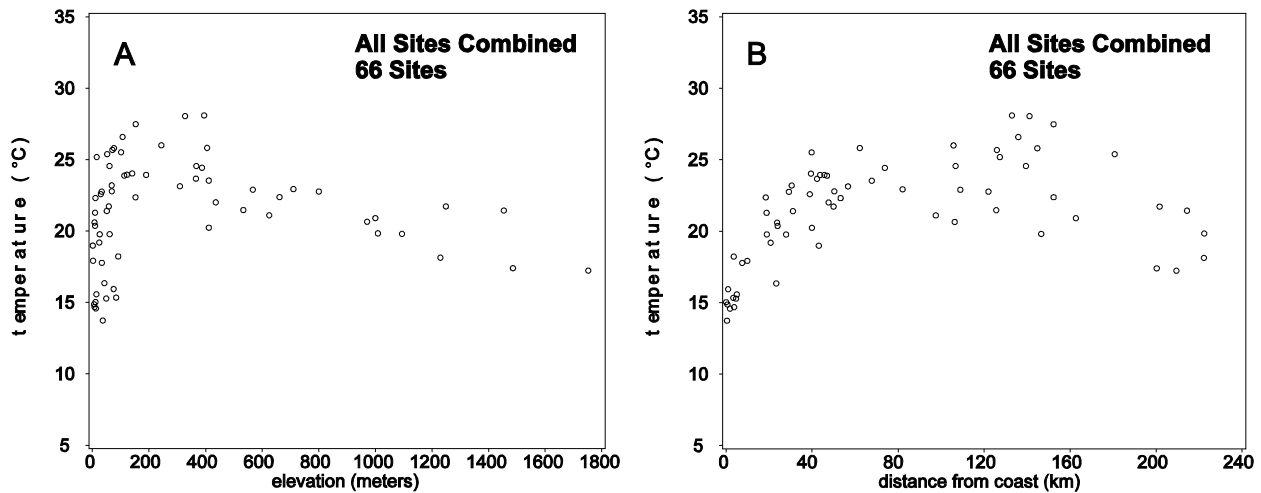


Figure 4.2. Relationship between August 1998 monthly average air temperature and elevation (A) and distance from the coast (B) for all sites combined (66 sites).

the graph. Air temperatures at the lower elevations were as low as or lower than air temperatures observed at elevations over 1000 meters (Figure 4.2-A). The relationship between monthly average air temperature and elevation is clearly not linear. The relationship was weak, as reflected by a low R^2 value of 0.0002.

Residents of Northern Coastal California are very familiar with the cooling effects of summertime oceanic air currents that tend to moderate temperatures during the summer months. For anyone who has driven from Arcata to Willow Creek or Weaverville on Route 299 in early August, they probably have experienced and appreciated the increasing air temperature while ascending in elevation, moving out of the affectionately termed ‘fog zone’ into the warmer, higher elevation areas. With this intuitive knowledge and first-hand experience of the warming trends in air temperature with increasing distance from the coast during the summer months, this relationship was examined in Figure 4.2-B.

Using 66 sites with August 1998 monthly average air temperatures in the analyses, a weak relationship ($R^2 = 0.15$) was observed (Figure 4.2-B). An overall positive slope of 0.02 was determined in the linear regression analysis. Visual inspection of Figure 4.2-

B revealed that at the lower values for distance from the coast, air temperature increased with increasing distance from the coast. The increasing trend seems to level off at approximately 80 km (~50 mi) from the coast.

Given the apparent relationship between air temperature and both elevation and distance from coast that was discernable in Figures 4.2 and 4.3, these relationships were explored in greater depth in the following sections.

Monthly Average Air Temperature Versus Elevation

The air temperature sites were broken into two groups, sites at distances less than or equal 80 km from the coast and sites at distances greater than 80 km from the coast.

Figure 4.3-A presents the relationship between August 1998 monthly average air temperature versus elevation for sites at distances less than or equal to 80 km (~50 mi) from the coast. There was a slight improvement in the linear regression model fit to the data, with an R^2 value of 0.27, compared to an R^2 value of 0.0002 for all sites combined (Figure 4.2-A). A slope of +0.01 was observed.

FSP Regional Stream Temperature Assessment Report

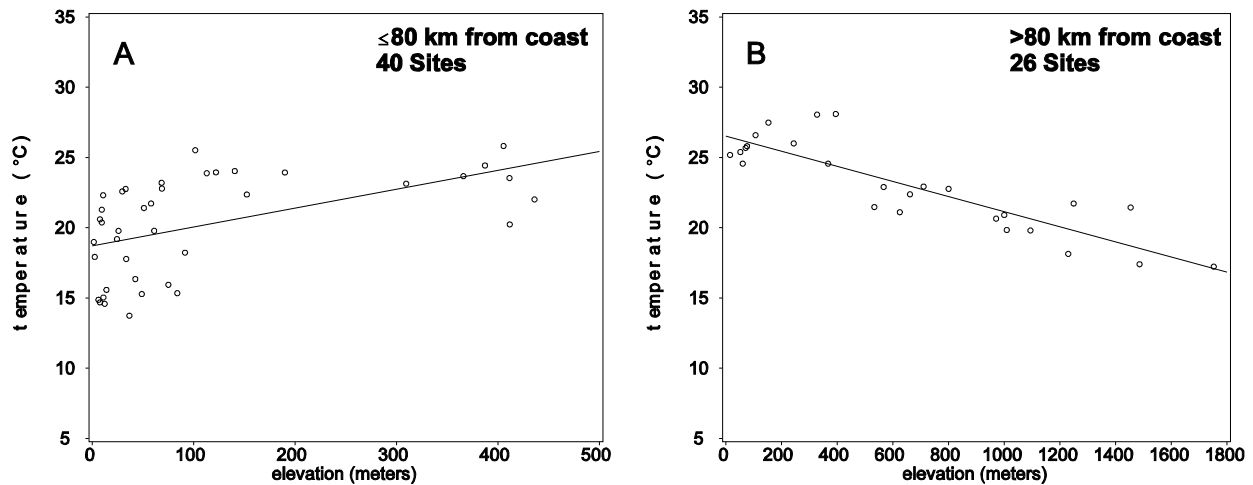


Figure 4.3. Relationship between August 1998 monthly average air temperature and elevation for 40 sites located ≤ 80 km (A) and 26 sites >80 km (B) from the coast.

Figure 4.3-B presents the same relationship for sites at distances >80 km (~ 50 mi) from the coast. The improvement in the linear regression model fit to the data was remarkable, with an R^2 value of 0.75 compared to an R^2 value of 0.0002 for all sites combined. A negative slope of -0.005 was found.

Monthly Average Air Temperature Versus Distance from Coast

Figure 4.2 illustrates the relationship between August 1998 monthly average air temperature versus distance from coast for all sites combined (66 sites). The R^2 value was 0.16 and the slope was +0.022. The relationship between August 1998 monthly average air temperature and distance from the coast was examined for the group of air temperature sites located at distances ≤ 80 km from the coast (Figure 4.4-A) and the group of sites located >80 km from the coast (Figure 4.4-B). For air temperature sites located >80 km (~ 50 mi) from the coast (Figure 4.4-B), the linear regression model relating August 1998 monthly average air temperature and distance from the coast was weak, with an R^2 value of 0.23 and a slope of -0.04. Air temperature sites located ≤ 80 km from the coast showed a great improvement in the linear regression model (Figure 4.4-A) with an R^2 value of 0.74 and a slope of 0.15.

There was a reversal in the importance of elevation and distance from the coast in explaining the variability in air temperature, depending upon the location of the air temperature site. For air temperature sites located at distances >80 km from the coast, elevation played a much greater role in explaining the variability in air temperature. Conversely, for air temperatures sites located ≤ 80 km from the coast, distance from the coast accounted for a large proportion of the variability in air temperature.

These changing relationships between air temperature with elevation and distance from coast should be borne in mind when attempting to model stream temperatures. Some researchers have used elevation as a surrogate for air temperature. We have demonstrated that surrogacy may or may not apply, depending on the location of the air or water temperature monitoring site with respect to distance from the coast. Relationships between air temperature versus distance from the coast and elevation vary seasonally as well. This seasonal variability is discussed later in the chapter.

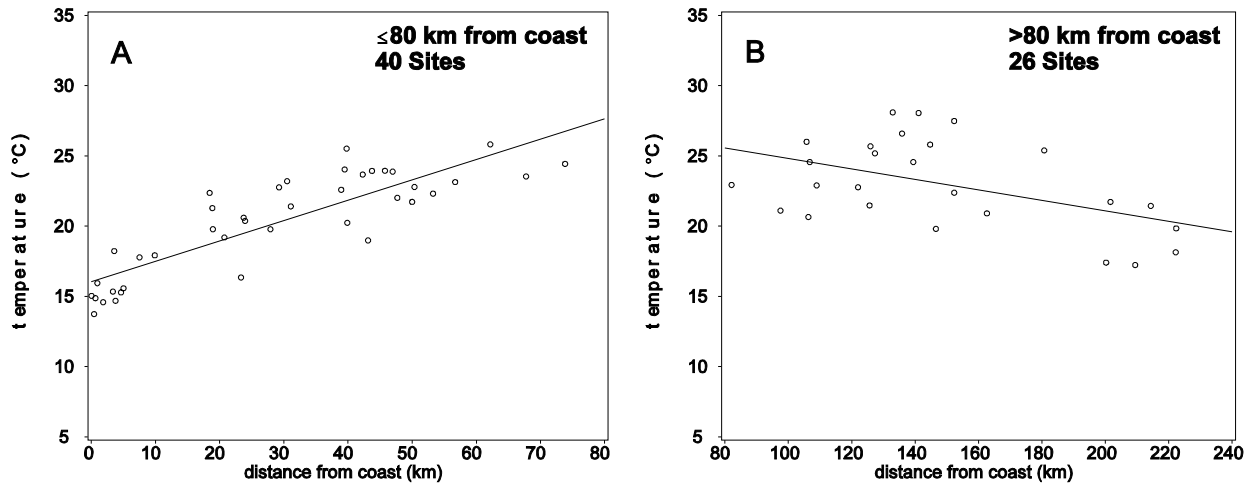


Figure 4.4. Relationship between August 1998 monthly average air temperature and distance from coast for 40 sites located ≤ 80 km (A) and 26 sites > 80 km (B) from the coast.

Monthly Average Air Temperature by Ecoprovince

Although stratification of the air temperature data into distance-from-coast classes greatly improved the linear regression models, the stratification was somewhat arbitrary. The observed relationship between air temperature versus elevation and distance from the coast undoubtedly plays a role in the distribution of plant communities and ecosystems across the region. Using Bailey’s ecophysiological regions (USDA, 1997) to stratify air temperature data was the next logical step. The area of interest defined for the regional stream temperature assessment encompasses two major ecoprovinces, the California Coastal Steppe Province (263) (CSP) and the Sierran Steppe-Mixed Forest-Coniferous Forest Province (M261) (Figure 4.5). Within the California Sierran Steppe-Mixed Forest-Coniferous Forest Province (SSP), air temperature data were limited to five ecosections, the Klamath Mountains Section (M261A), the Northern California Coast Ranges Section (M261B), the Northern California Interior Coast Ranges Section (M261C), the Southern Cascades Section (M261D), and the Modoc Plateau (M261G). The four sections were aggregated together and represent those ecophysiological areas

for which both stream temperature and air temperature were used in the regional assessment. The relationship between elevation and distance from the coast is shown in Figure 4.6 for each ecoprovince. The highest elevation at which air temperature sites were located in the CSP was approximately 160 m (525 ft) at about 20 km from the coast, compared to about 1800 m (~5900 ft) in the SSP. The relationship between distance from the coast and elevation for the SSP was nearly linear. However, there were several low lying sites located a considerable distances from the coast (100 to 160 km).

Table 4.1 shows the air temperature versus distance-from-coast linear regression model fit to the air temperature sites in the CSP. The regression line fit to the data (Figure 4.7-A) had an R^2 value of 0.6925, a marked improvement over the all-sites-combined model ($R^2 = 0.1547$).

August 1998 monthly average air temperature versus elevation for each ecoprovince are compared to the ≤ 80 km and > 80 km from the coast air temperature groups in Table 4.1. For the SSP the linear regression model was greatly improved over the all-sites-combined model, with an R^2 value of 0.6517.

FSP Regional Stream Temperature Assessment Report

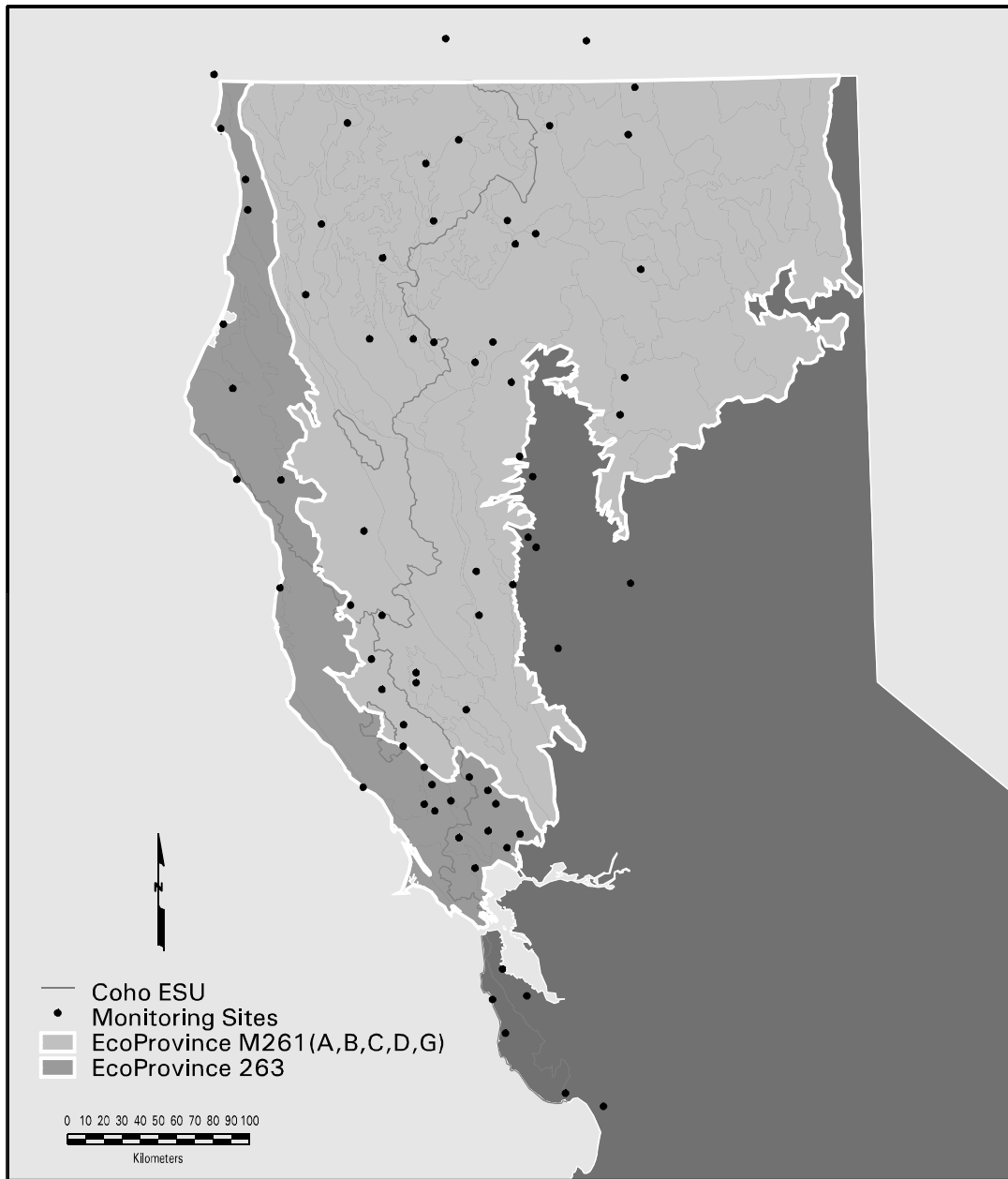


Figure 4.5. Distribution of air temperature monitoring sites in the Coastal Steppe, Mixed Forest and Redwood Forest Province (263) and the Sierran Steppe-Mixed Forest - Coniferous Forest Province (M261).

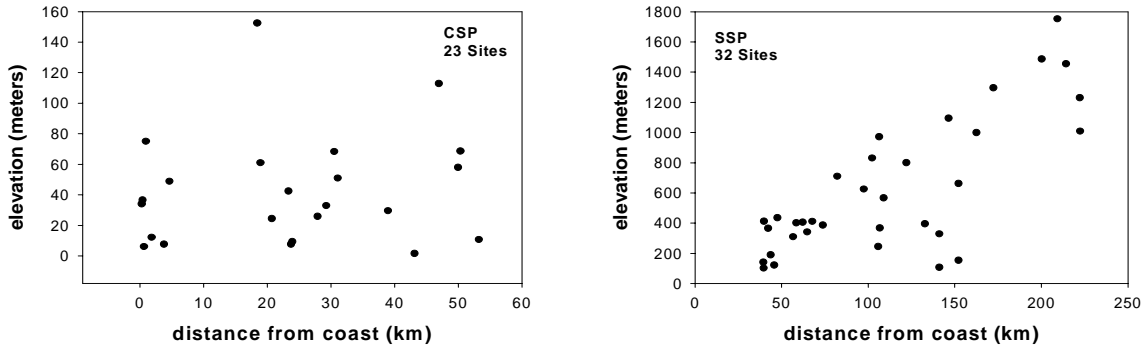


Figure 4.6. Relationship between distance from the coast and elevation for air temperature sites located in each ecoprovince.

Table 4.1. Linear Regression Models of August 1998 Monthly Average Air Temperature Versus Distance from Coast and Elevation by Air Temperature Site Groups.

Group	n	intercept	slope	R ²	F	pr (F)
<u>Air vs. Distance from Coast</u>						
All Sites	66	21.3529	-0.0001	0.0002	0.0158	0.9004
≤80 km	40	18.7101	0.0134	0.2730	14.2703	0.0005
CSP ¹	22	17.9130	0.0350	0.1550	3.6685	0.0699
>80 km	26	26.5164	-0.0054	0.7531	73.2154	0.0001
SSP ²	29	26.0759	-0.0052	0.6517	50.5287	0.0001
<u>Air vs. Elevation</u>						
All Sites	66	19.6663	0.0216	0.1547	11.7129	0.0011
≤80 km	40	16.0482	0.1448	0.7378	106.9030	0.0001
CSP	22	15.5061	0.1583	0.6925	45.0362	0.0001
>80 km	26	28.5377	-0.0372	0.2325	7.2700	0.0126
SSP	29	25.2738	-0.0219	0.2128	7.3001	0.0118

¹CSP = California Coastal Steppe Province

²SSP = Sierran Steppe-Mixed Forest-Coniferous Forest Province

This value is slightly less than the >80 km model, but has more of an ecological basis. The plot for the SSP (interior) air temperature versus elevation ecoprovincial model is shown in Figure 4.7-B.

There was a great improvement in the ecoprovincial linear regression models when coast distance was used as an independent variable. For the CSP, a

strong R² value (0.6925) was found (Table 4.1, Figure 4.7-A). For the SSP, more of the variability in August 1998 monthly average air temperature was accounted for using elevation as the independent variable (Table 4.1, Figure 4.7-B).

FSP Regional Stream Temperature Assessment Report

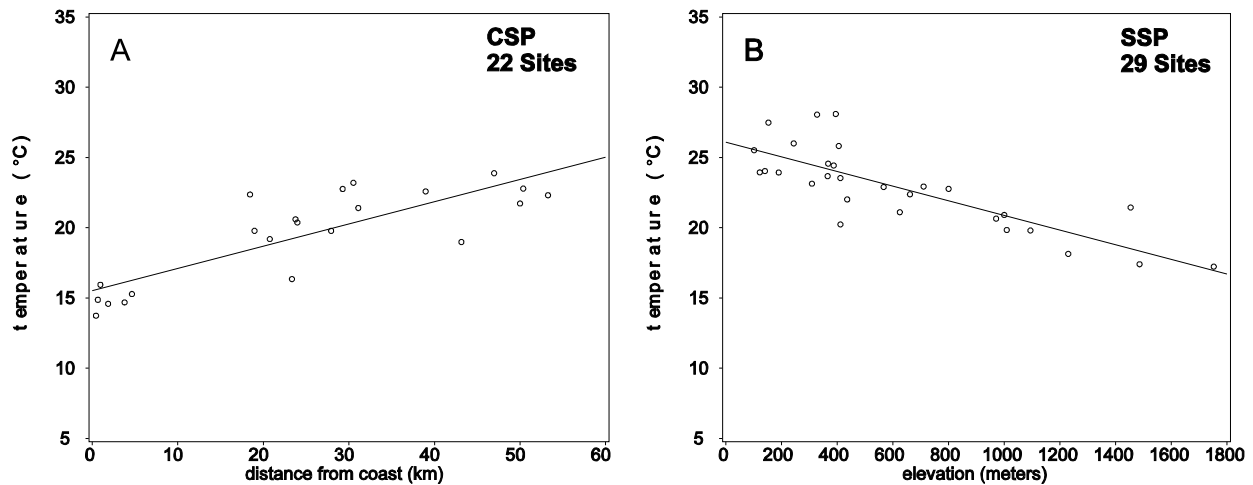


Figure 4.7. August 1998 monthly average air temperature versus distance from coast for 22 sites in the Coastal Steppe (A) and air temperature versus elevation for 29 sites in the Sierran Steppe-Mixed Forest-Coniferous Forest Province (B). Linear regression equations are presented in Table 4.1.

Seasonal Variation in Relationships

While it has been shown that elevation accounts for a large proportion of the variability in air temperatures for the SSP and distance from coast for the CSP, only August 1998 monthly average air temperature was used to develop these relationships. The relationship between air temperature and the two independent variables, elevation and distance from coast, changes seasonally. Linear regression analyses were performed on monthly average air temperatures for all months.

The winter months of December and January exhibited negative slopes for both air-versus-coast-distance and air-versus-elevation models for all air temperature site groups. The marine influence serves to make winter air temperatures warmer than those further inland and at higher elevations but cooler in the summer. This would account for the change in slope with season. The highest R^2 values were noted for the air-versus-elevation relationships for all sites combined, the >80 km-from-coast, and SSP groups. Moving into the warmer months, the slopes for the ≤ 80 km and CSP groups began to shift from negative to positive values for the air-elevation models. During the transition from winter to summer the R^2 values for these two groups steadily increased for the

air-versus-coast distance relationships, and decreased for the air-versus-elevation relationships. The air-versus-elevation R^2 values for the >80 km and SSP groups remained high across all months and their accompanying slopes remained negative across all months.

These results clearly demonstrate the need to consider both the temporal and spatial relationships between air temperature versus elevation and distance from coast. If either elevation or distance from coast are to be used as surrogates for air temperature to predict water temperature, the geographic and seasonal variations in these relationships must be taken into account.

Ecoprovincial Differences in Air Temperature

The difference in the relationship between monthly average air temperature and distance from the coast, and monthly average air temperature and elevation has been demonstrated in the previous section. What has not been explored is the relative difference between air temperatures in the CSP and the SSP. Figure 4.5 shows the distribution of the 72 air temperature sites in these two ecoprovinces.

Chapter 4 - Regional Trends in Air Temperature

Figure 4.8 presents the August average and average maximum air temperatures for the CSP and SSP for 1990 through 1998. Only air temperature sites with August data for all nine years were used in the analyses. There were 22 sites in the SSP and 12 sites in the CSP with which to make comparisons across the nine years. The August averages were compared to the 30-yr long-term average derived for each site using the PRISM model. That is, at each of the 34 air monitoring sites the 30-yr long-term average and average maximum for August was determined from the GIS data set developed from the PRISM model. PRISM data for air temperature sites in each ecoprovince were averaged to obtain the ecoprovincial long-term August average.

The CSP August average air temperatures were lower than SSP averages for all years. The cooling influence of marine air currents is responsible for the cooler air temperatures observed in the CSP compared to the SSP. The graph serves to illustrate that some years were warmer than the long-term

average, and that these warmer years did not necessarily transcend ecoprovinces. For example, while 1996 exhibited above normal air temperature for the SSP, the CSP was about normal. Conversely, 1993 exhibited above normal air temperatures for the CSP, while SSP air temperatures were below normal. August was the month used in the comparison since this is the month when the highest water temperatures normally occur for most sites. Comparison of other ecoprovincial monthly average air temperatures (i.e., June, July, and September) to the long-term average for that month showed slightly different patterns.

The purpose of this comparison is to provide researchers with qualitative information on the year-to-year variability that is observed in each ecoprovince. If a group of water temperature sites was monitored across multiple years, this information could assist in determining whether trends in water temperature may be due to differences in air temperature across years.

FSP Regional Stream Temperature Assessment Report

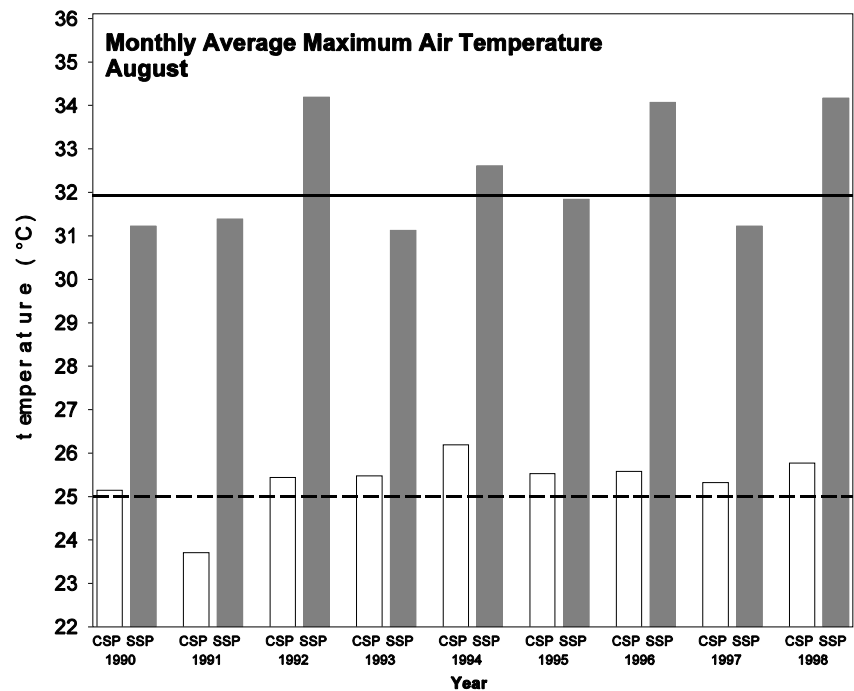
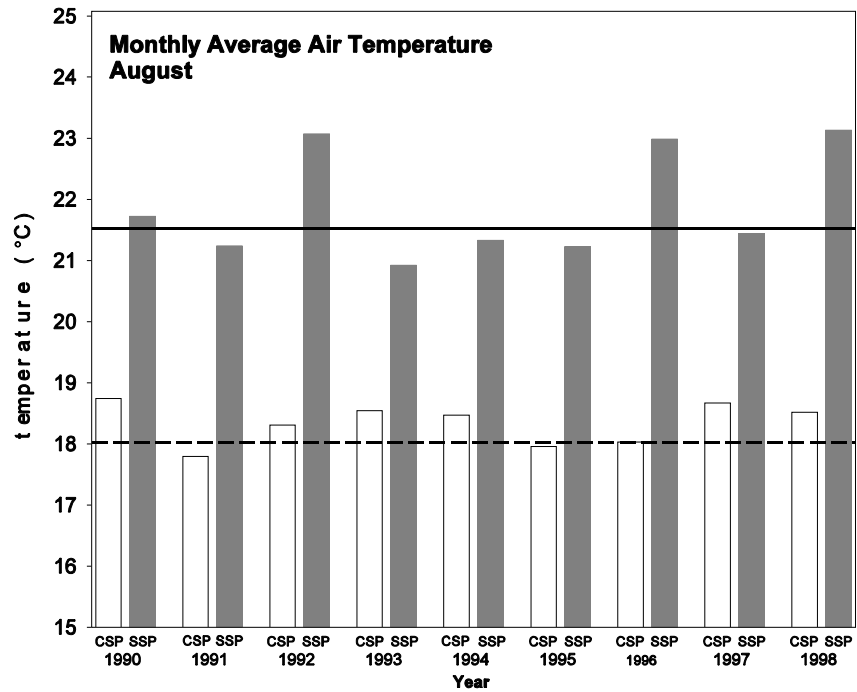


Figure 4.8. Comparison of ecoprovincial air temperatures for August 1990 - 1998. Ecoprovince CSP = California Coastal Steppe Province (12 coastal sites) and SSP = Sierran Steppe-Mixed Forest-Coniferous Forest Province (22 interior sites). Dashed and solid horizontal lines represent 30-yr long-term averages derived from the PRISM model for the coastal and interior ecoprovinces, respectively. PRISM monthly average calculated as max+min/2.

Air Temperature By Evolutionarily Significant Unit

Similar air temperature comparisons were performed by coho salmon evolutionarily significant units (ESU). There were 15 air temperature sites in the SONCC ESU with August air temperature for years 1990 through 1998 and 8 sites in the Central California ESU. The 30-year long-term averages derived by averaging the PRISM air temperature values at each of the 23 air temperature sites revealed that the ESU averages were very similar (Figure 4.9). We expected the SONCC ESU to exhibit higher long-term average temperatures than the CC ESU because of the greater inland areal extent of the SONCC ESU. The SONCC ESU transcends both the CSP and SSP ecoprovinces, whereas the CC ESU is mostly associated with the CSP ecoprovince. The more coastal distribution of sites in the SONCC ESU with complete August data for all nine years could account for the lower-than-expected 30-year long-

term average. Weitkamp et al. (1995) reported that the average annual sunshine along the coast in the Central California ESU is higher than anywhere further north, averaging 2200-2800 hours per year, while the SONCC receives 2000-2200 hours per year of sunshine. If one only considers the coastal portion of the SONCC, the somewhat lower hours of sunshine may result in cooler air temperatures. However, we consider the SONCC as a whole (both the coastal and inland portions), and believe that, on average, it is most likely warmer than the CC ESU.

Both ESUs showed above normal August average air temperatures in 1990, 1992, 1996, 1997 and 1998 (Figure 4.9). Not unlike ecoprovincial trends in air temperature across years, August average air temperatures did not vary similarly in the two ESUs. In some years the CC ESU was above normal while the SONCC was below normal and in other years the opposite trend was observed.

FSP Regional Stream Temperature Assessment Report

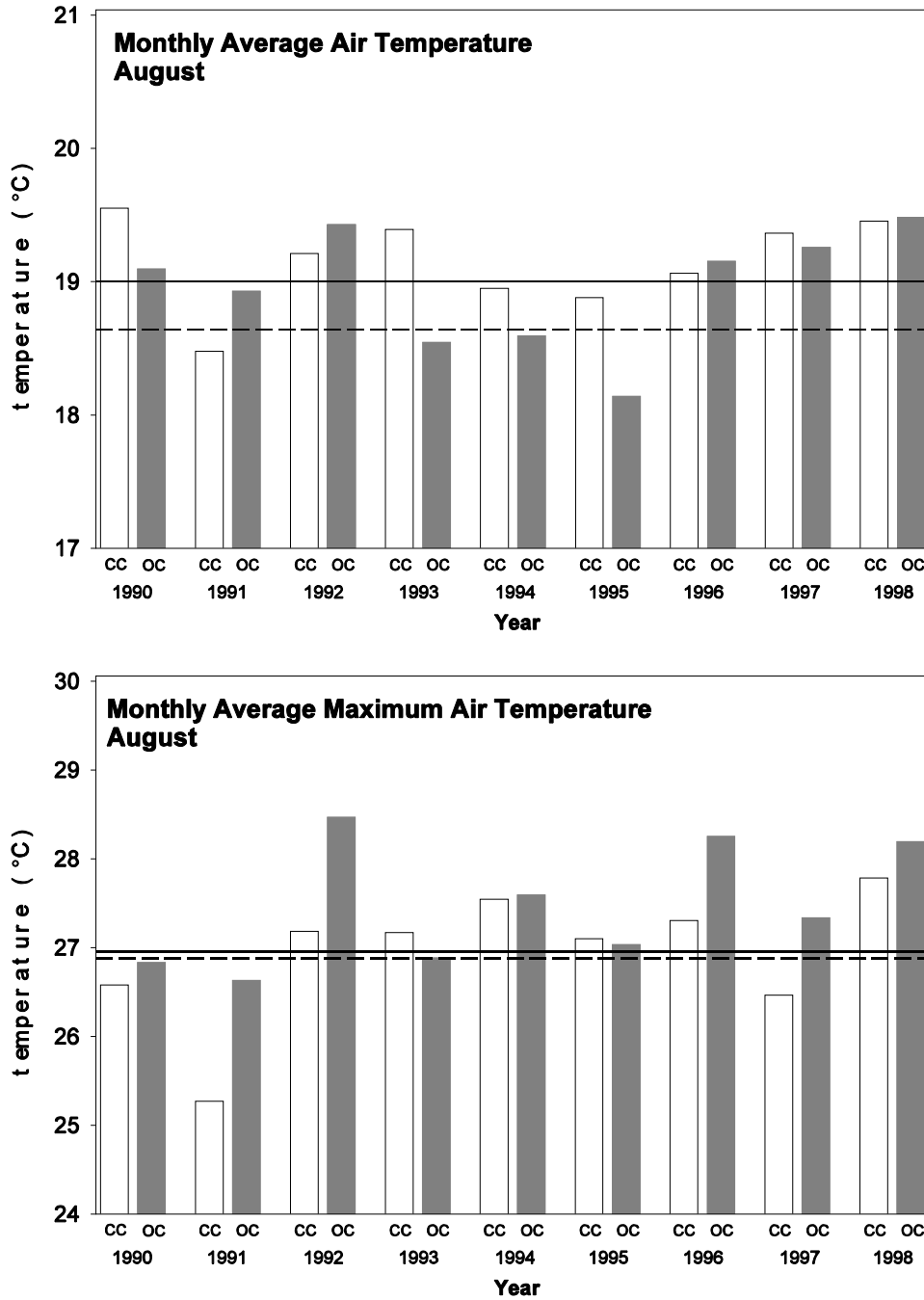


Figure 4.9. Comparison of ESU average air temperatures for August 1990 - 1998. CC = Central California ESU (8 sites) and OC = Southern Oregon Northern Coastal California ESU (15 interior sites). Dashed and solid horizontal lines represent 30-yr long-term averages derived from the PRISM model for the CC and SONCC ESUs, respectively. PRISM monthly average calculated as $\text{max} + \text{min} / 2$.

Variation in Basin-Level Air Temperatures

Figure 4.8 serves to illustrate the variation in air temperatures between years and between ecoprovinces. The SSP exhibited higher air temperatures than the CSP. The CSP and SSP are comprised of hydrologic units (HUCs) that also possess unique air temperature regimes.

Figure 4.10 shows the hydrologic units (HUCs) that comprise the range of the coho salmon in Northern California. The inset table in Figure 4.10 lists the HUC ID number and the HUC name.

PRISM-derived 30-year averages for August are displayed with respect to the HUC boundaries in Figure 4.11. Figure 4.12 presents the 30-year average maximum August air temperature. The coastal zone is much cooler than the more interior portions of the region. The coastal HUCs with southeast-to-northwest orientations, like the Lower Eel, Mad-Redwood, and South Fork Eel, and combined Upper, Middle, and Lower Eel HUCs have large temperature gradients from the upper headwaters to the coast. Air temperature gradients can be as much as 5°C to 15°C from headwaters to coast.

HUC-level averages were calculated to develop a picture of how average temperatures vary across HUCs. Table 4.2 presents the HUC-level 30-year August average minimum, average, and maximum air temperatures and the standard deviation and range in temperatures within each HUC. The minima and maxima are the lowest and highest August average temperature values in the HUC in any given 4-km grid cell. Those HUCs with southeast-to-northwest orientations have higher average values due to the contribution of higher interior air temperatures to the average. HUCs that are predominately along the coast have lower average air temperatures. HUCs that are completely in the interior have higher averages than coastal HUCs.

At the time of writing of this report only 1961-1991 30-yr average PRISM data for each month were available for the regional stream temperature assessment. More recently it has been learned that monthly average PRISM air temperature data for individual years may be available but have not been acquired to date. With monthly average PRISM data for each year, more localized air temperature estimates will be possible. This will greatly improve the predictive power of air temperature in the statistical models presented in Chapter 10.

Zone of Coastal Influence

PRISM data sets were used to develop a relationship between the 30-year average maximum monthly air temperature (AVGMAX) and the inland extent of the coastal effect. The PRISM AVGMAX raster data sets were converted from a 4-km grid spacing to a 1-km cell size using a bilinear resampling technique (Arc/Info GRID). The first derivative (slope) was calculated for the July and August AVGMAX data. These grids represent the rate of change in air temperature over distance. The rate averaged 0.30 C°/km for both coho ESUs. The maximum rates of change for July and August were 1.60 C°/km and 1.66 C°/km respectively. Figure 4.13 illustrates the variability of this rate over the coho ESUs for the month of July. A high rate of change is evident, roughly paralleling the coast from 2.8 to 32 km inland. Using the rate-of-change grids, a linear feature representing the maximum rate of change was derived. The rate of temperature change along this line varies between 0.43 C°/km and 1.43 C°/km with a mean of 0.78 C°/km. This line is an approximation of the maximum inland extent of the coastal cooling effect and is hereafter referred to as the zone of coastal influence (ZCI). ZCI is also our best approximation of the fog zone. It has not been validated. The extent of inland fog varies daily, seasonally, and from year to year.

FSP Regional Stream Temperature Assessment Report

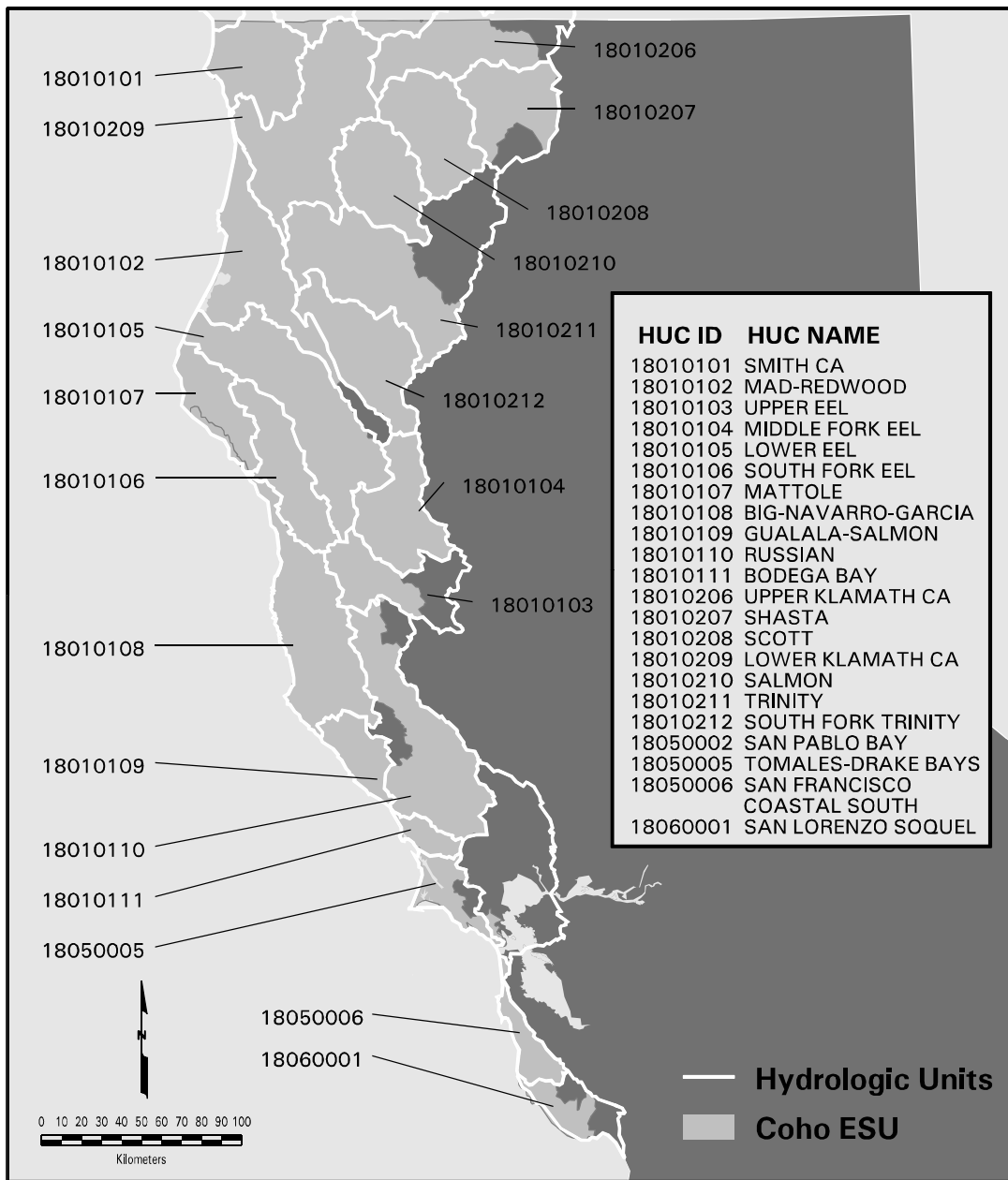


Figure 4.10. Hydrologic units that comprise the range of coho salmon in Northern California. The shaded area represents the coho ESU boundary.

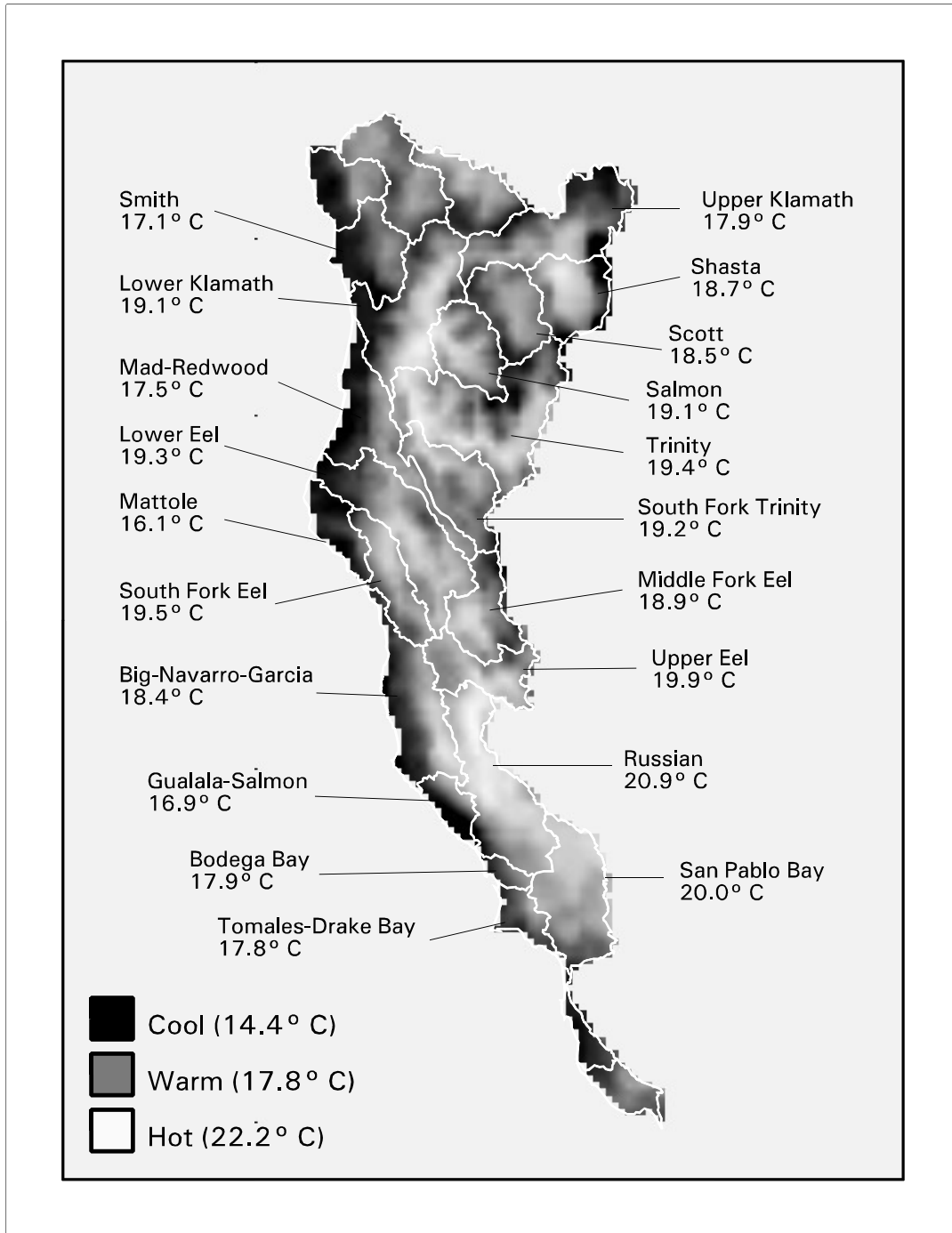


Figure 4.11. PRISM-derived August monthly average air temperatures across HUCs that comprise the range of the coho in Northern California.

FSP Regional Stream Temperature Assessment Report

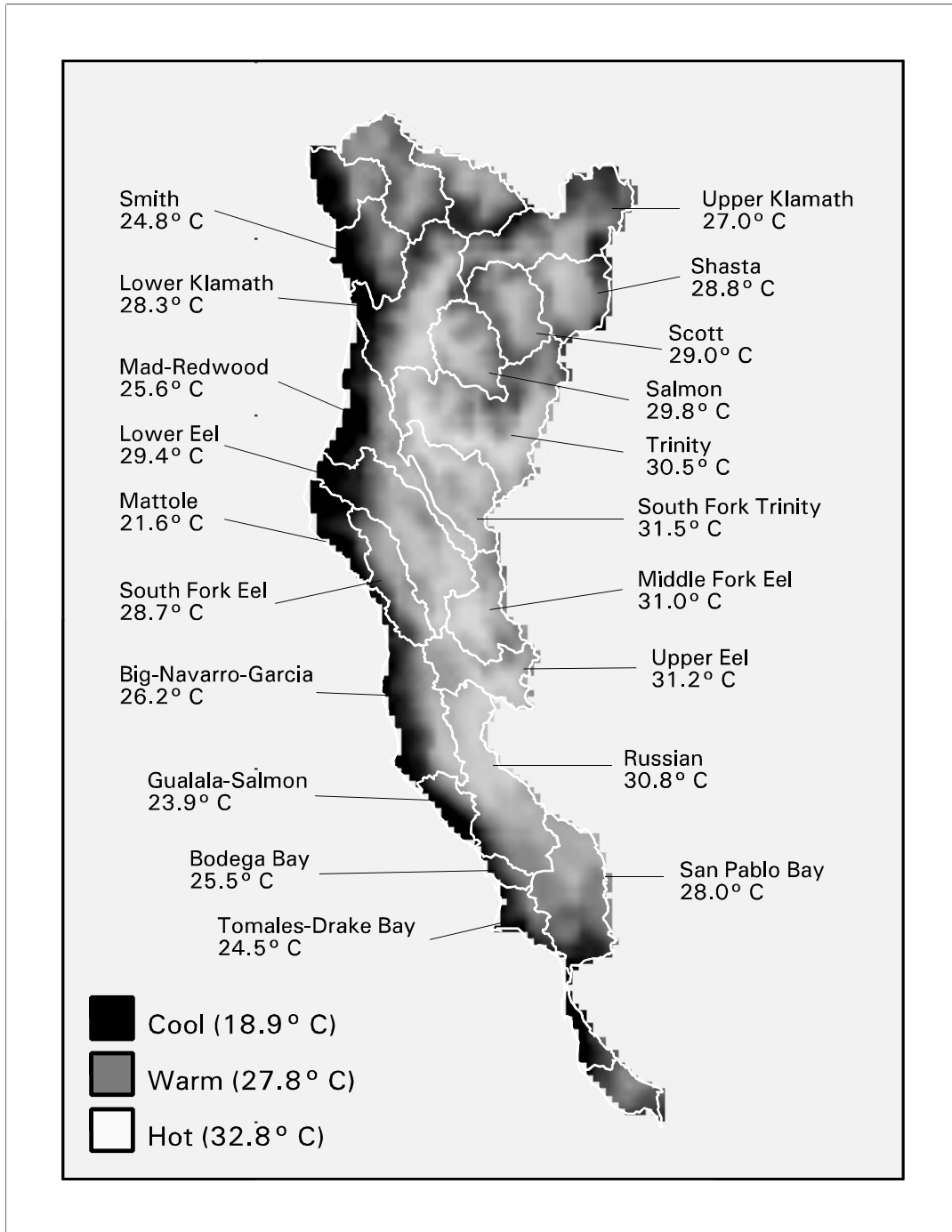


Figure 4.12. PRISM-derived August monthly average maximum air temperatures across HUCs that comprise the range of the coho in Northern California.

Chapter 4 - Regional Trends in Air Temperature

Table 4.2. PRISM 30-Year August Average Air Temperature Statistics for Hydrologic Units that Comprise the Range of the Coho Salmon in Northern California.

HUC Name	Minimum	Maximum	Range	Average	Std. Dev.
Smith	13.9	19.8	5.9	17.1	1.48
Mad-Redwood	14.5	20.4	5.9	17.5	1.94
Upper Eel	16.8	21.9	5.1	19.9	1.07
Middle Fork Eel	14.9	21.7	6.8	18.9	1.84
Lower Eel	14.7	21.6	6.9	19.3	1.68
South Fork Eel	15.9	21.5	5.6	19.5	1.27
Mattole	14.7	20.1	5.4	16.1	1.25
Big-Navarro-Garcia	14.6	22.1	7.5	18.4	2.16
Gualala-Salmon	13.6	21.2	7.6	16.9	2.45
Russian	14.8	22.7	7.8	20.9	1.45
Bodega Bay	15.3	19.9	4.6	17.9	1.35
Upper Klamath	13.1	21.1	8.1	17.9	1.89
Shasta	8.1	22.3	14.2	18.7	2.81
Scott	15.1	20.4	5.3	18.5	1.27
Lower Klamath	15.1	22.4	7.3	19.1	2.15
Salmon	15.5	21.9	6.4	19.1	1.67
Trinity	13.4	22.4	9.0	19.4	1.99
South Fork Trinity	15.1	22.4	7.3	19.2	1.34
San Pablo Bay	15.7	21.9	6.2	20.0	1.26
Tomales-Drake Bays	15.8	20.6	4.8	17.8	1.36
San Francisco Coastal South	15.0	17.9	2.9	16.1	0.76
San Lorenzo Soquel	15.8	20.1	4.3	18.1	1.08

NOTE: August Minimum, Maximum, Range, Average, and Standard Deviation are statistics based on the August average air temperature across all 4-km cells that comprise the HUC.

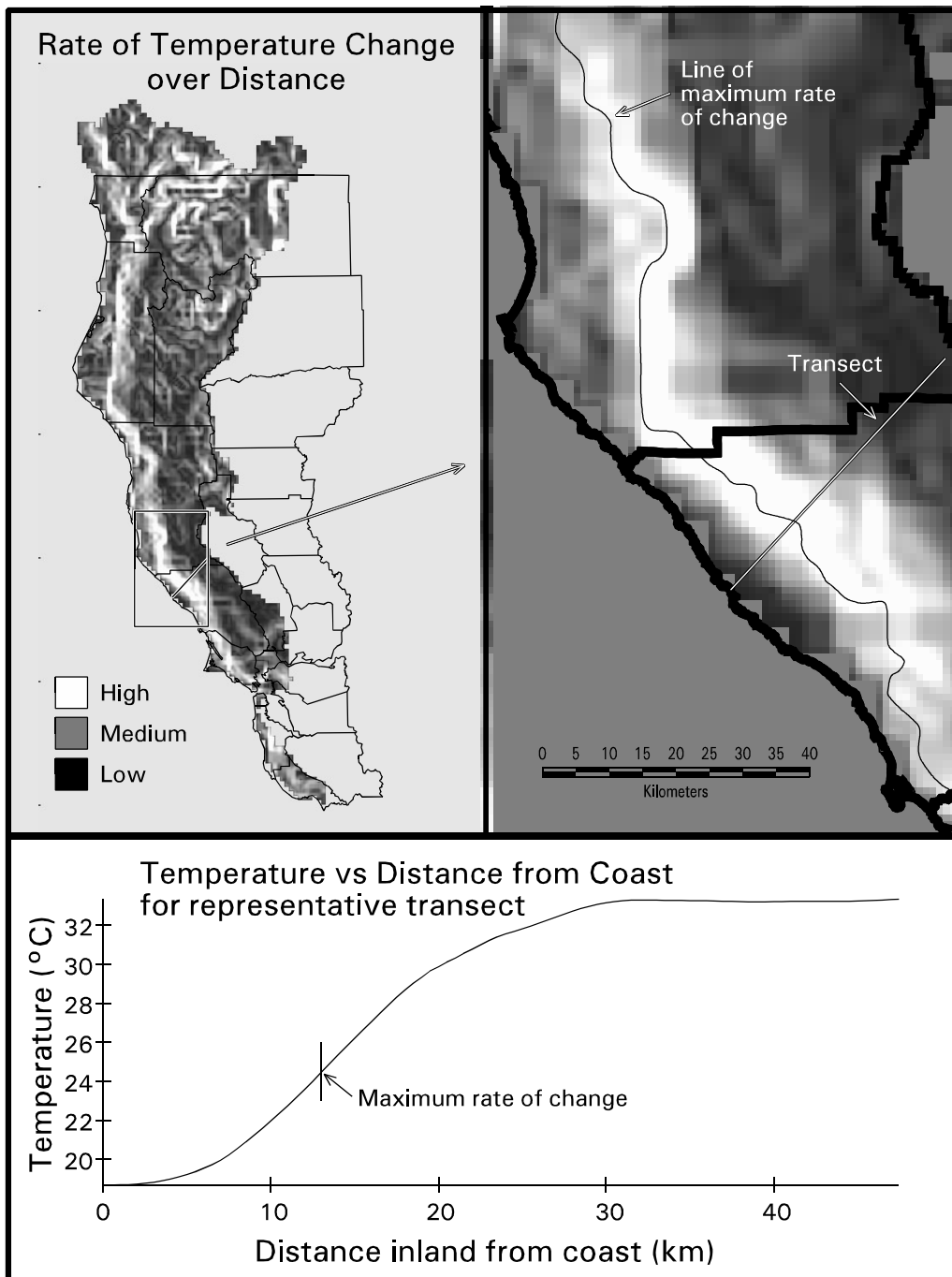


Figure 4.13. Derivation of the zone of coastal influence. Maximum rate of change determined using 30-yr PRISM August maximum average grid coverage across the range of coho salmon. Maximum rate of change is shown for a representative transect.

Mean Annual Air Temperature and Estimated Groundwater Temperature

Groundwater temperature is reportedly within $\pm 1^{\circ}\text{C}$ to 3°C of mean annual air temperature (Collins, 1925; Sullivan et al., 1990). Using PRISM 30-yr air temperature data the mean annual air temperature was calculated within each 4-km grid cell. The resulting spatial display shown in Figure 4.14 presents the estimated groundwater temperature throughout the HUCs within the range of the coho salmon. HUC-level average groundwater temperatures are indicated. It is interesting to note that in some locations, the estimated groundwater temperature is within a few degrees of the Maximum Weekly Average Temperature (MWAT) threshold of 18.3°C that is often used as a target temperature for

coho salmon streams. The Forest Science Project is acquiring and analyzing well-monitoring data from the U.S. Geological Survey and other sources to validate these groundwater temperature estimates.

If these groundwater estimates are accurate, then many headwater streams in the range of the coho salmon originate in areas of high air and groundwater temperature. Given the natural warming trend of streams in a longitudinal direction, very little downstream travel distance would be needed before stream temperatures exceed various chronic and acute thermal stress thresholds for juvenile coho salmon and other salmon species that have been developed in the laboratory and applied to field conditions.

FSP Regional Stream Temperature Assessment Report

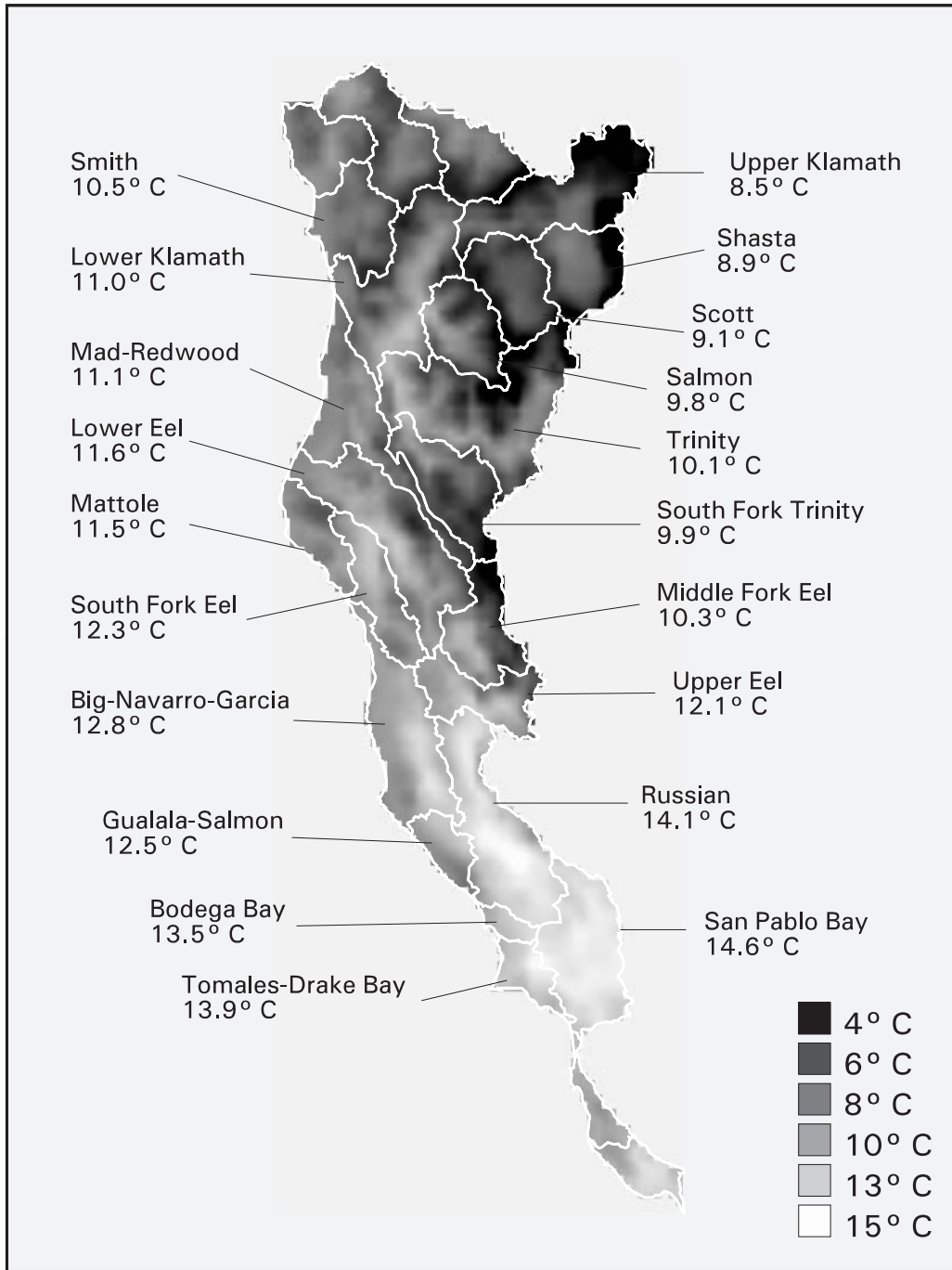


Figure 4.14. Groundwater temperature estimated from PRISM 30-yr mean annual air temperature in HUCs that comprise the range of the coho salmon in Northern California.

Summary

Air temperatures did not follow expected adiabatic cooling trends across the entire study area. Near the coast, air temperature was more a function of distance from the coast rather than elevation. Near the coast, summertime air temperatures increased with increasing elevation. Modelers should use caution when using elevation as a surrogate for air temperature. In the interior portion of the study area, air temperatures followed a more expected trend: decreasing air temperature with increasing elevation. The relationship between air temperature and the two independent variables, distance from the coast and elevation varied seasonally. During the winter months air temperatures in the coastal portion of the study area conformed more to the negative relationship with elevation.

The 1990-1998 CSP August average air temperatures were lower than SSP averages for all years. The cooling influence of marine air currents is most likely responsible for the cooler air temperatures observed in the CSP compared to the SSP. Some years were warmer than the long-term average. Warmer years did not necessarily coincide between ecoprovinces. For example, while 1992 exhibited above normal air temperature for the SSP, the CSP was below normal. Conversely, 1993 exhibited above normal air temperatures for the CSP, while SSP air temperatures were below normal.

Air temperatures exhibit appreciable gradients within and across the HUCs that comprise the range of the coho salmon in Northern California. Hydrologic units that are predominantly coastal have cooler air temperatures whereas those that have a somewhat southeasterly to northwesterly orientation show strong thermal gradients. Some HUCs are 10°C to

15°C warmer in the upper reaches than near the coast. Interior HUCs have warmer air temperatures throughout their drainage area, with cooler air temperatures at higher elevations.

The zone of coastal influence (ZCI) was derived from 30-yr long-term PRISM air temperature data by defining the steepest rate of change in air temperature along transects at increasing distances from the coast. The ZCI is an approximation of the fog zone, which intuitively would have a cooling influence on water temperatures due to its associated cooler air temperatures and solar energy interception.

Spatial trends in air temperature across the region must be understood in order to predict their influence on water temperatures. A useful air temperature database has been developed to characterize air temperature regimes across Northern California. In the next chapter we will explore the influence of these significant air temperature gradients on regional water temperatures. Acquisition of the monthly average PRISM air temperature data for individual water temperature years will greatly improve our understanding of the role air temperature plays in influencing water temperatures at large spatial scales.

Groundwater temperature was estimated from PRISM 30-yr mean annual air temperature. At some locations in the range of the coho salmon in Northern California, groundwater temperature is within a few degrees of a commonly applied MWAT threshold of 18.3°C. Some headwater streams may originate in areas with high air and groundwater temperature. Very little downstream travel distance would be needed before these streams would exceed various chronic and acute thermal stress thresholds. These exceedances could conceivably occur with natural longitudinal warming of streams.

Chapter 5

AIR AND WATER TEMPERATURE RELATIONSHIPS

Introduction

The previous chapter examined regional trends in air temperature throughout the range of coho salmon in Northern California. It was shown that air temperatures vary greatly across the region. This chapter examines whether air temperature measured at remote sites can be useful in explaining the variability in water temperature. Ideally, air temperature monitored at stream-side would provide the most representative information on the equilibrium temperature of a stream. However, very few sites in the regional assessment data set had air temperature collected at the stream temperature monitoring location. Due to the paucity of stream-side air temperature data we evaluated whether NOAA and other remote air temperature station data may have some explanatory power with respect to water temperature. These data are referred to as *macroair* temperature throughout this chapter.

At 23 water temperature sites, air temperature was monitored in close proximity to the water temperature sensor. These data will be referred to as *microair* temperatures. Analyses were performed on data from this limited number of sites, comparing trends in macroair versus microair temperatures, and air versus water temperatures.

Use of remote estimates of air temperature may result in inaccurate estimates of water temperature. This was observed by Sullivan and coworkers (1990) using data from six NOAA stations and is borne out in this report, using 72 remote air sites. In model sensitivity analyses, Bartholow (1989) and Sinokrot

and Stefan (1994) ranked air temperature as the single most important parameter for predicting water temperature, followed by solar radiation. However, as Bartholow (1989) points out, many other factors, including humidity, wind speed, riparian canopy, as well as factors in combination with air temperature, contribute to equilibrium water temperatures. The variability of these conditions make trying to predict water temperatures from remote air temperatures difficult. Given the importance of air temperature in predicting water temperature at daily, seasonal, and yearly temporal scales, it is perplexing that more data contributors did not measure stream-side air temperature.

Various studies (Collins, 1925; Moore, 1967; Kothandaraman and Evans, 1972) indicate that mean water temperature is generally within a few degrees of mean air temperature measured at stream-side. Moore (1967) found that for Oregon streams air temperature was a reasonable index of water temperature, but, because of other factors affecting water temperature, some Oregon streams were warmer and some were cooler than air temperature. The correlation between air temperature and water temperature is largely a function of upstream riparian conditions along a thermal reach, and to other factors controlling water inflow into the channel. However, air temperature influences both mean and maximum water temperatures regardless of riparian cover or stream size (Sullivan et. al., 1990). As streams increase in size at points more distant from the watershed divide, riparian characteristics become less influential in controlling water temperature. Large streams, because of their width relative to flanking

FSP Regional Stream Temperature Assessment Report

vegetation, naturally have less shade (Essie, 1998). Water temperature becomes more a function of air temperature.

At some sites where air temperature was monitored near the stream, good correlation was found with remote air temperature. We found that microair correlated better with water temperature than did macroair at 10 water temperature sites where air temperature was monitored at stream-side.

At 154 FSP sites that were monitored across three consecutive years (1996-1998), year-to-year changes in air temperature were shown to have some influence on water temperatures. The level of influence was dependent upon the stream's size, as estimated by the distance from the watershed divide.

Determining Nearest Remote Air Station

For many aspects of stream temperature analysis, ambient air temperature data are needed. If air temperature is not recorded in the immediate vicinity of the stream temperature site, data from remote air stations must be used to estimate local air temperatures. However, as Sullivan et al. (1990) pointed out, if remote or approximated air temperature data are used in predicting stream temperatures, then one can only hope for remote or approximated predicted stream temperature values.

The simplest method of determining the nearest air site to a stream temperature site is to use a minimum straight-line distance. However, as noted in the previous chapter, *Regional Trends in Air Temperature*, distance from coast and elevation are important parameters for describing regional variability in air temperature regimes within the study area. As such, these parameters should also be included in the model to select the most appropriate air temperature site. Using four parameters (UTM X-coordinate, UTM Y-coordinate, elevation, and distance to coast), four-dimensional Euclidian distances were calculated between each stream site and each air site. Air temperature sites with the smallest Euclidian distance were matched with water temperature sites for analysis. Monthly mean stream

temperatures for June through September 1998 at 546 sites and corresponding monthly mean air temperature data were used to examine the strength of the relationship. Figure 5.1-A shows the linear regression of monthly mean stream temperatures to mean air temperatures using the four-dimensional Euclidian distance criteria. The relationship was highly variable ($R^2 = 0.15$).

Because of the relatively low R^2 value for the four-dimensional model, additional parameters were added to the model in an attempt to improve the estimate. These additional parameters were long-term minimum and maximum air temperatures at each air station estimated from the PRISM data model. PRISM 30-year long-term monthly air temperature metrics for June through September (1961 - 1991) resulted in eight additional parameters being included in the model. Twelve-dimensional Euclidian distances were calculated between each stream site and each air site. Figure 5.1-B shows the regression of monthly mean stream temperatures to monthly mean air temperatures using the 12-dimensional Euclidian distance model. Although there was only a slight improvement in the R^2 , it was felt that, based on best professional judgement and personal knowledge of the climate regimes in Northern California, the 12-parameter method appeared to provide more realistic matchings between air and water temperature sites. The most notable changes were in the coastal areas, where the four-dimensional model selected air sites that were closer to the water site yet were 20 to 50 km inland. The 12-dimensional model was more sensitive to coastal versus inland air temperature differences. Moreover, the 12-dimensional model was better at selecting air sites that were more representative of air temperature at the water site based on the PRISM 30-year long-term values for the water site. This often meant that for a coastal water site the model might select a coastal air site that was 84 km away as opposed to an inland site that was only 20 km away. The mean distance between air stations and stream temperature sites using the 12-dimensional Euclidian distance method was 25 km, with a range of 0.3 to 84 km.

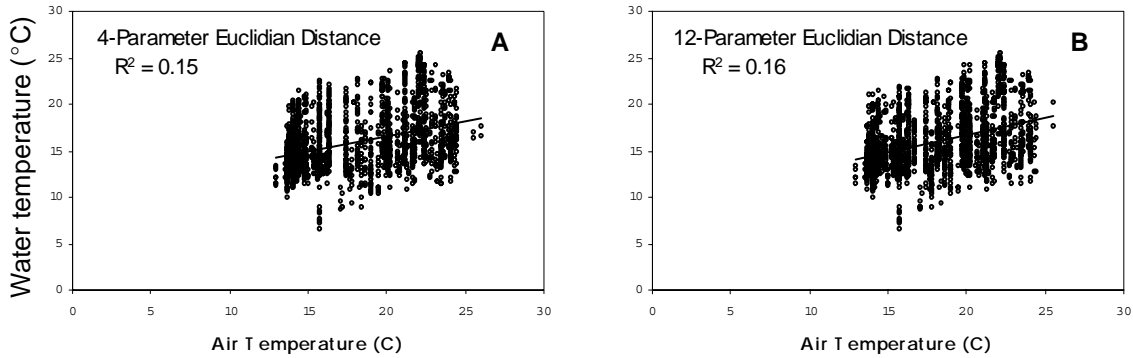


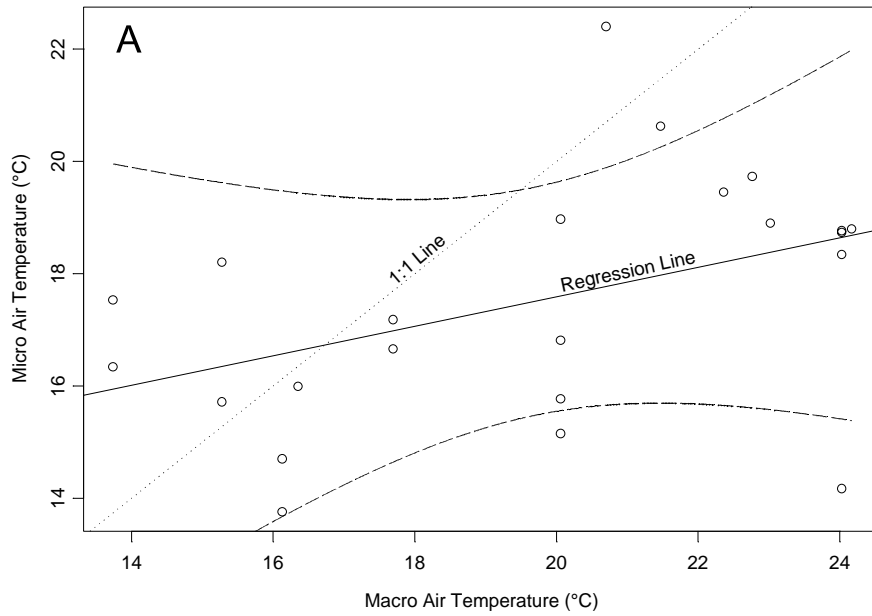
Figure 5.1. Comparison of linear regressions for monthly average air temperatures versus monthly average water temperatures using (A) four- and (B) 12-dimensional minimum Euclidian distance models. June, July, August, and September 1998 monthly averages are plotted for 546 water temperature sites.

Micro- and Macro-Air Temperature Relationships

To determine how well remote air temperature might predict local air temperature at a water temperature site, we acquired stream-side air temperature data. There were 40 water temperature sites where stream-side air temperature was monitored. Of these 40 sites, 23 sites had complete microair temperature data for comparison to data collected at macroair temperature sites selected using the 12-dimensional Euclidian distance model described above. Figure 5.2 shows comparisons between August monthly macro- and

micro-air average and maximum temperature data. The monthly average microair temperature generally fell below the line of one-to-one correspondence (Figure 5.2-A), while the monthly maximum microair temperature was above this line (Figure 5.2-B). While there was an obvious positive correlation between average micro- and macro-air temperature ($R^2 = 0.1902$) and maximum micro- and macro-air temperature ($R^2 = 0.1790$), microair temperatures exhibited a 5-10°C range at certain macroair temperature values.

Average August Air Temperature



Maximum August Air Temperature

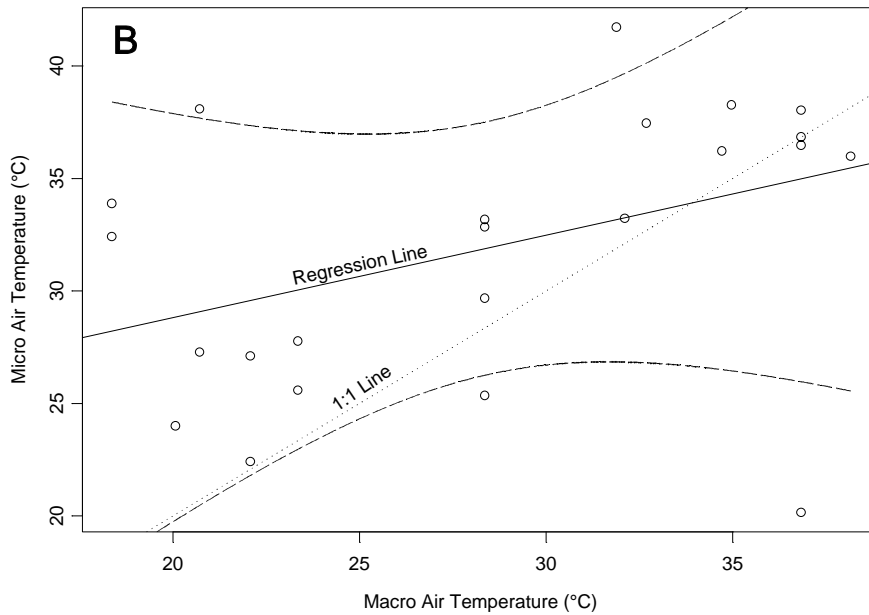


Figure 5.2. Comparison of August monthly average (A) and maximum (B) macro- versus micro-air temperature. Regression line and line of one-to-one correspondence is shown. Dashed lines represent 95% confidence bounds for predicting microair temperature from macroair temperature.

Comparison of Macroair and Stream Temperatures

Monthly average air temperature data from the nearest 12-dimensional Euclidian distance site was merged with its corresponding monthly average stream temperature at each site. Analyses were performed to explore the relationships between air-water temperatures across the entire study area, i.e., the two coho salmon ESUs in Northern California, and smaller spatial scales (e.g., ecoprovinces, HUCs, zone of coastal influence).

Figure 5.1 illustrates the rather poor correlation between macroair and water temperature exhibited for all 1998 sites in the study area. While a positive correlation was observed, the ability to predict water temperature from macroair temperature alone would not be of sufficient accuracy to be useful for most purposes. This is further evidenced by the poor correlations between macro- and micro-air temperatures at 23 sites shown in Figure 5.2. Stefan and Preud'homme (1993) found that as the time interval increased, better relationships between air and water temperature were realized at a given site. Relying on macroair temperature data, we are unfortunately limited to monthly averages at most sites. Going to the next time step, yearly averages, may provide better correlations at single sites, but then biological relevancy is lost. At a yearly temporal scale we are limited by not having stream temperature data spanning an entire 12-month period. Thus, we are limited to making macroair-water temperature comparisons of June, July, August, and September monthly averages. Using a larger temporal scale (e.g., yearly average) will not solve the problem that is inherent in this regional assessment, and that is spatial variability.

Figure 5.3 compares the monthly minima, means, and maxima for air-water temperature relationships for 1998 FSP sites for the months of June, July, August, and September. Figure 5.3-C is the same data as shown in Figure 5.1-B, but with a one-to-one line of correspondence drawn instead of the linear regression line. Monthly minimum water temperatures nearly always exceeded monthly

minimum air temperatures (Figure 5.3-A), whereas for monthly maxima, the opposite was observed (5.3-B). The opposite minimum-maximum relationships can be related to the specific heat of water. Specific heat is the amount of energy required to raise a unit mass of a material 1°C. The specific heat of water is ~1.0 calorie/gram/°C while air has a specific heat of ~0.24 calories/gram/°C, both at zero degrees Celsius and one atmosphere pressure. Thus, it takes about one fourth the energy to raise air temperature 1°C than it does water. Water is slow to cool down and slow to heat up, much slower than air. While air temperatures can reach higher levels in the day and lower levels in the evening, water is in a constant state of disequilibrium. Water temperatures seek to come into equilibrium with air temperatures during the day, but insufficient time is available during daylight hours for the slower heating water to reach the maximum air temperature. After sundown, air temperatures decrease more rapidly than water temperatures. Given adequate time, water temperature would eventually equilibrate with minimum and maximum air temperatures. But water temperatures never have enough time to catch up. Sunrise comes and the process begins again. Moreover, streams are flowing bodies of water. The air temperature regime changes as water moves down through the watershed.

The above discussion focuses on minimum and maximum temperatures. Figure 5.3-C shows that average water temperatures frequently exceed average air temperatures. It must also be remembered that these are macroair temperatures, and may be 5°C to 10°C different than microair temperatures at stream-side (Figure 5.2). Also, given the spatial variability in air temperature regimes across Northern California as presented in Chapter 4, water temperature at one location may have come into equilibrium with much warmer air temperature at a more upstream location. This spatial lag could partially explain many instances of water temperature exceeding air temperature at certain locations. Additionally, average water temperature will be lower than average air temperature because water generally exhibits higher daily minima than air.

FSP Regional Stream Temperature Assessment Report

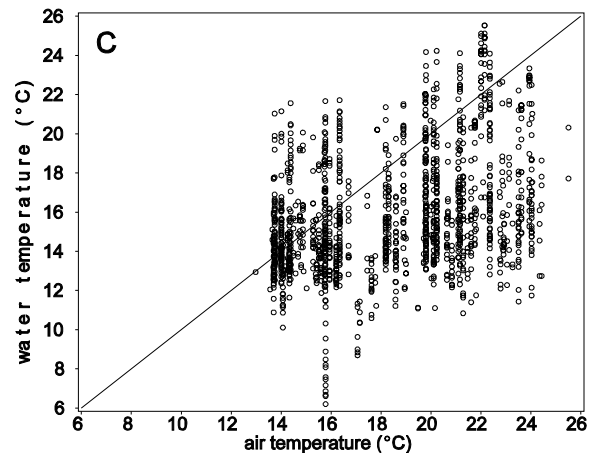
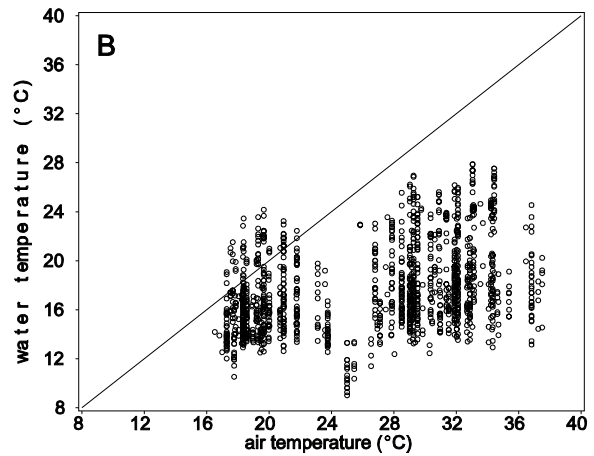
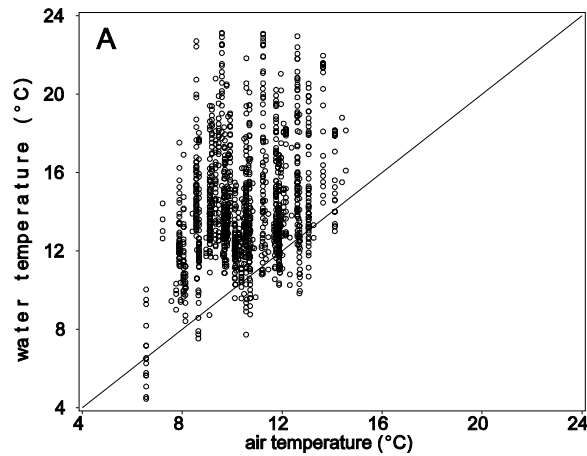


Figure 5.3. Comparisons of (A) monthly minimum, (B) monthly maximum, and (C) monthly average June, July, August, and September macroair versus water temperatures for 1998 Forest Science Project sites. Air temperature data are from air sites selected using a 12-dimensional Euclidian distance model. One-to-one line of correspondence is shown.

Ecoprovincial Comparisons

Water temperature sites and their matched 12-dimensional Euclidian macroair sites were grouped by CSP and SSP ecoprovinces. Figure 5.4 shows the relationship between the monthly average macroair and water temperature in each ecoprovince for all summer months combined. Figure 5.4-A shows that many monthly average water temperatures in the CSP exceeded monthly average macroair temperatures over most of the range in macroair temperature. At monthly average macroair temperatures as low as 14°C, water temperatures over 21°C were observed. Interestingly, at the highest air temperatures, the highest corresponding water temperatures were well

below the line of one-to-one correspondence. The lower water temperatures observed at higher air temperatures may indicate that the macroair temperature may not adequately reflect localized climate conditions. Additionally, this seems to suggest that water temperatures may only reach some maximum value, and will not go much above this value, even with continually increasing air temperatures. The maximum equilibrium concept was also postulated by Sullivan et al. (1990). As discussed above, water temperature would eventually attain the same temperature as air, given sufficient equilibration time. However, the diurnal cycles in air temperature change at a faster rate than water. Another factor that may account for

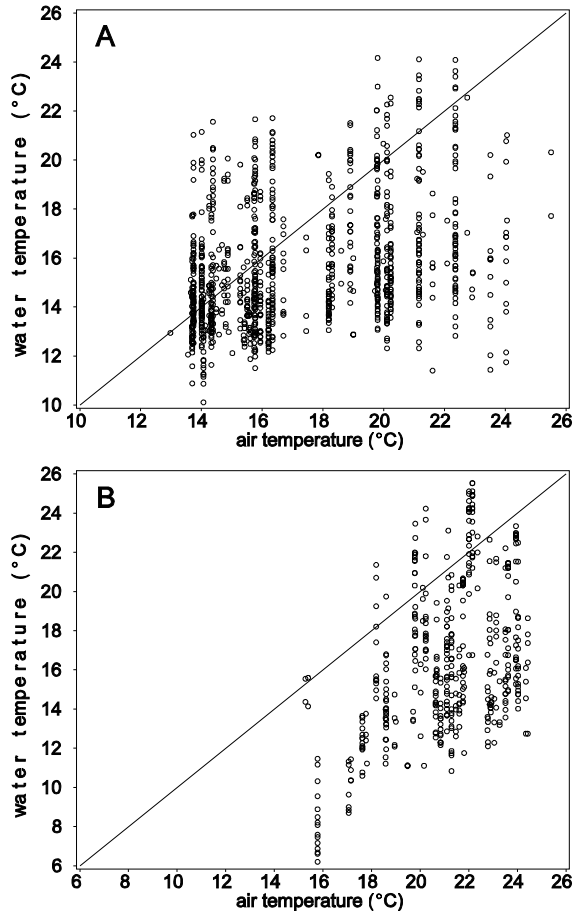


Figure 5.4. Relationship between 1998 monthly (June, July, Aug, Sept) average macroair and water temperatures for A) CSP and B) SSP ecoprovinces.

the observed maximum-equilibrium phenomenon is that other important meteorological variables co-vary with air temperature and solar radiation, such as humidity. As air temperature increases, humidity decreases, which, in turn, increases evaporation at the air-water interface. Increased evaporation tends to have a cooling influence on water temperature.

In the SSP, water temperatures exceeding the macroair temperature monthly averages were not observed until the air temperatures attained values over $\sim 18^{\circ}\text{C}$ (Figure 5.4-B). Generally, there appeared to be a more discernable increasing trend in water temperature with increasing air temperature in

the SSP. Similar to the CSP, at the highest air temperatures, water temperatures fell below the line of one-to-one correspondence.

Water temperature tends to approach air temperature as water travels down through a watershed (Hynes, 1970; Sullivan et al., 1990). However, as presented in Chapter 4, interior air temperatures in Northern California are often 10°C to 15°C warmer than air temperatures near the coast, where most drainages find their eventual outlet. Next, we will examine how air-water temperature relationships vary by HUC and by watershed position within a HUC.

Air-Water Temperatures and Watershed Position

The difficulty in developing good predictions of water temperature from remote air temperature is illustrated in Figure 5.5 for the Lower Eel and Big-Navarro-Garcia HUCs. The plotted monthly average was calculated by averaging 1998 July and August averages. There were 60 sites in the Lower Eel HUC and 113 sites in the Big-Navarro-Garcia HUC. However, only five air sites in each HUC were matched with multiple water sites. For a given monthly average air temperature at a macroair site, the associated water temperatures ranged up to 15°C in some instances.

The variation in water-to-macroair temperature ratio (W:A_RATIO) with distance from the watershed divide was investigated in each hydrologic unit (HUC) comprising the range of the coho salmon in Northern California (Figure 5.6). Two HUCs were not included, the Salmon and Russian, due to insufficient data points. July and August monthly mean temperatures were averaged together to generate the plots in Figure 5.6.

All HUCs showed a general increase in the W:A_RATIO with increasing divide distance. More mainstem sites were over unity than tributary sites. The Scott and Upper Klamath did not exhibit any sites with W:A_RATIO values over unity. These two HUCs are among the warmest in terms of air

Chapter 5 - Air and Water Temperature Relationships

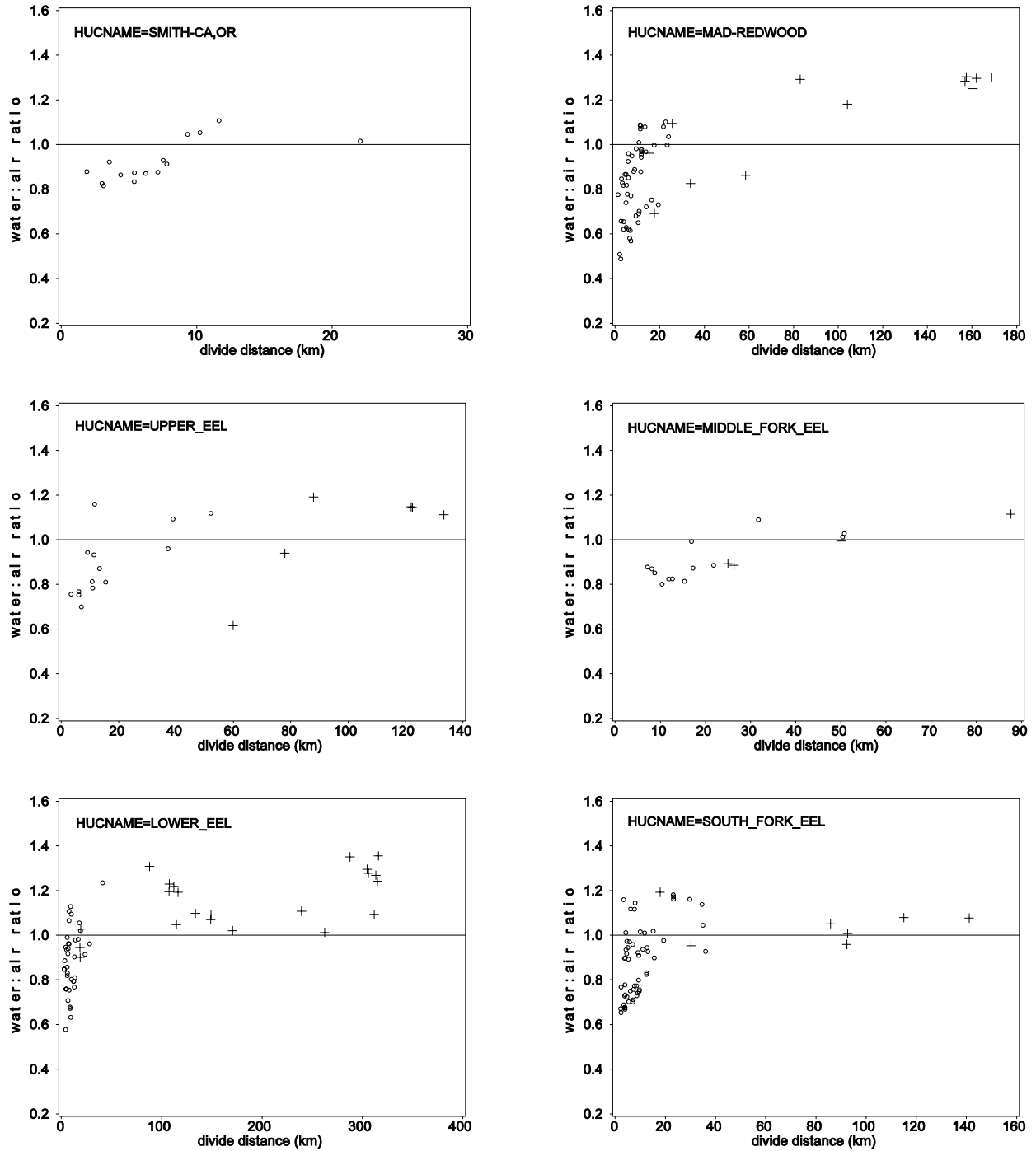


Figure 5.6. Change in water:air temperature ratio with distance from watershed divide by HUC. Macroair and water temperatures are monthly averages for July/August combined, 1998. Open circles are tributary sites and crosses are mainstems.

FSP Regional Stream Temperature Assessment Report

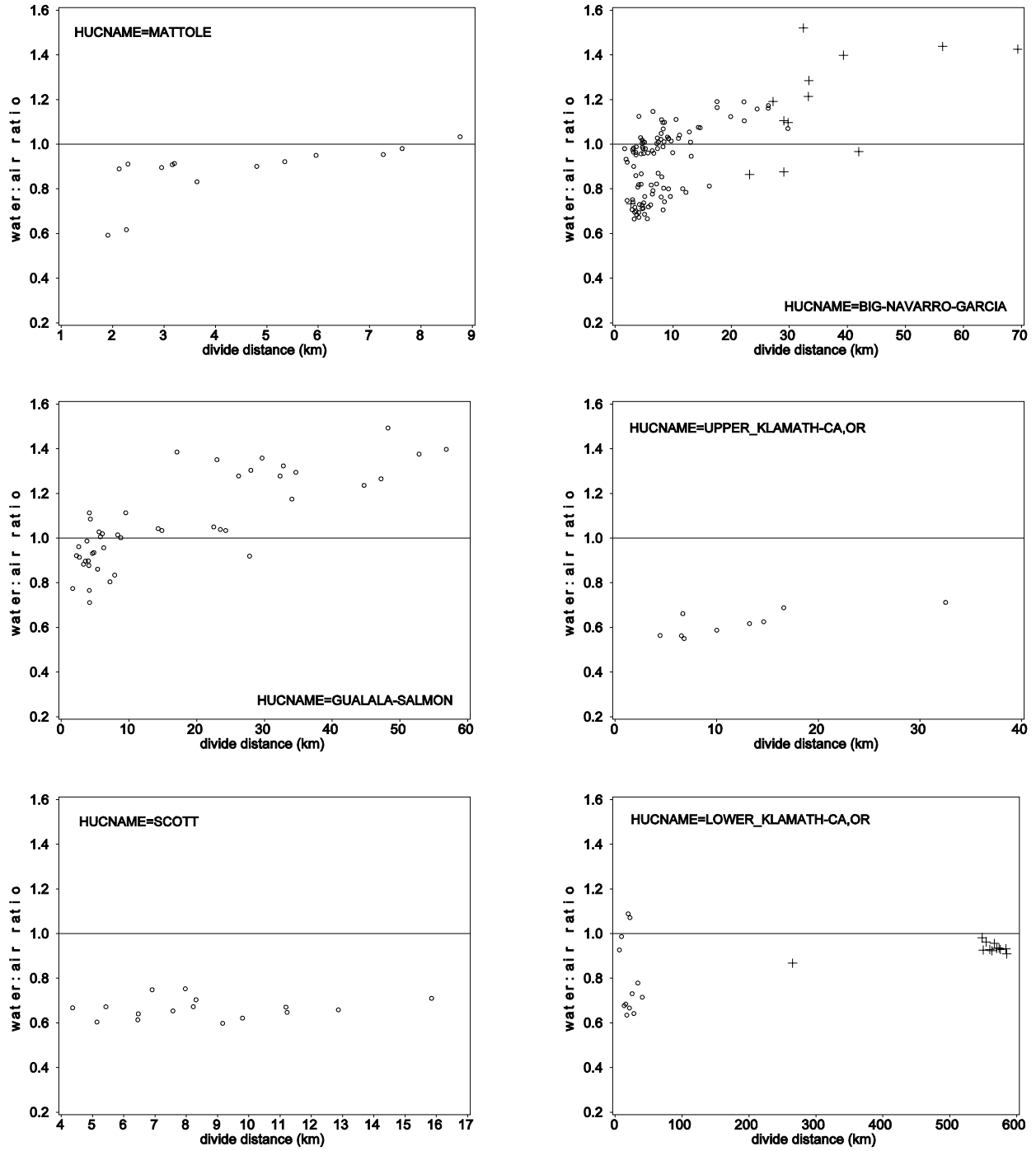


Figure 5.6. (continued)

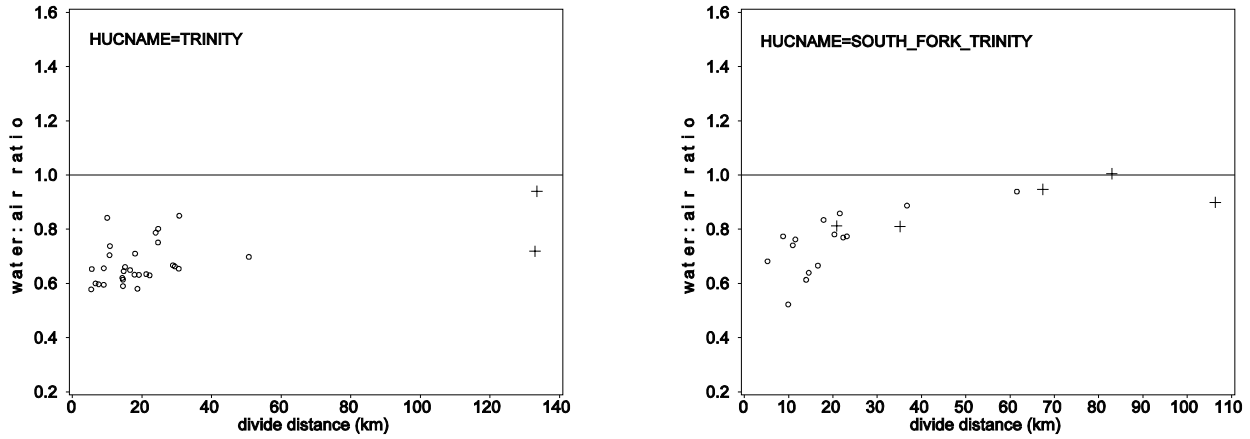


Figure 5.6. (continued)

PRISM Air Temperature and Watershed Position

The 30-year long-term average maximum air temperature from the PRISM data set was used to examine air temperature regimes in selected hydrologic units. Although year-to-year variations in air temperature cannot be discerned from the data, more representative air temperatures at each water site are obtained, given PRISM's 4-km grid resolution. Figure 5.7 presents the 30-year August average maximum air temperature at each Mad-Redwood HUC water site plotted by divide distance. Symbols denote whether the highest 1998 daily maximum temperature at either a tributary or mainstem site exceeded 26°C. Only one mainstem site exceeded 26°C at a divide distance of about 60 km. The August average maximum air temperature at the site was ~29°C (84°C). There was about a 7°C decrease in the August average air temperature at mainstem sites located 80 km or more from the watershed divide. The decrease in air temperature and concomitant lack of mainstem sites that exceeded 26°C is most likely due to cooling influence of the coastal zone.

The four HUCs that comprise the Eel River basin (Upper, Middle, Lower, and South Fork) are presented in Figure 5.8. August average maximum air temperatures at water sites in the four Eel River

HUCs were markedly higher than in the Mad-Redwood HUC.

August average maximum air temperature ranged between 30°C to 34°C (86°F to 93°F) at all tributary and mainstem sites along the 140 km divide distance of the Upper Eel River HUC (Figure 5.8-A). All but one mainstem site exceeded 26°C. At divide distances less than 20 km, all but one tributary site were below 26°C. This site fell in the 0-24% canopy class.

In the Middle Fork Eel River HUC, August average maximum air temperatures at each stream temperature monitoring site showed a similar range as in the Upper Eel River HUC. At air temperatures above 32°C (90°F) both tributary and mainstem sites exhibited daily maximum stream temperatures over 26°C. (Figure 5.8-B). Three sites on the Middle Fork Eel River between 20 km and 50 km from the watershed divide had XY1DX values under 26°C. However, at a site further downstream (~90 km) air temperature increased by about 3°C and the highest daily maximum water temperature exceeded 26°C. This trend supports the concept that large rivers tend

FSP Regional Stream Temperature Assessment Report

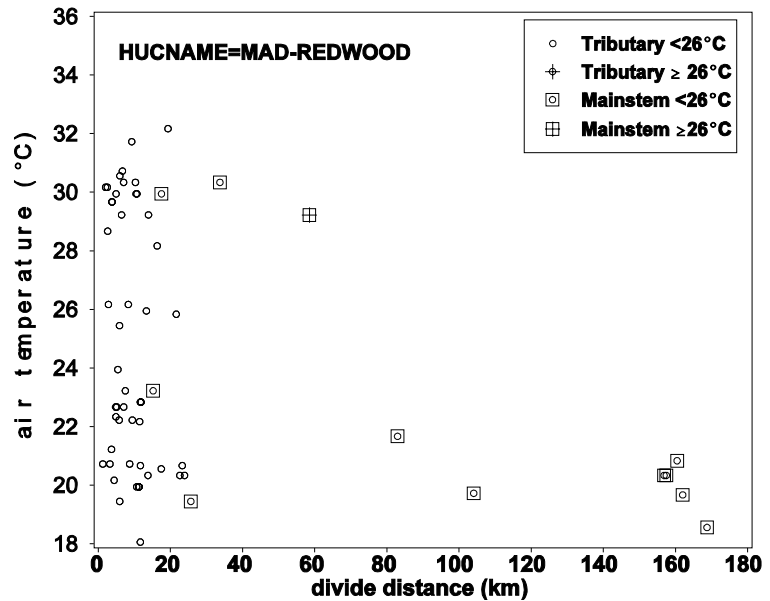


Figure 5.7. PRISM 30-year August average maximum air temperatures at each stream temperature monitoring site versus divide distance in the Mad-Redwood HUC. Open circles are tributary sites and squares are mainstem sites. Crosses indicate that the highest 1998 daily maximum temperature exceeded 26°C.

to come into equilibrium with air temperature (Sullivan et al., 1990). August average maximum air temperatures at sites on the mainstem Eel River in the Lower Eel HUC showed about a 14°C (25°F) decrease between 100 km and 320 km from the watershed divide (Figure 5.7-C). Despite the large decrease in air temperatures, mainstem sites continued to have XY1DX values over 26°C until sites at about 300 km from the watershed divide were reached. Mainstem water temperatures seem to have equilibrated to the higher interior air temperatures, imparting thermal inertia that requires considerable cooling from the zone of coastal influence before water temperatures begin to reequilibrate. The North Fork Eel River enters the Eel River in an area where August average maximum air temperatures are near 32°C (~90°C). Two sites on the North Fork Eel River had water temperatures that appear to be influenced by warm air temperatures in the interior portion of the HUC.

August average maximum air temperatures were lower at two water temperature sites on the South Fork Eel River at divide distances less than 40 km than sites further downstream (>80 km divide distance). Generally, it is believed that both air and water temperatures increase longitudinally. Exceptions to this commonly observed phenomenon have been shown for Northern Coastal California. The South Fork Eel River conforms to the norm, but for a different reason. The South Fork Eel River is oriented such that the upper reaches are located within the zone of coastal influence. The South Fork Eel River enters the main Eel River outside of the zone of coastal influence where air temperatures are higher. Thus, two mechanisms are working simultaneously to account for the longitudinal increase in air and water temperature.

In the four HUCs that comprise the Eel River Basin, the majority of tributary sites with XY1DX values exceeding 26°C were associated with warm August average maximum air temperatures.

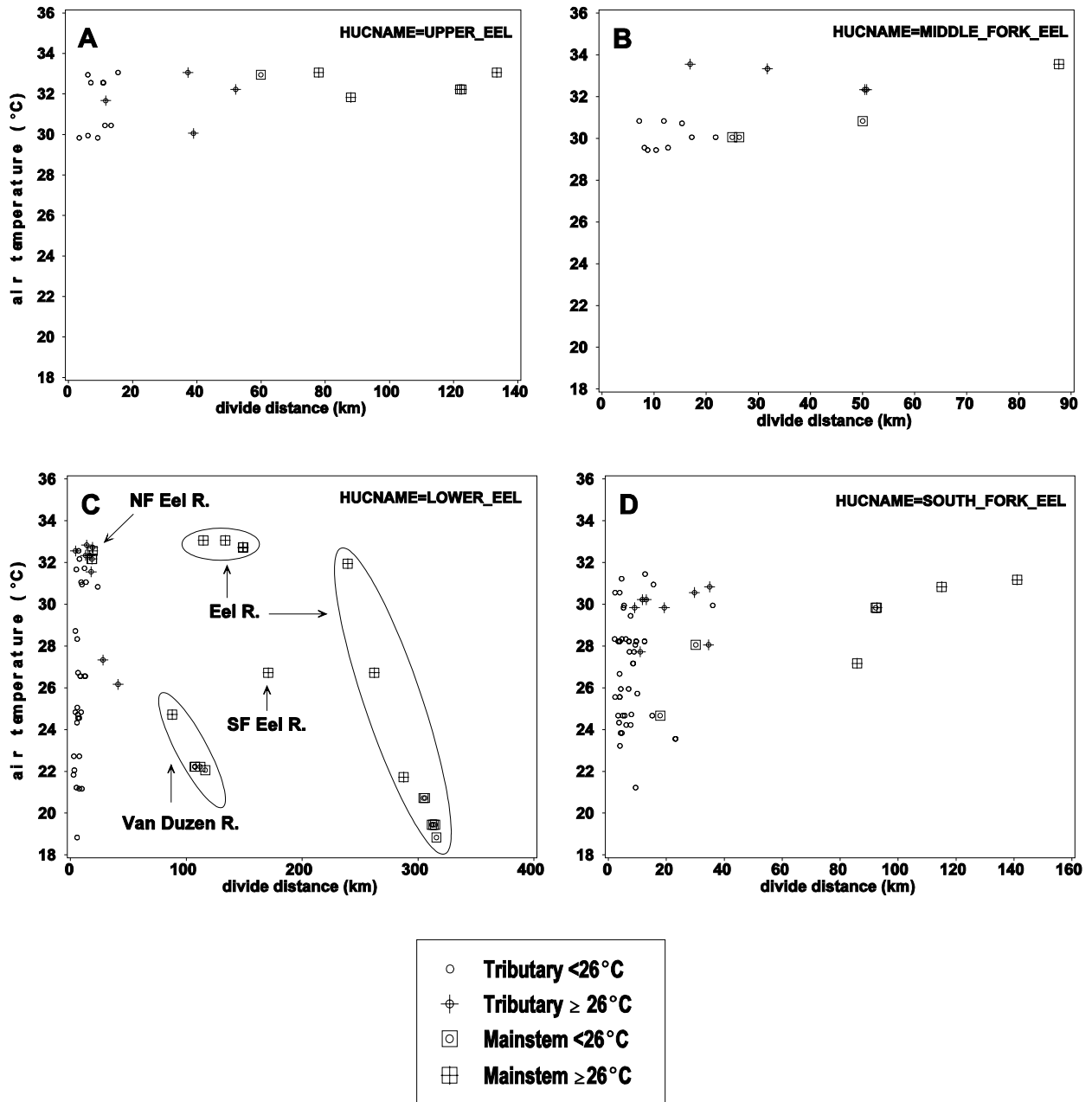


Figure 5.8. PRISM 30-year August average maximum air temperatures at each stream temperature monitoring site versus divide distance in Eel River HUCs. Open circles are tributary sites and squares are mainstem sites. Crosses indicate that the highest 1998 daily maximum stream temperature exceeded 26°C.

Water-Macroair Temperature Relationships and Canopy

Figure 5.9 presents a bar graph of the average W:A_RATIO by canopy class within each divide distance class. The graph illustrates that in the lowest canopy class (0 - 24%), the W:A_RATIO is closer to the 1:1 reference line in the lower divide distance classes (i.e., 1 and 2, representing 1 to 50 km) than at higher canopy class values. This trend suggests that in smaller headwater streams with little or no canopy, the water temperature may tend to exceed air temperatures more than in similar size streams with more developed canopy. The lack of sites at higher divide distances that had canopy values in the 50-74% and 75-100% classes indicates that streams may be becoming too wide for stream-side vegetation to provide adequate shading.

Air temperature is largely influenced by solar radiation (Miller and Thompson, 1975). The rate of heating and eventual maximum temperature is greater

in the sun than in the shade for both air and water (Essig, 1998). Plots of PRISM air temperature versus divide distance similar to those shown in Figure 5.8 were used to focus on the possible effects of canopy on stream temperature at different air temperature regimes. Stream temperature sites that were located at distances less than 50 km from the watershed divide in the four HUCs that comprise the Eel River basin are presented in Figure 5.10. Sites that exhibited highest 1998 daily maximum stream temperatures over 26°C were generally located in areas of warmest air temperatures. Sites with less than 50% canopy were most frequently those with stream temperature excursions above 26°C. Some sites with canopy greater than or equal to 50% exhibited XY1DX values greater than 26°C. These sites were located predominantly in areas of high air temperatures and at greater distances from the watershed divide.

The relationship between canopy and divide distance is explored in greater detail in Chapter 9.

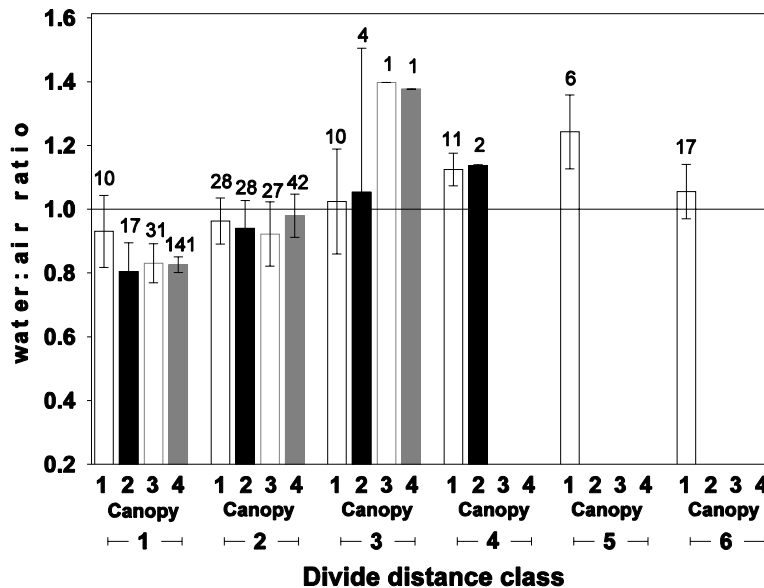


Figure 5.9. Change in water:air temperature ratio at four different canopy classes at six different divide distance classes. Based on the average of July and August monthly averages for 1998. Canopy classes: (1) 0-24%, (2) 25-49%, (3) = 50-74%, (4) = 75-100%. Divide distance classes: (1) 1 - 10 km, (2) 10 - 50 km, (3) 50 - 100 km, (4) 100 - 150 km, (5) 150 - 200 km, and (6) greater than 200 km. Error bars represent ± 1 standard deviations. Above each error bar is the number of sites in the class.

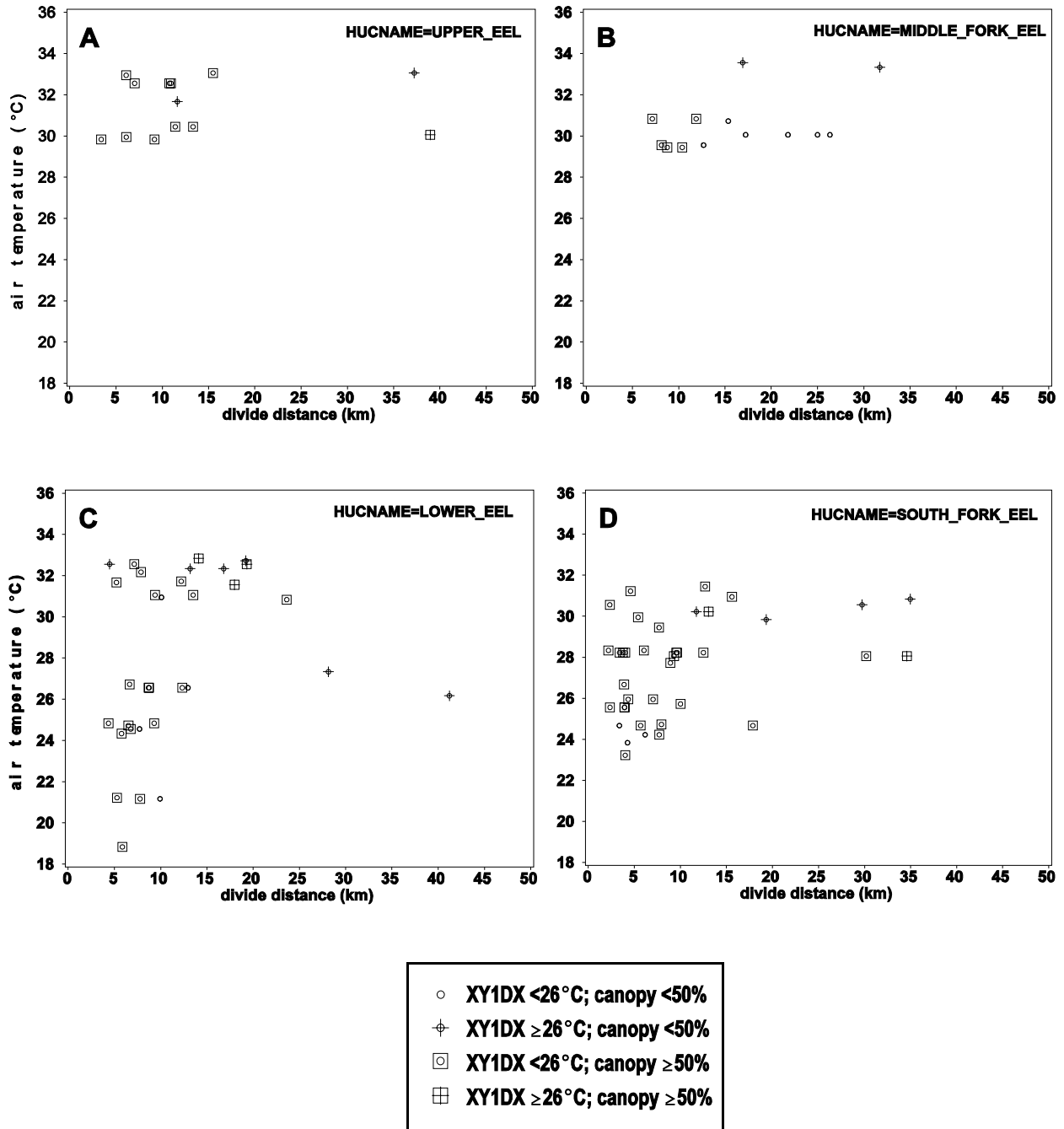


Figure 5.10. PRISM 30-year August average maximum air temperatures at stream temperature monitoring sites located less than 50 km from the watershed divide versus divide distance in Eel River HUCs. Open circles are stream temperature sites with highest 1998 daily maximum water temperature (XY1DX) less than 26°C and crosses are sites with XY1DX ≥26°C. Square indicates 1998 canopy ≥50%, no square indicates canopy <50%.

Water-Air Temperature Relationships and Flow

An important factor that we have not addressed is the influence of flow on the water-air relationship. In large systems the contribution of groundwater influx becomes proportionally less at increasing distances from the watershed divide. In fact, some systems may become losing streams (Kjelstrom, 1992; Donato, 1998). The water in these larger systems experiences exposure to atmospheric heating proportionate to its travel time from the source. As flow drops so does velocity, giving more time for water to approach thermal equilibrium with the overlying air (Essig, 1998). In many geographic locations larger systems at lower elevations will equilibrate with warmer air temperatures. In the case of Northern Coastal California, large systems have time to equilibrate with cooler maritime air temperatures. This was indeed the case in the Eel and Mad River systems (see Chapter 7).

Flow data were recorded at very few FSP stream temperature monitoring sites, fewer than air temperature measurements. In future updates to FSP's regional stream temperature assessment, it is hoped that more stream flow data will be available.

Water Temperature Versus Micro- and Macro-Air Temperature

Microclimate refers to the "layer of air from ground" or water level "to a height of two meters" (Geiger 1965, cited in Bartholow, 1989) and is represented by the microair temperature. Stream-side average air temperatures are, generally, less than ambient (remote) air temperatures, and large variability can be seen over relatively short distances (Troxler and Thackson, 1975). Many of the remote air sites in the present study were at lower elevations than the elevations at the water sites with which they were matched. Moreover, some of the air sites in our study were used for fire predictions and were located on south-facing slopes, which are warmer than other slope aspects. For regional-type assessments such as the current study, models developed from more readily available remote air temperature data proved

to be poor in predicting water temperatures.

This section demonstrates the value of measuring microair temperatures in predicting the variability in stream temperatures. Ten water temperature sites out of 1090 had both micro and macro air temperatures available at daily intervals. One site in the Eel Basin had two microair temperatures recorded at the location: one at 0.15 m and another at 2 m above the water. The microair at 0.15 m was used for analyses unless otherwise noted. Most sites were located in the central and more northern portions of the region-wide study area, and all sites were within 40 km of the coast. Microair temperature was collected in close proximity to the water temperature sensor, all within 600 meters of the stream temperature monitoring site. The macroair site was determined using the 12-dimensional Euclidian distance method as described in the section *Determining Nearest Remote Air Station* in this chapter. Comparisons were made using the daily mean, daily minimum, and daily maximum temperatures during the period between July 21 through August 19. Data regarding habitat and canopy were available for only a few sites, thereby precluding their use in exploring associations between air-water temperature relationships and site-specific attributes.

To characterize relationships between water and air temperatures, regression analyses were performed on daily mean, daily minimum, and daily maximum water temperatures in combination with micro- and macro-air temperatures for all sites combined and for each site separately. A summary of results are presented in Table 5.1.

The strongest overall correlation for all sites combined was between daily mean water and daily mean microair temperatures ($R^2 = 0.61$). Daily maximum water versus daily maximum microair temperature also had a moderate overall relationship ($R^2 = 0.59$). Although these are only moderate relationships, it indicates that the variables tended to respond in somewhat similar manners (i.e., to similar meteorological influences). Relationships between daily air and water minimum temperatures for all sites combined showed much variability. Daily

Table 5.1. Linear Regression Models for Water Temperature versus Microair and Macroair Temperatures.

Stream	Relationship	Mean			Minimum			Maximum		
		intercept	slope	R ²	intercept	slope	R ²	intercept	slope	R ²
All Sites	water vs. microair	6.02	0.67	0.61	9.91	0.34	0.22	8.27	0.46	0.49
	water vs. macroair	11.21	0.34	0.22	16.21	0.07	0.00	11.43	0.30	0.31
Hall Creek	water vs. microair	14.37	0.06	0.15	14.35	0.07	0.30	15.87	-0.03	0.05
	water vs. macroair	14.05	0.08	0.26	14.09	0.08	0.13	14.78	0.03	0.04
Redwood Creek	water vs. microair	13.05	0.39	0.76	12.52	0.47	0.75	16.40	0.25	0.69
	water vs. macroair	12.00	0.35	0.77	13.16	0.40	0.74	14.85	0.25	0.71
Redwood Creek	water vs. microair	15.07	0.33	0.64	16.68	0.25	0.28	17.90	0.23	0.59
	water vs. macroair	14.41	0.28	0.73	16.39	0.26	0.60	16.40	0.22	0.52
Minor Creek	water vs. microair	11.54	0.30	0.69	10.70	0.39	0.68	13.06	0.21	0.71
	water vs. macroair	11.49	0.23	0.71	12.68	0.25	0.62	12.15	0.18	0.70
Minor Creek	water vs. microair	11.76	0.31	0.74	11.41	0.37	0.83	15.17	0.17	0.55
	water vs. macroair	10.93	0.27	0.73	11.04	0.35	0.73	14.48	0.17	0.52
Eel River	water vs. microair	18.63	0.20	0.23	14.55	0.45	0.46	23.70	0.07	0.01
	water vs. macroair	16.03	0.34	0.43	19.44	0.20	0.14	19.12	0.20	0.05
Rattlesnake Creek	water vs. microair	12.95	0.39	0.72	11.31	0.48	0.73	16.97	0.29	0.64
	water vs. macroair	16.18	0.22	0.34	12.61	0.45	0.44	20.12	0.16	0.37
Cedar Creek	water vs. microair	12.75	0.22	0.59	14.17	0.09	0.06	14.61	0.16	0.47
	water vs. macroair	12.94	0.16	0.48	11.03	0.33	0.44	13.80	0.15	0.59
Rock Creek	water vs. microair	7.38	0.53	0.81	7.60	0.58	0.83	11.14	0.29	0.58
	water vs. macroair	12.04	0.19	0.38	8.62	0.52	0.66	14.15	0.10	0.30
Sprowl Creek	water vs. microair	10.89	0.39	0.71	12.70	0.33	0.39	13.01	0.25	0.66
	water vs. macroair	13.64	0.22	0.50	13.78	0.26	0.22	14.85	0.16	0.64

minimum water temperature had a somewhat weak relationship to daily minimum microair temperatures ($R^2 = 0.22$), while the relationship between daily minimum water and daily minimum macroair temperatures was not significant.

Comparing R^2 values from Table 5.1 for individual sites gives a somewhat different impression than the all-sites-combined regressions. For instance, as previously noted, the combined-site relationship between daily mean water and microair temperatures was relatively weak. However, the strongest individual site relationships were seen with daily minimum water temperatures versus daily minimum microair temperatures for Minor Creek and Rock Creek ($R^2 = 0.83$).

Some general observations can be made. Daily mean water temperatures were better estimated than daily minimum or maximum water temperatures using microair data. At some sites, little difference was observed between R^2 for correlations between daily means of water-macroair versus water-microair.

Proximity of the remote air site to the stream-side air site did not seem to account for the degree of similarity in R^2 values. If daily extremes in water temperature are of interest, then microair stations should be used.

Variability in the relationship between water temperature and microair temperatures can be illustrated by using hourly data for two sites located in the Eel Basin (Figure 5.11). The first site was located on Rattlesnake Creek approximately 18.6 km from the coast (left graph). The second site was located on the Eel River near Nashmead Bar approximately 35.9 km from the coast (right graph). Water temperature regimes were similar for both sites during the period of study. The Rattlesnake Creek and Eel River sites had average water temperatures of 20.8°C and 23.5°C, respectively. For both sites, the mean water temperature was within 0.6°C of the mean microair temperature for the study period. The diurnal fluctuation in microair temperature at the Eel River site was much greater than at the Rattlesnake Creek site. However, the diurnal water temperature

FSP Regional Stream Temperature Assessment Report

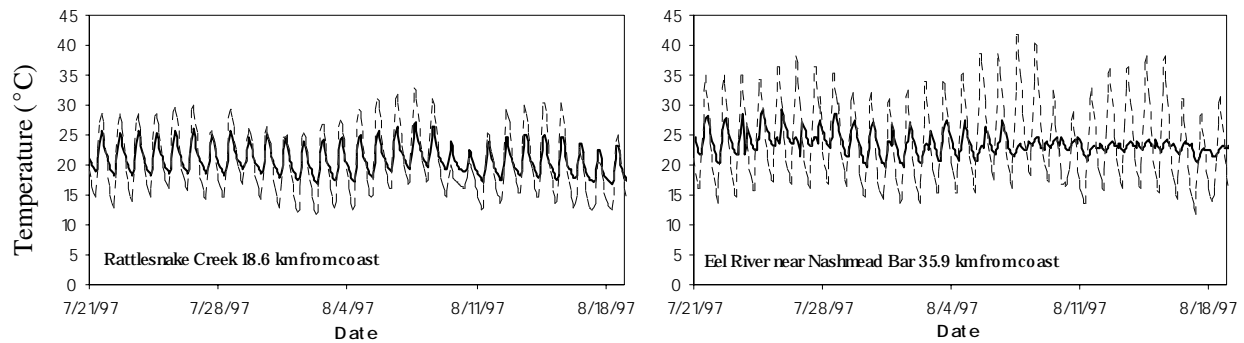


Figure 5.11. Hourly water and micro air temperatures for (A) Rattlesnake Creek and (B) the mainstem Eel River near Nashmead Bar in the Eel River Basin, for period of 21 July to 19 August 1997. Solid line is water temperature and dashed line is air temperature.

fluctuation in the mainstem Eel River was of an amplitude similar to the tributary site. This trend exemplifies the concept of thermal inertia of large mainstem systems. It should also be noted that the daily minimum air temperatures on the days when the highest daily maximum water temperatures occurred were near a commonly used MWAT threshold (i.e., 16.8°C). Essig (1998) reported that at some locations in Idaho water warms to above state temperature standards even without exposure to direct or indirect solar radiation. Daily minimum air temperatures at some sites are so warm that stream heating can occur throughout the evening. He reported that in some regions of Idaho July minimum air temperature, ~15°C, exceeds Idaho's salmonid spawning instantaneous maximum temperature (13°C).

Figure 5.11 helps to illustrate the value of having hourly observations to examine aspects of the air-water temperature relationship that are not readily apparent by looking at summary temperature metrics, such as daily mean and range or monthly averages. Unfortunately, hourly observations were not available for the macroair temperature data. Graphs

of daily minimum, mean, and maximum water, microair, and macroair are presented in Appendix C for each of the 10 sites discussed above.

Distance Above Water Surface

At the Rock Creek site, two microair data sets were available, one collected at 0.15 m above the stream and the other at 2 m. Visual inspection of plots in Figure 5.12 shows that mean and maximum microair temperatures collected at 2 m above the water surface were consistently warmer than the microair temperature at 0.15 m, and minimum temperatures were consistently cooler. The 2-m microair trends more closely followed the macroair trends (Table 5.2). The 0.15-m microair trends more closely followed the water temperature trends (compare R^2 values for mean temperatures). This indicates that water is having a moderating influence on microair temperatures, the influence increasing with decreasing distance from the water surface. The effects of evaporative cooling are more apparent with decreasing distance above the water surface.

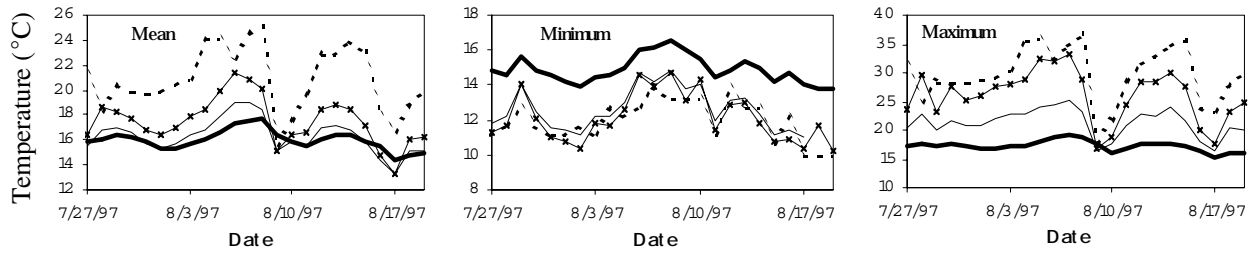


Figure 5.12. Daily mean (left), minimum (middle), and maximum (right) temperatures for water and microair sites located on Rock Creek, a tributary of the South Fork Eel River, and a macroair station located 17 km north. This site had two microair temperatures recorded at 0.15 m and 2 m above the water surface. Bold solid line = water temperature, dashed line = macroair, thin solid line = microair at 0.15 m, solid line with 'x' = microair at 2 m.

Table 5.2. Linear Regression Models Comparing Microair Temperatures Measured at 0.15 m and 2 m above the Water Surface to Water Temperature and Macroair Temperatures for a Site on Rock Creek.

Relationship	Mean			Minimum			Maximum		
	intercept	slope	R ²	intercept	slope	R ²	intercept	slope	R ²
water vs. micro air (0.15 m)	7.38	0.53	0.81	7.60	0.58	0.83	11.14	0.29	0.58
water vs. micro air (2 m)	9.78	0.36	0.71	8.83	0.50	0.82	13.28	0.15	0.54
micro air (0.15 m) vs. macro air	8.15	0.39	0.55	3.08	0.79	0.61	8.84	0.42	0.70
micro air (2 m) vs. macro air	5.57	0.57	0.62	1.27	0.91	0.61	3.93	0.74	0.67
micro air (0.15 m) vs. micro air (2 m)	3.84	0.71	0.97	2.14	0.86	0.99	7.16	0.54	0.98

Year-to-Year Variability in Water-Air Relationships

Stream temperature data from 154 sites were available that spanned three consecutive years (1996-1998). The data set was explored to determine whether year-to-year differences in air temperature had a noticeable effect on water temperatures in each year. Figure 5.13 shows the geographic distribution of the 154 sites.

Combined July-August average macroair temperatures were estimated at each of the 154 water temperature sites using the 12-dimensional Euclidian model. Figures 5.14-A and 5.14-B show that 1996 had the highest monthly maximum and the lowest monthly minimum average air temperature. Only 15 macroair temperature sites were matched with the 154 water temperature sites. Figure 5.5 illustrates the large source of variability introduced into the analyses by having a limited number of macroair stations available to match up with a multitude of water temperature sites.

FSP Regional Stream Temperature Assessment Report



Figure 5.13. Geographic distribution of 154 sites where stream temperature was monitored across three consecutive years, 1996 through 1998. Sites had uninterrupted data for the time period between July 21 and August 19.

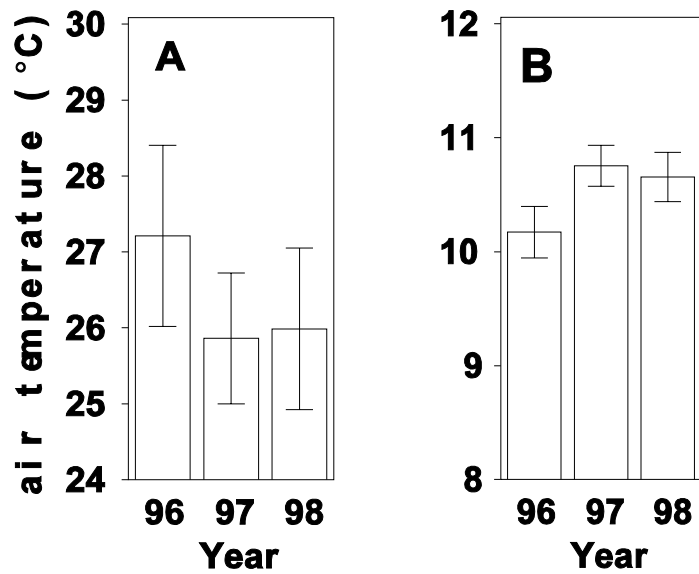


Figure 5.14. Average July-August monthly maximum (A) and minimum (B) macroair temperature associated with 154 stream temperature sites over three consecutive years (1996-1998). Error bars represent ± 2 standard deviations.

CDF graphs were produced for four stream temperature metrics. The cumulative distributions for XY1DX, XYA7DA, and XYA7DX were very similar for all three years (Figure 5.15-A through C). Inset bar graphs indicate that 1997 was a few tenths of a degree Celsius higher for average values of XY1DX, XYA7DA, and XYA7DX. These differences would be of little or no biological significance. There was a noticeable difference in the distribution of IY1DI values, with 1996 having lower daily minimum temperatures than either 1997 or 1998 (Figure 5.15-D). The inset bar graph in Figure 5.15-D also illustrates a lower daily minimum temperature in 1996.

While average air temperatures were generally warmer in 1996 based on macroair temperatures at 15 remote sites, stream temperature metrics dealing with daytime temperatures showed only slight differences across years. The 1996 July-August monthly minimum air temperature was significantly lower than 1997 and 1998, suggesting that 1996 may have had more cloud-free days. Fewer cloudy days would result in higher daytime air temperatures and lower nighttime temperatures. Minimum water temperature seems to be more sensitive to year-to-year changes in minimum air temperature. The discrepancy between the year showing the highest air temperature (1996) and the year showing the highest water temperature suggests that the 15 remote air temperature sites may not be representative of conditions at the stream site. Using only a small number of remote air temperature sites, caution should be exercised when making broad generalizations about climatic conditions from one year to the next to explain trends in stream temperatures.

The total hours spent above 26°C was calculated for each site sampled over three consecutive years. Because of the strict temporal window imposed on the data, that is each site having complete uninterrupted data for the time period between July 21 and August 19, each site had equal total time. Thus, direct comparisons can be made between sites and between years of the total hours above 26°C, because all sites had equal total hours in their data sets. Figure 5.16 presents a CDF graph of the proportion of sites that spent less than x hours above

26°C. It is of interest to note that the y-axis begins at 0.8 at the x-axis zero origin. This means that 80% of the sites did not have any hours above 26°C. At an arbitrary reference value of 50 hours, between 88% and 91% of the sites had less than 50 hours over 26°C. This represents a difference of roughly 3% of the sites in the three-year period, which is about 4 or 5 sites. Essentially, there appears to be only a slight difference in the total hours spent above 26°C across the three years.

Using a threshold of 26°C may limit the ability to discern differences between years by focusing on sites that routinely exhibit high temperatures. The same cumulative distribution for sites that had less than x hours above 18°C was examined to see if there was a more discernable difference between years. The sum degrees over 18°C was also examined. Figure 5.17 shows that even at this lower threshold, very similar CDF curves were observed. See Chapter 7 for a more detailed discussion of the derivation of the sum degree temperature metric.

The similarity in stream temperatures at 154 sites monitored over three consecutive years is striking. At least at the 154 sites examined here, it appears that stream temperatures show very little year-to-year variability. This constancy has also been noted for streams in Idaho (Essig, 1998) and select streams throughout the United States (Vannote and Sweeney, 1980). With a large enough data set one could conceivably predict future stream temperatures from historical trends, and using a similar CDF approach, detect departures from expected temperatures regimes. Differences could be due to much larger changes in air temperatures, larger than those observed in the 1996-1998 period examined here. Changes may also be detectable as riparian vegetation develops as the result of natural regeneration or restoration efforts. Conversely, changes in the CDF curve for a watershed or sub-basin may be detected due to cumulative effects of channel aggradation from flooding, or watershed- or basin-wide cumulative effects from timber harvest, agriculture, urbanization, or all of the above.

FSP Regional Stream Temperature Assessment Report

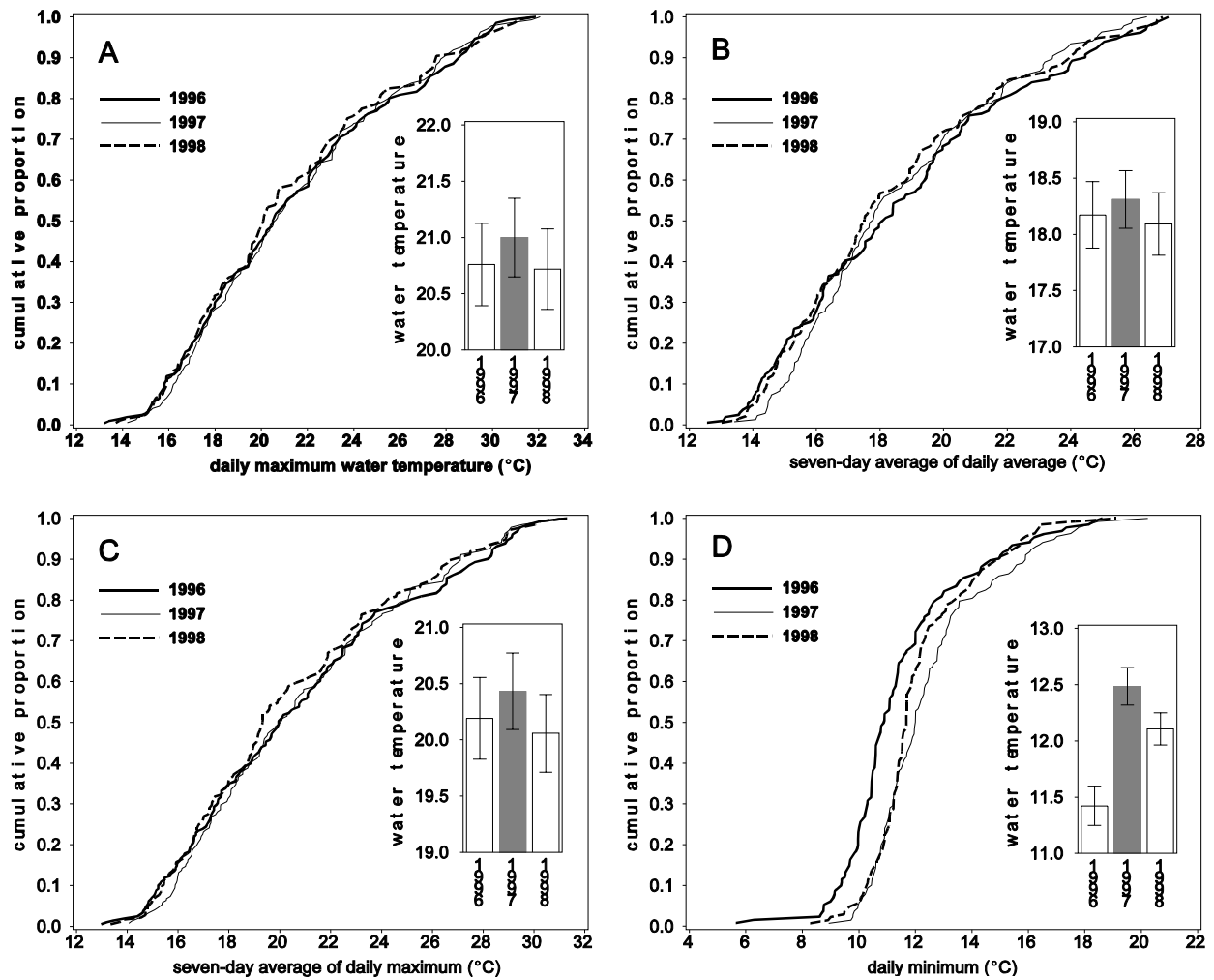


Figure 5.15. Cumulative distributions of temperature metrics (A) highest daily maximum (XY1DX), (B) highest seven-day moving average of the daily average (XYA7DA), (C) highest seven-day moving average of the daily maximum (XYA7DX), and (D) lowest daily minimum (IY1DI) for 154 sites that had stream temperatures measured during three consecutive years (1996 through 1998) and having continuous observations between July 21 and August 19. Inset bar graphs show the average stream temperature metrics for each year with ± 2 standard deviation error bars.

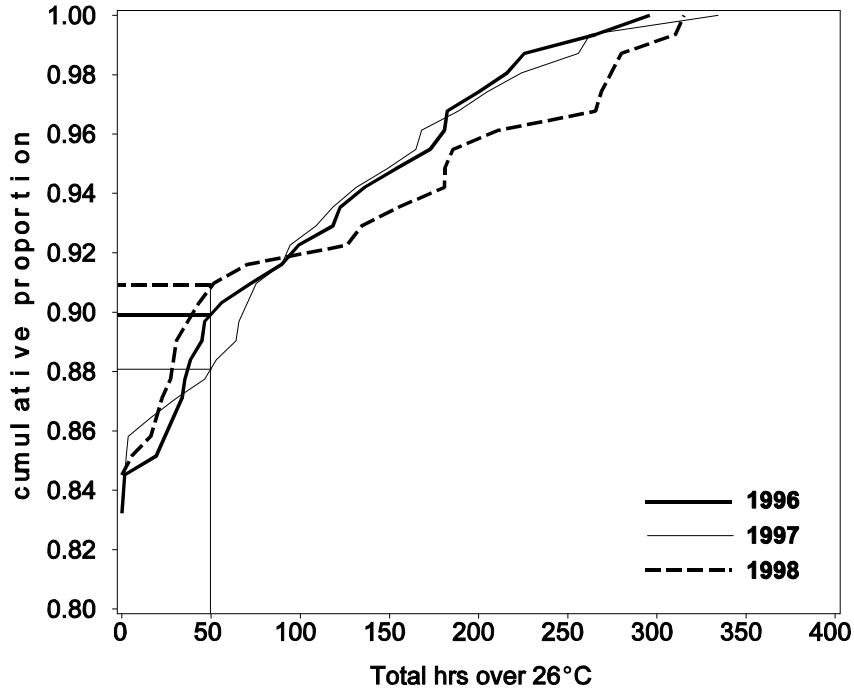


Figure 5.16. Cumulative distribution of proportion of sites that had less than x total hours over 26°C water temperature. Distribution based 154 sites that had stream temperatures measured during three consecutive years (1996 through 1998) and had continuous observations between July 21 and August 19.

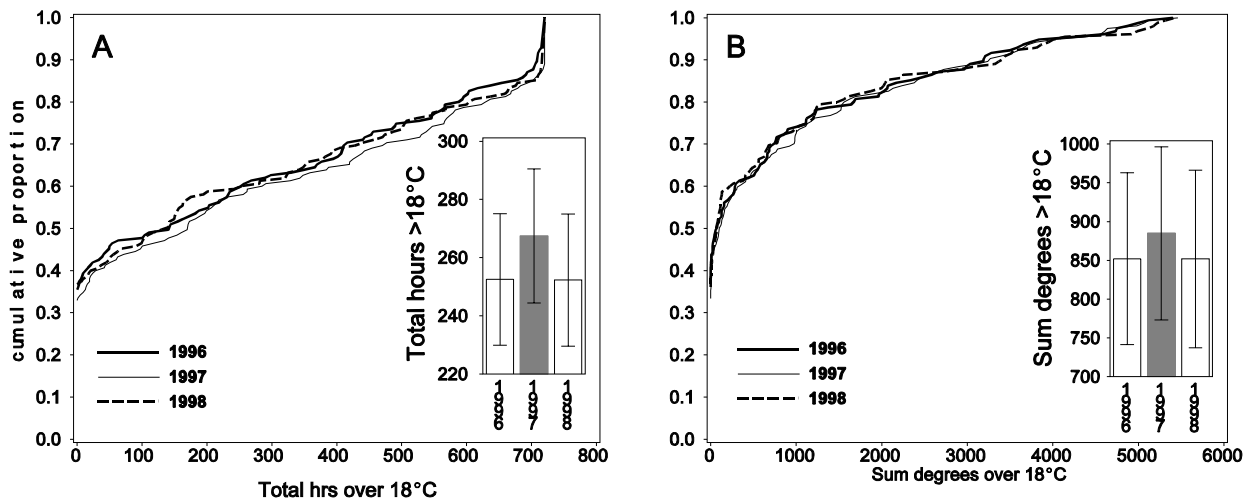


Figure 5.17. Cumulative distribution of proportion of sites that had (A) less than x total hours over 18°C water temperature and (B) less than x cumulative degrees over 18°C. Distribution based 154 sites that had stream temperatures measured during three consecutive years (1996 through 1998) and had continuous observations between July 21 and August 19. Inset bar graphs show the average stream temperature metrics for each year with ± 2 standard deviation error bars.

FSP Regional Stream Temperature Assessment Report

Temporal predictability is a very important aspect of a streams's thermal regime. Aquatic biota have developed a dependency on the temporal predictability of running waters (Vannote and Sweeney, 1980).

Larger streams respond to air temperature changes to a greater extent than smaller streams (Sullivan et al., 1990; Bartholow, 1989). To corroborate this finding the monthly average maximum water temperature (July and August combined) was calculated for sites at each divide distance class. The associated monthly average maximum air temperature (July and August combined) at each divide distance was also calculated from the nearest 12-dimensional Euclidian air site. Average monthly water and air temperatures were plotted versus divide distance class for each year (Figure 5.18). The warmest year for the 154

sites combined was 1996, followed by 1998, and 1997 being cooler. At divide distances up to approximately 100 km, average monthly maximum stream temperatures showed a nearly identical rate of increase. Air temperatures in 1996 were about 3°C higher than 1997 or 1998. However, the effects of higher 1996 air temperatures on stream temperatures did not manifest themselves until water arrived at sites located over 100 km from the watershed divide. The number of sites in the higher divide distance classes was smaller than in the 1 to 3 classes. However, the trend supports the concept that as stream systems become large, air temperature has more of an influence on water temperature than other site-specific attributes. The mainstem sites at higher distances from the watershed divide account for the slight differences in CDFs observed across the three years shown in Figures 5.15 - 5.17.

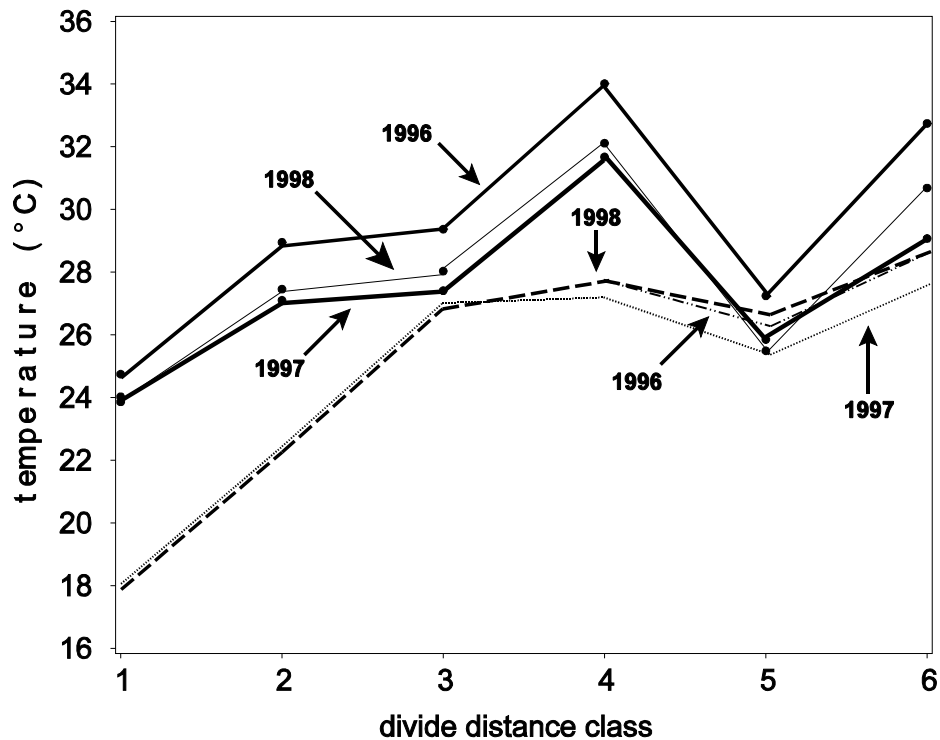


Figure 5.18. Change in monthly average maximum water (broken lines) and air temperatures (solid lines) at six different divide distance classes at 154 sites monitored in 1996, 1997, and 1998. Divide distance classes: (1) 1 - 10 km, (2) 10 - 50 km, (3) 50 - 100 km, (4) 100 - 150 km, (5) 150 - 200 km, and (6) greater than 200 km.

Summary

The success of describing air-water relationships may be somewhat dependent on the region being studied. Greater success in predicting water from air temperatures may be experienced in regions with relatively small air temperature gradients within the study area as opposed to regions with abrupt changes. As presented in Chapter 4, areal air temperature patterns observed in Northern California often exhibit large temperature gradients within relatively short distances (see Chapter 4, Figure 4.10 and 4.11). Air temperatures obtained from 12-dimensional Euclidian distance air stations were found to show some correlation with water temperatures at a regional scale. August monthly macroair versus microair temperature comparisons revealed that remote sites may not be very representative of stream-side air temperatures.

Monthly mean water temperatures in the SSP seemed to vary more closely with monthly mean macroair temperatures than water temperatures in the CSP.

The water-to-macroair temperature ratio increased with increasing distance from the watershed divide. The divide distance at which the ratio began to exceed unity varied by HUC, but generally fell between 6 km and 10 km. HUCs with tributaries that originate in the warm interior portions of the study area and drain into the zone of coastal influence exhibited greater numbers of sites with water-to-air ratios greater than one. HUCs that lie entirely within the interior portion of the study area exhibited fewer sites with water-to-air temperature ratios exceeding one. Water-to-air ratios can exceed one because water temperatures have increased, air temperatures have decreased, or both. Given the fact that water temperatures normally tend to increase in a longitudinal downstream direction and that air temperatures decrease in the zone of coastal influence, in coastal HUCs of Northern Coastal California the exceedance of one in water-to-air ratio is most likely due the simultaneous increase in water temperature and decrease in air temperature in the downstream direction.

Microair temperatures generally showed greater correlations with water temperature than remote macroair temperatures, and correlations were greatest for daily maximum and daily minimum water temperatures. Moore (1967) noted that air temperature affects water temperature through the advection of heat from air to water or vice versa, but not to the degree that might seem to be indicated by the correlation between the two. The close correlation is caused largely by the fact that solar radiation affects both water and air temperature. Some sites in the present study showed little difference between microair and macroair relationships with water temperature. Local environmental conditions probably play a role in the similarities in micro- and macro-air temperatures and water temperatures at some sites. To model water temperatures at hourly, daily, or weekly time steps, the data suggests that microair temperature data are needed.

At a subset of sites where stream temperature was monitored for three consecutive years, very small year-to-year variability was observed. While 15 macroair temperature sites associated with 154 water site indicated that 1996 was relatively warmer than 1997 or 1998, stream temperatures showed very little difference in any of the daytime temperature metrics examined. The 1996 daily minimum stream temperature was lower than 1997 or 1998. July-August monthly average minimum macroair temperatures were also significantly lower than the subsequent two years. Lower nighttime and higher daytime temperatures in 1996 suggest that there may have been more cloud-free days. Cumulative distributions of the total hours spent above 26°C indicated that about 80% of the sites did not exceed this threshold in any of the three years. In a comparison of air and stream temperatures at increasing distances from the watershed divide, larger systems seemed to respond more to year-to-year variations in air temperature than smaller systems. This agrees with other research findings from other geographic areas (Bartholow, 1989; Sullivan et al., 1990).

The discrepancy between the year showing the highest air temperature (1996) and the year showing the highest water temperature suggests that the 15

FSP Regional Stream Temperature Assessment Report

remote air temperature sites may not be representative of conditions at the stream site. Caution should be exercised when making broad

generalizations about climatic conditions from one year to the next to explain trends in stream temperatures.

Chapter 6

GEOGRAPHIC POSITION AND STREAM TEMPERATURES

Introduction

California's climate and ecosystems are varied. Within the state's borders lie glaciers and deserts. The state spans ten degrees of latitude from 42°N at its border with Oregon to 32°N at its border with Mexico. Landsberg (1958) reported that average annual air temperature decreases about 0.8°C (1.5°C) for each degree increase in latitude in the middle latitudes (40° to 50°N). Within the study area of the present assessment, i.e., the California portion of the Southern Oregon Northern Coastal California and the Central California evolutionarily significant units, about five degrees of latitude are covered, from 42°N at the Oregon-California border to about 37°N near San Francisco, CA.

This chapter examines the influence of broad-scale geographic position on stream temperatures. These factors include distance from the coast, ecoprovince, zone of coastal influence, north-south distribution (latitude), and elevation. Do local site factors completely control water temperatures or can some regional scale patterns be observed? The environmental variable that exerts its influence across all of these geographic factors is predominantly air temperature. Similar patterns that were observed for air temperature variability across the region are expected to be seen for variability in water temperature. However, local site-specific factors also influence water temperature, such as canopy, flow, gradient, and topographic shading. These other factors will confound the response of water temperatures to purely geographic phenomena.

Four different stream temperature metrics were explored for their variation with geographic position. The highest daily maximum (XY1DX) for the year, the highest seven-day moving average of both the daily average (XYA7DA) and maximum (XYA7DX) for the year, and the lowest daily minimum for the year were examined for 520 sites monitored in 1998. These sites had uninterrupted data for the time period July 21 to August 19, 1998.

We found that some trends in stream temperature are discernable at broad regional scales. However, given the large variability in the relationships, site-specific factors appear to play an important role. Geographic position may serve as a surrogate for macroair temperature in any given year. However, by using geographic position as a surrogate for air temperature, one loses the ability to explain year-to-year changes in water temperature that may be due to changes in air temperature.

Distance from Coast and Stream Temperatures

The distance from the coast was calculated for each site using a GIS. This distance was calculated as the nearest direct line from the stream temperature monitoring site to the coast. Figure 6.1-A shows the number of sites in each 10-km coast-distance class. The distribution revealed that a larger proportion of sites were near the coast, with 80% of the sites being within 40 km of the coast. The SONCC ESU has a maximum distance from the coast of 165 km and a

FSP Regional Stream Temperature Assessment Report

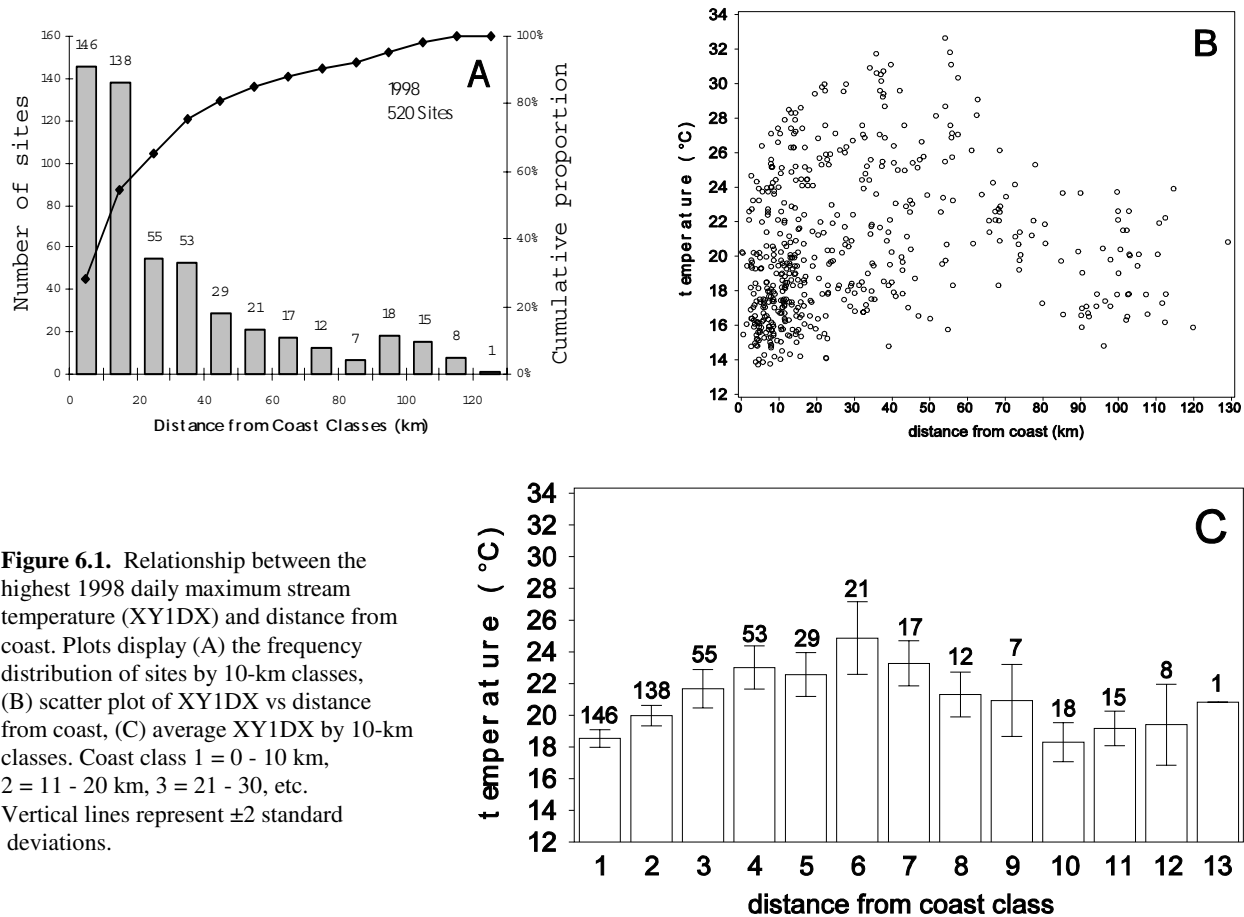


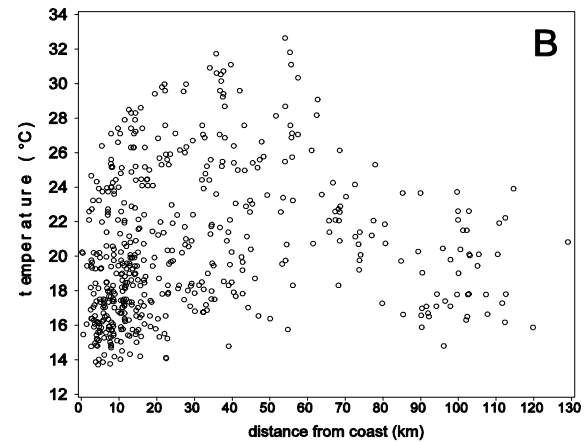
Figure 6.1. Relationship between the highest 1998 daily maximum stream temperature (XY1DX) and distance from coast. Plots display (A) the frequency distribution of sites by 10-km classes, (B) scatter plot of XY1DX vs distance from coast, (C) average XY1DX by 10-km classes. Coast class 1 = 0 - 10 km, 2 = 11 - 20 km, 3 = 21 - 30, etc. Vertical lines represent ± 2 standard deviations.

minimum of 52 km. The Central California ESU has a maximum coast distance of 56 km and a minimum of 0.4 km.

Daily Maximum and Distance from the Coast

Figure 6.1-B is a scatter plot of the highest daily maximum temperature versus distance from the coast.

There is considerable scatter in the data. However, there appears to be an increasing trend in XY1DX values up to about 50 to 60 km from the coast and then a decreasing trend as distance from the coast continues to increase. Although the trend is not as clearly defined as that observed for air temperature (see Figure 4.2), a weak trend is apparent in the data. The trend becomes more apparent when XY1DX



values are grouped by coast-distance classes of 10-km increments (Figure 6.1-C). The highest class average for XY1DX was in class 6, that is 50 to 60 km from the coast.

Figure 6.1 includes stream temperature measured at all sites in 1998 that had continuous data between July 21 and August 19. These sites included tributaries and mainstem rivers. Mainstem rivers that drain to the coast and large inland rivers (e.g., Klamath River) may have influenced the observed trend in XY1DX with coast distance. Without bankfull width or stream order to group streams together, it is difficult to compare streams of similar size. Watershed area was used as a surrogate to group streams of similar size.

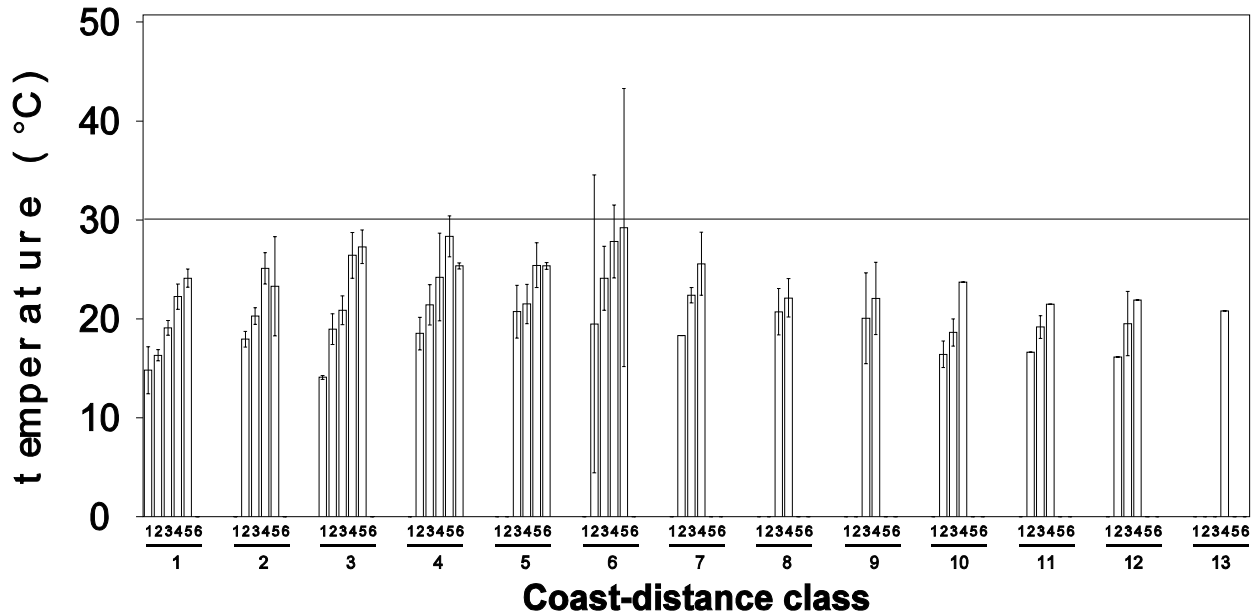


Figure 6.2. Variation in the highest 1998 daily maximum stream temperature (XY1DX) by watershed area (1-6) and coast distance class (1-13). Watershed area classes: 1 = 0 - 100 ha, 2 = 101 - 1000 ha, 3 = 1001 - 10,000 ha, 4 = 10,001 - 100,000 ha, 5 = 100,001 - 1,000,000 ha, 6 = >1,000,000 ha. Coast-distance classes: 1 = 0 - 10 km, 2 = 11 - 20 km, 3 = 21 - 30, etc. Horizontal reference line drawn at 30°C for visual comparison across classes.

Figure 6.2 (above) shows the change in 1998 XY1DX values with watershed area at different coast-distance classes. Two sites dropped out of the analyses because they lacked watershed area values. The average XY1DX values in the same coast-distance classes were greater in larger watershed area classes. This supports other documented studies that reported an increase in stream temperature with increasing watershed area and distance from the watershed divide (Allan, 1995; Sullivan et al., 1990). The greatest increase in XY1DX with watershed area was observed in coast-distance class 3 (i.e., 21 - 30 km from the coast). In coast-distance class 3, the cooling influence of ocean currents on air temperature is waning, but also elevation is increasing. See Chapter 4 for a discussion on the variation in air temperature with distance from the coast and elevation. Streams in coast-distance class 3 may be at the transition between being inside and outside of the zone of coastal influence. The relationship between stream temperature and

watershed position is explored in greater depth in Chapter 7.

The distribution of the highest 1998 seven-day moving average of the daily average (XYA7DA) and highest seven-day moving average of the daily maximum (XYA7DX) showed similar patterns.

Daily Minimum Temperature and Distance from Coast

The distribution of the lowest 1998 daily minimum (IY1DI) measured at each site was plotted against coast distance (Figure 6.3). There was clearly a decrease in IY1DI values at greater distances from the coast. The moderating influence of coastal air temperatures on water temperatures can account for the higher IY1DI values nearer to the coast. Proximity to the coast has a moderating effect on extremes in stream temperature, i.e., both lower daily maxima and higher daily minima.

FSP Regional Stream Temperature Assessment Report

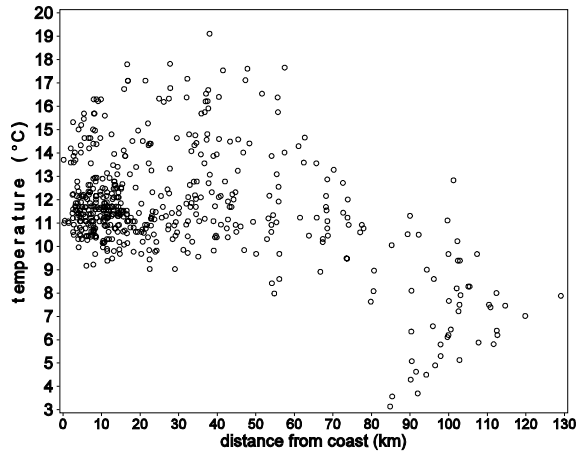


Figure 6.3. Variation in lowest 1998 daily minimum stream temperature (IY1DI) as a function of distance from coast.

UTM X-Coordinate (Longitude) and Stream Temperatures

UTM x-coordinate (a surrogate for longitude or easting) serves as a crude surrogate for distance from coast. Longitude does not follow the curves in the coastline. Therefore, it would be less precise and redundant to examine the variation in stream temperature with x-coordinate. There appears to be a west-to-east trend in water temperature based on the above distance-from-coast analyses. We suspect that this trend is largely a function of air temperature. However, there is considerably more scatter in water temperatures with coast distance than was observed with air temperatures. Obviously, there are more factors influencing water temperatures than simply macro-scale air temperatures. Local channel and riparian conditions and micro-scale air temperatures also play a role in the observed scatter seen in the data.

Ecoprovincial Stream Temperatures and Distance from the Coast

The data were stratified by ecoprovince and the relationship between the four temperature metrics and coast distance were examined. The three metrics

show a general increase with increasing distance from the coast in the CSP and a decrease with increasing distance from the coast in the SSP (Figure 6.4). The series of graphs in Figure 6.4 reveals that there is overlap between the two ecoprovinces between ~15 km and 55 km from the coast. The CSP extends inland up to about 55 km in some locations, and the SSP comes within about 20 km of the coast in some locations.

UTM Y-Coordinate (Latitude) and Stream Temperatures

It is generally believed that air temperature increases in a north-to-south direction. This large scale geographic phenomenon operates at a global scale, and may manifest itself more regionally as a north-to-south stream temperature pattern within the range of the coho salmon in Northern California.

The distribution of sites with respect to UTM y-coordinate classes is shown in Figure 6.5-A. The majority of sites (438) were located between UTM y-coordinates 4,300,000 and 4,600,000 (43 and 46 in Figure 6.5-A). A UTM y-coordinate of 4,300,000 equates with a latitude of approximately 37°N and a UTM y-coordinate of 4,600,000 equates with a latitude of approximately 42°N.

The four previous temperature metrics (XY1DX, XYA7DA, XYA7DX, and IY1DI) were evaluated for possible dependency on the UTM y-coordinate value, explained above as a surrogate for latitude. Figure 6.5-B shows the change in XY1DX values with UTM y-coordinate. Y-coordinate values increase in a northerly direction. A left-to-right unit change on the graph (e.g., 42 to 43) represents a change of 100 km northward. For reference in Figure 6.5-B, the Oregon-California border is at about 46.5 and San Francisco is near 41. The distribution of XY1DX values is quite scattered. However, there does appear to be a greater number of sites with higher XY1DX values at more southerly locations. A similar pattern was observed for XYA7DA and XYA7DX (graphs not shown). In the more interior ecoprovince (SSP), the decrease in stream temperature with increasing latitude appears more

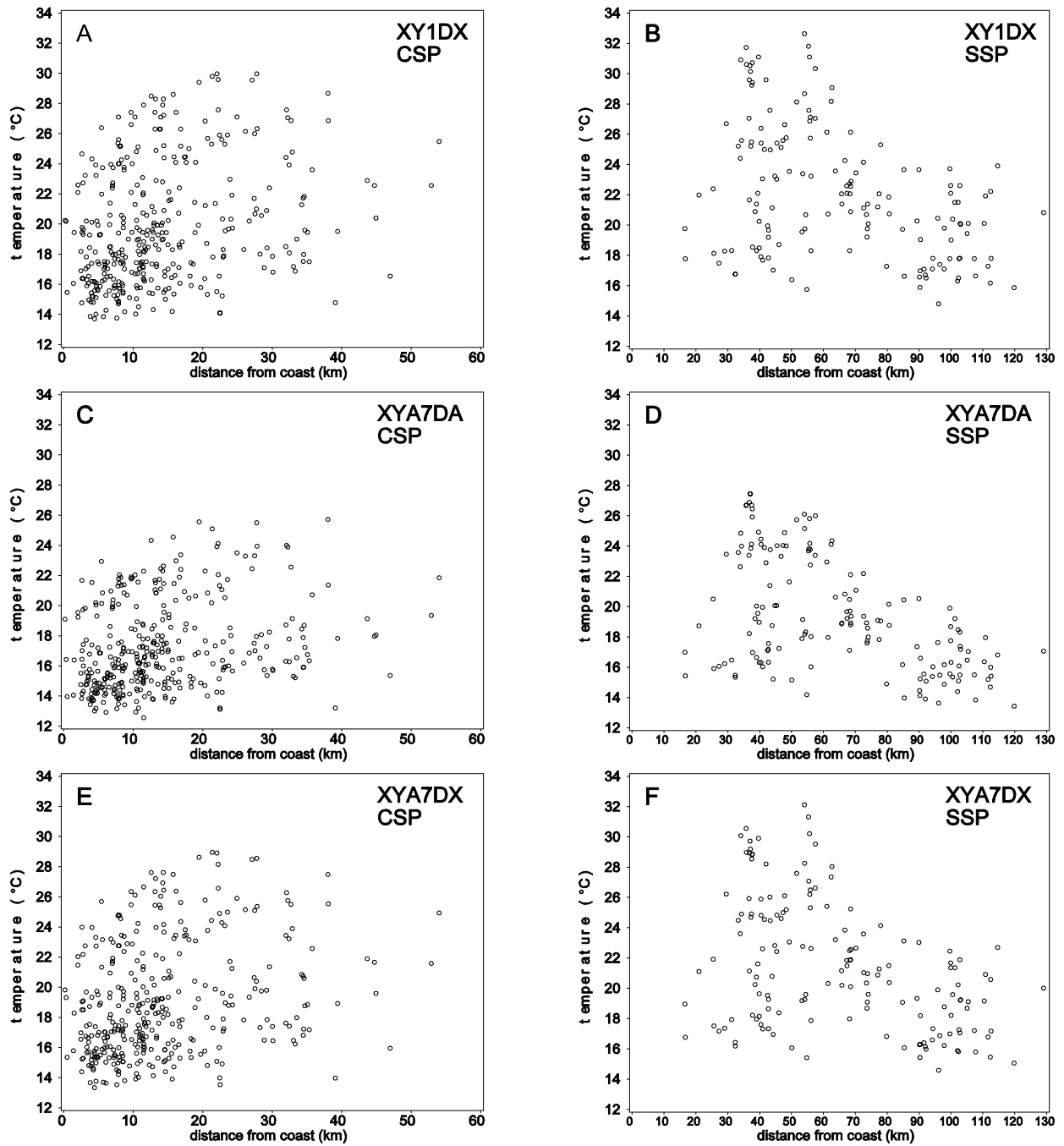


Figure 6.4. Comparison of 1998 temperature metrics versus distance from coast by ecoprovince. (A) XY1DX - CSP, (B) XY1DX - SSP, (C) XYA7DA - CSP, (D) XYA7DA - SSP, (E) XYA7DX - CSP, and (F) XYA7DX - SSP.

FSP Regional Stream Temperature Assessment Report

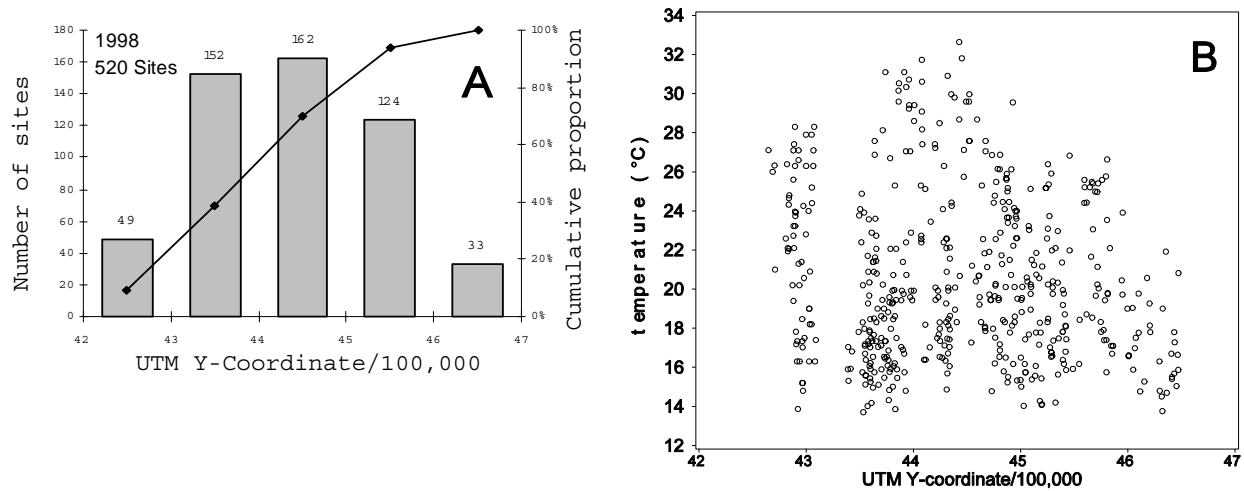


Figure 6.5. Variation in 1998 XY1DX values with Y-coordinate. (A) Frequency distribution of number of sites by UTM Y-coordinate class. (B) Scatterplot of XY1DX versus UTM Y-coordinate. Left-to-right on the graph is a south-to-north direction. X-axis values are UTM Y-coordinates divided by 100,000. San Francisco, CA is at approximately 41 and the Oregon-California border is at approximately 46.5.

defined, whereas the coastal ecoprovince (CSP) displays considerable scatter (Figure 6.6). The CSP ranges from 0 km from the coast to ~55 km inland while the SSP ranges from ~20 km to nearly 130 km inland.

Using the same coast distance classes as presented in Figure 6.1-C, the variation in XY1DX values with Y-coordinate was examined. This analysis essentially aggregates temperature sites into 13 north-south transects paralleling the coast, each transect being 10 km in width. The variation in XY1DX along each transect in a south-to-north direction by UTM y-coordinate classes is presented in Figure 6.7. Not all y-coordinate classes were represented, therefore south-to-north trends were not well defined. However, there does appear to be a general decreasing trend in XY1DX from y-coordinate classes 1 to 5. Whether there is more of a south-to-north cooling trend along the coast than inland cannot be determined from the data due to an under representation of sites in coast-distance classes in each of the five y-coordinate groupings.

Zone of Coastal Influence and Stream Temperatures

Using 30-yr long-term average PRISM air temperature data the ZCI was determined by calculating the steepest rate of change in air temperature for August. August is the month when the majority of highest XY1DX, XYA7DA, and XYA7DX values occur for most sites throughout the range of coho salmon in Northern California. The ZCI is our best approximation of the inland extent of the *fog zone*. See Chapter 4 for a more detailed explanation of how the ZCI was developed.

Figure 6.8-A shows the average XY1DX class values for sites combined (518) with ZCI values of zero or one. Sites with ZCI = 0 were outside the approximated zone of coastal influence and those with ZCI = 1 were considered inside the ZCI. The average XY1DX value for the ZCI = 0 group was 21.7°C and 18.7°C for the ZCI = 1 group. The two groups were significantly different ($p < 0.0001$)

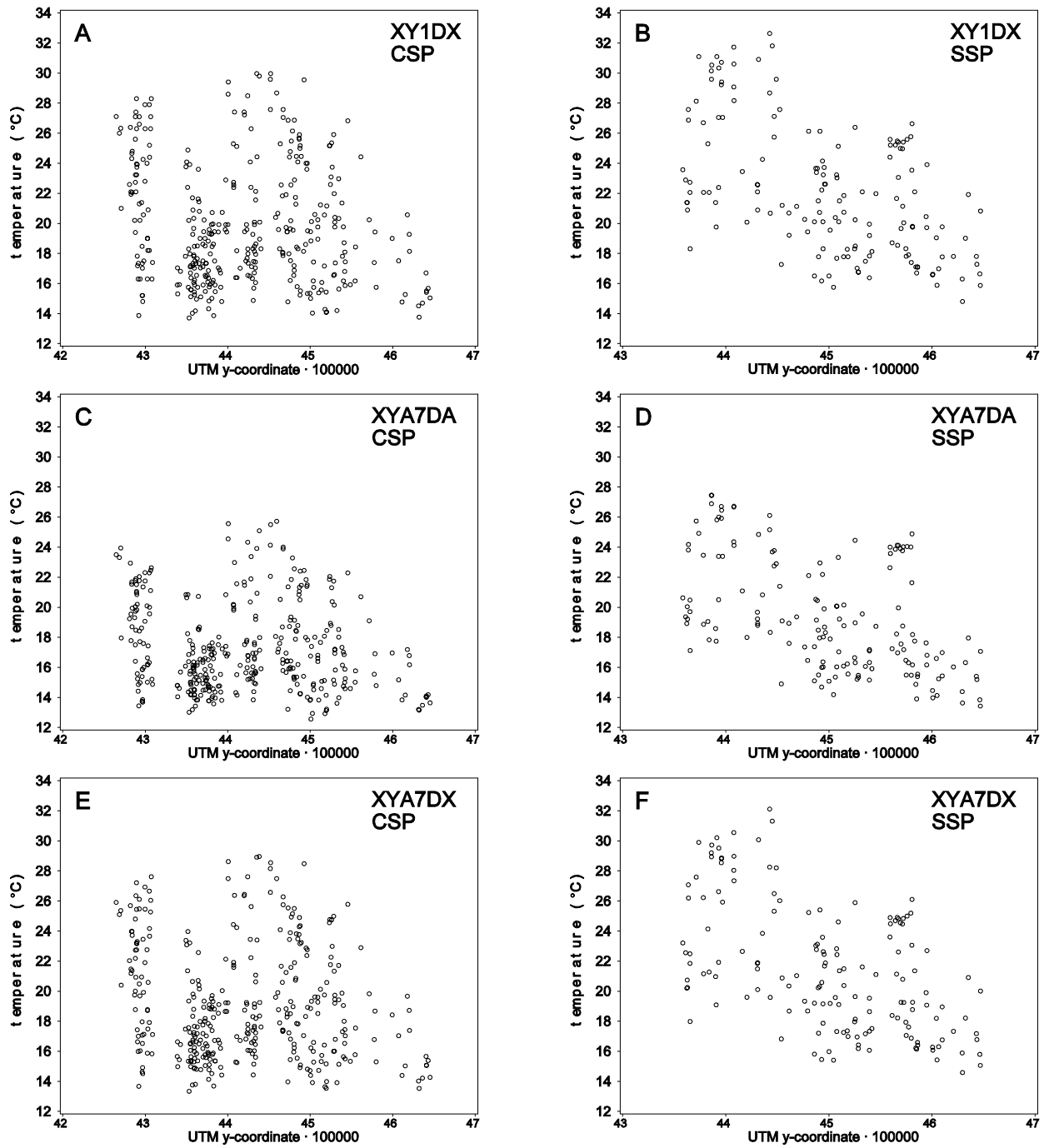


Figure 6.6. Comparison of 1998 temperature metrics versus UTM y-coordinate (northing) by ecoprovince. A) XY1DX - CSP, B) XY1DX - SSP, C) XYA7DA - CSP, D) XYA7DA - SSP, E) XYA7DX - CSP, and F) XYA7DX - SSP.

FSP Regional Stream Temperature Assessment Report

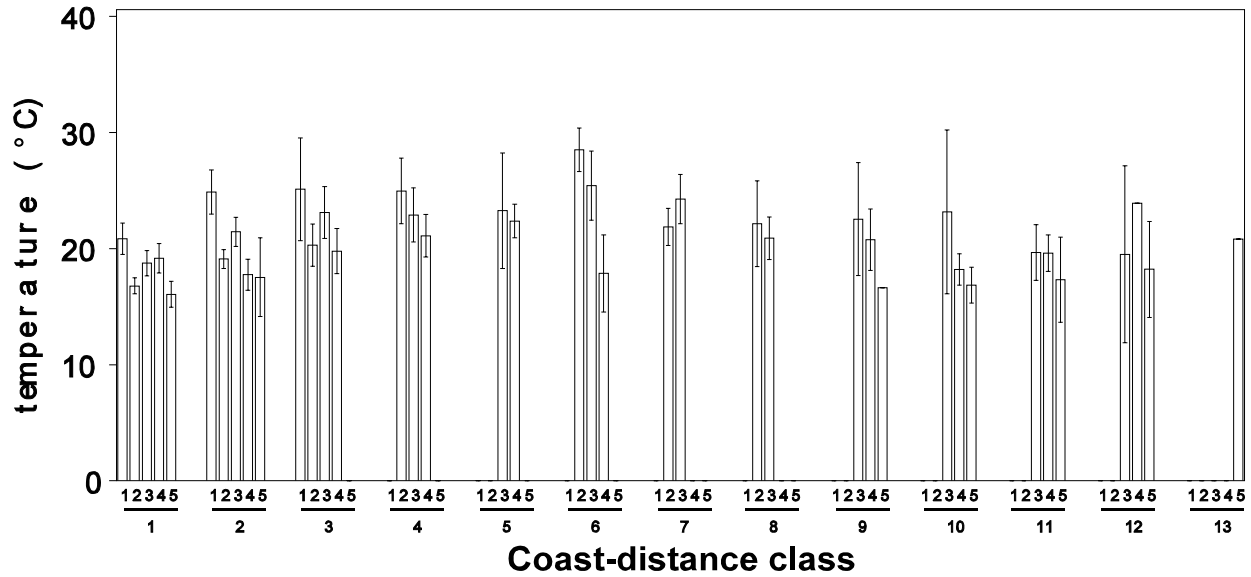


Figure 6.7. Average XY1DX values by UTM y-coordinate (latitude) and distance-from-coast classes. UTM y-coordinates divided by 100,000. Y-coordinate classes are 1 = 42-43, 2 = 43-44, 3 = 44-45, 4 = 45-46, 5 = >46. Coast-distance classes (1 - 13) as defined in Figure 6.2 caption.

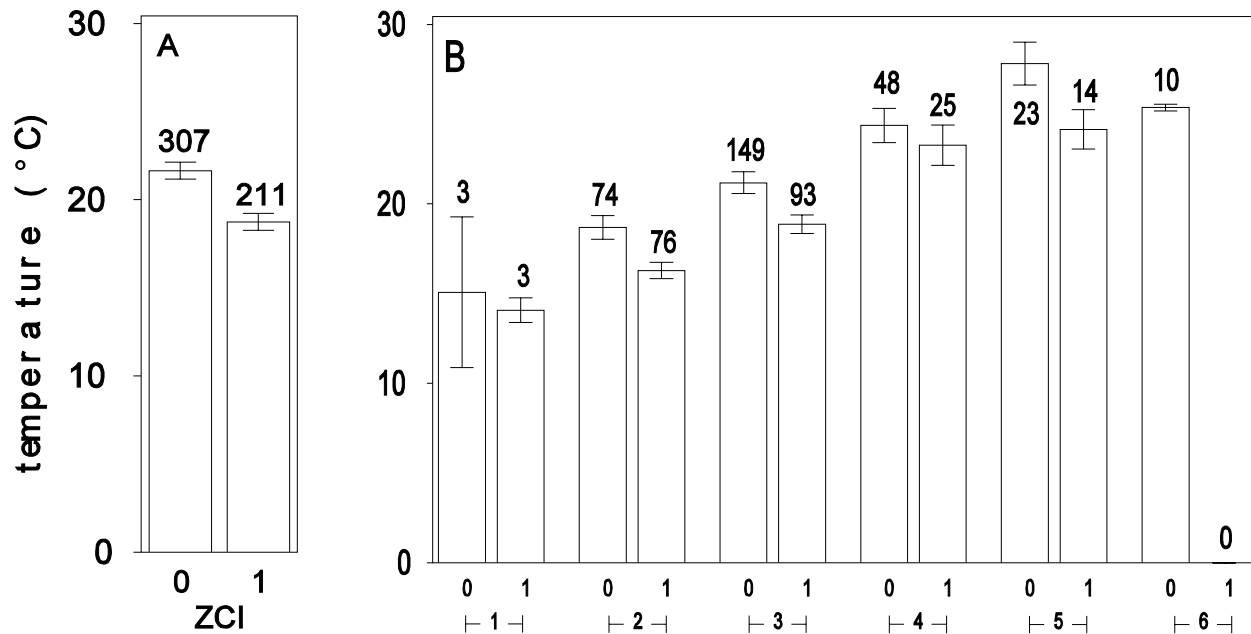


Figure 6.8. Average XY1DX for sites within and outside of the zone of coastal influence (ZCI) for (A) all sites combined and (B) by watershed area class. ZCI = 0 outside, ZCI = 1 inside. Watershed area classes 1 - 6 as defined in Figure 6.2 caption. Error bars represent ± 2 standard deviations. Number of sites shown above error bar.

based on analysis of variance results using PROC GLM (SAS, 1985). Streams of similar size were grouped together using watershed area as a surrogate for stream size. Figure 6.8-B shows that for all watershed area size classes (watershed area class 6 had no sites inside the ZCI) the average XY1DX for sites outside the ZCI was approximately 1°C to 2°C higher than the average for sites inside the ZCI. Analysis of variance showed that both ZCI and watershed area classes were significantly different ($p < 0.0001$), however the interaction term was not.

Elevation and Stream Temperature

Elevation is expected to have an influence on stream temperature in that air temperature is believed to decrease with increasing elevation. Air temperature, in turn, influences water temperature. A decrease in air temperature at higher elevations is well documented and known to be driven by adiabatic cooling processes. Adiabatic cooling deals with the cooling of parcels of air as they rise, or are forced upward, through the atmosphere. An example would be the cooling of an air parcel as it rises over a mountain range. A reasonable hypothesis is that streams at higher elevations should have cooler water temperatures.

This hypothesis may prove false, however, based on the discussion in Chapter 4, where it was demonstrated that air temperature variation is more a function of distance from the coast rather than elevation in areas under the influence of maritime air currents. In the more interior areas, air temperature was shown to have the more traditional inverse relationship with elevation. Does water temperature vary with elevation as does air temperature?

Daily Maximum and Elevation

It is instructive to examine the distribution of elevation values for stream temperature monitoring sites. Sites were grouped into elevation classes. The number of sites in each elevation class and the cumulative proportion are shown in Figure 6.9-A. The distribution of water temperature sites is dominated by sites at elevations less than 400 m (~1300 ft). Approximately 80% (~416 sites) of the

520 sites monitored in 1998 had elevations below 400 m.

Figure 6.9-B shows the relationship between elevation and the highest 1998 daily maximum stream temperature (XY1DX). There was not a clear relationship between the two variables. Generally, elevations between 200 and 600 m exhibited some of the highest XY1DX values (~32°C). At elevations greater than 600 m, XY1DX values were usually below ~26°C. All XY1DX values were greater than 13°C across all elevations. Examination of plots of XYA7DA and XYA7DX revealed similar patterns. These graphs are not shown for sake of brevity.

Daily Minimum and Elevation

There was more of a discernable trend in the lowest 1998 daily minimum stream temperature (IY1DI) and elevation (Figure 6.10). The lowest 1998 IY1DI observed between July 21 and August 19 was about 3°C, at around 1300 m (~4300 ft). The highest IY1DI was about 19°C at ~50 m elevation (Figure 6.10-A). The decreasing trend in IY1DI is shown by elevation class in Figure 6.10-B. The same data were stratified by ecoprovince in Figure 6.11. There was a much greater range in daily minimum temperatures in the SSP than in the CSP. Maritime air temperature probably moderates daily minimum water temperature in the CSP. At higher elevations of the CSP, which are more inland, much cooler evening air temperatures are attained, resulting in lower daily minimum water temperatures. Some sites at higher elevations in the SSP may also be more influenced by snowmelt and colder groundwater inflow.

Daily minima occur in the late evening and early morning hours after sundown and prior to sunrise. In the absence of incoming solar radiation, the daily minimum water temperature attained at a site is more a function of air temperature. The daily maximum temperature reached at a site will also play a role in what daily minimum can be reached. Radiative heat from the substrate can continue to contribute heat input after sundown. Sites that reach high daily maxima may not have sufficient time to come into equilibrium with late evening and early morning air temperatures before the sun rises and the heating cycle begins again.

FSP Regional Stream Temperature Assessment Report

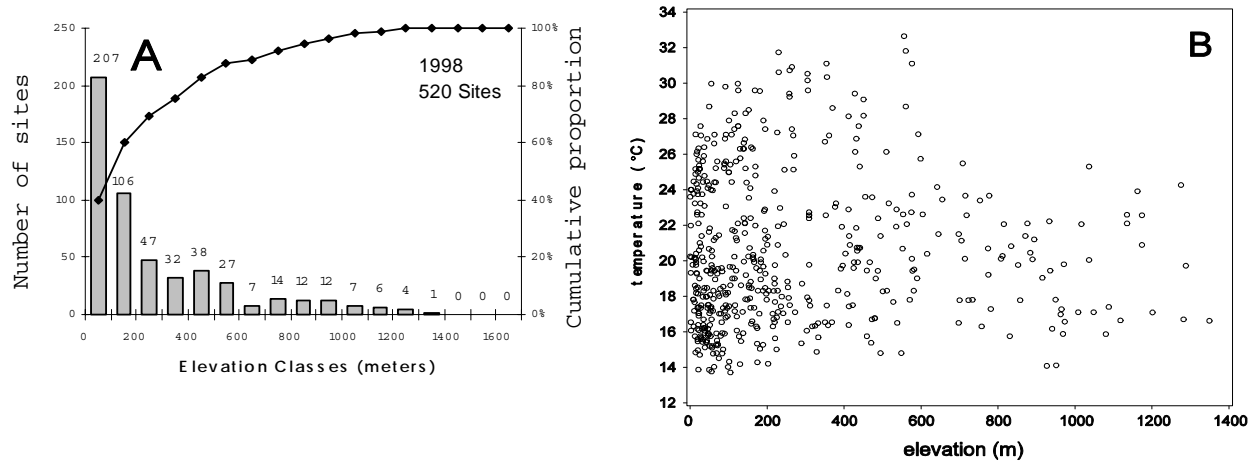


Figure 6.9. Relationship between the highest 1998 daily maximum water temperature (XY1DX) and elevation. Plots display (A) the frequency distribution of sites by elevation classes and (B) scatter plot of XY1DX vs elevation.

As pointed out in Figure 6.6, there is overlap in sites within the CSP and SSP between about 20 km and 55 km from the coast. Thus, stratification of water temperature sites by ecoprovince may not adequately characterize the sites that are influenced by coastal air temperatures. Sites were stratified by ZCI and average IY1DI values were plotted by elevation class. Figure 6.12 shows that there is a large decrease in IY1DI values with increasing elevation for the sites outside the ZCI. Not all elevation classes were represented by sites inside the ZCI. Only elevation classes 1 through 3 were found inside the ZCI. A less distinctive decrease in IY1DI was noted with increasing elevation for sites inside the ZCI.

Summary

Stream temperatures across Northern California appear to vary with geographic position. The variation in water temperature with respect to distance from the coast, UTM y-coordinate (latitude), ecoprovince, zone of coastal influence, and elevation was large for the highest 1998 values of the daily maximum (XY1DX) and the seven-day moving average

of the daily average (XYA7DA) and daily maximum (XYA7DX) stream temperatures. These three temperature metrics are indicative of day time stream temperatures, a time when solar radiation may be more influential in controlling air and water temperature. Large variation in day-time temperature metrics suggests that local site-specific factors may play a greater role in controlling stream temperatures through their influence on both local microair temperatures and direct and diffuse solar radiation.

Variation in daily minimum temperature in relation to various geographic position factors was not as great, with much clearer trends discernable. Geographic position factors are largely surrogates for macroair temperature. Since the daily minimum stream temperature, in this case the lowest 1998 daily minimum observed at each site (IY1DI), occurs at the time when solar radiation is absent, the reduced scatter in IY1DI values suggests that air temperature may be asserting more influence on this stream temperature metric than on those metrics that have more of a solar heating and daily maximum air temperature component. While air temperature is

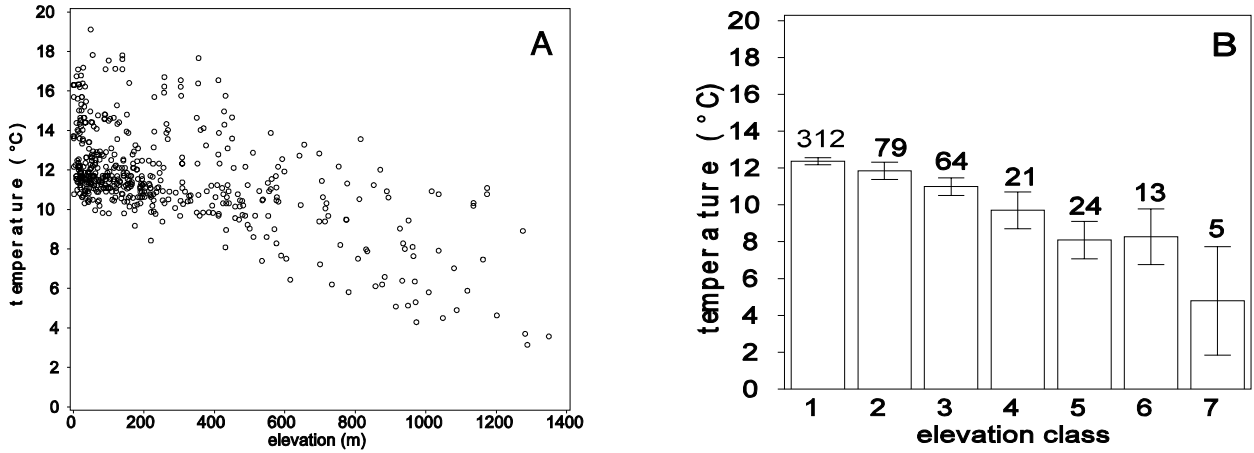


Figure 6.10. Relationship between the lowest 1998 daily minimum water temperature (IY1DI) and elevation. (A) scatterplot of IY1DI versus elevation, (B) average IY1DI by elevation class. Error bars are ± 2 standard deviations. Number of sites shown above error bar. Elevation class 1 = 0 - 200 m, 2 = 201 - 400 m, 3 = 401 - 600 m, 4 = 601 - 800 m, 5 = 801 - 1000 m, 6 = 1001 - 1200 m, 7 = >1200 m.

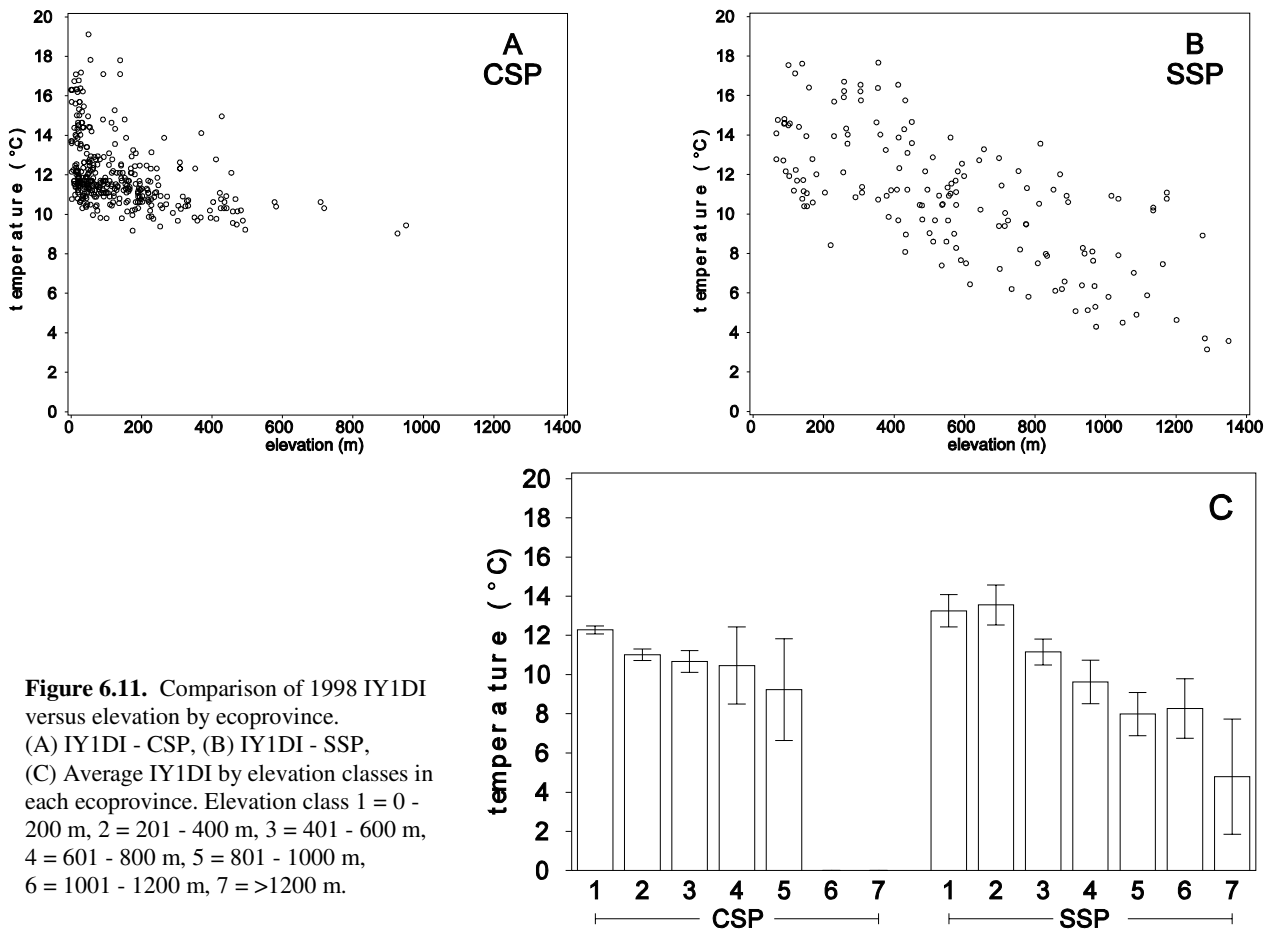


Figure 6.11. Comparison of 1998 IY1DI versus elevation by ecoprovince. (A) IY1DI - CSP, (B) IY1DI - SSP, (C) Average IY1DI by elevation classes in each ecoprovince. Elevation class 1 = 0 - 200 m, 2 = 201 - 400 m, 3 = 401 - 600 m, 4 = 601 - 800 m, 5 = 801 - 1000 m, 6 = 1001 - 1200 m, 7 = >1200 m.

FSP Regional Stream Temperature Assessment Report

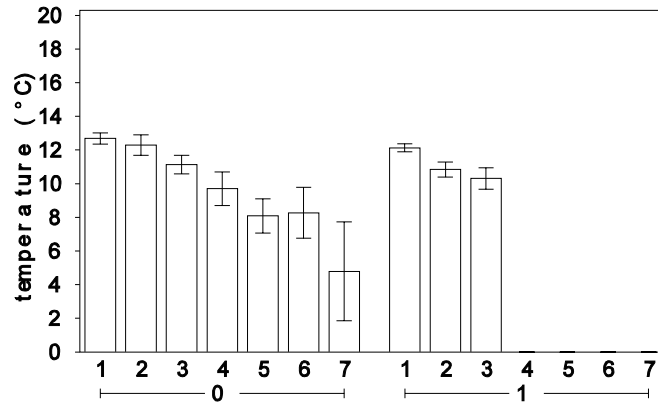


Figure 6.12. Average IY1DI values by elevation class for sites outside (group 0) and inside (group 1) the ZCI. Elevation classes as defined in Figure 6.10 caption.

known to influence water temperatures, the large variation observed for XY1DX, XYA7DA, and XYA7DX suggests that other factors are important in explaining the observed variability across the region.

These factors include canopy closure, watershed area, distance from the watershed divide, flow, gradient, and channel orientation. These factors are explored in greater depth in the following chapters.

WATERSHED POSITION AND STREAM TEMPERATURE

Introduction

Water temperature has a tendency to increase with increasing distance from the watershed divide and with increasing drainage area (Allan, 1995; Sullivan et al., 1990). Water temperature near the source is the coolest, usually close to groundwater temperature. Groundwater temperature is usually within $\pm 1\text{--}3^\circ\text{C}$ of mean annual air temperature (Collins, 1925; Allan, 1995; Sullivan et al., 1990). Seasonal temperature variation in springs and some headwater streams is slight. For example, a spring source in northern Colorado remained between 8°C and 10°C over the year, despite much greater annual variation in air temperature at this site (Ward and Dufford, 1979).

Because long rivers originate at higher elevations with generally cool climates and flow into warmer lowlands, a longitudinal temperature increase is the norm. Longitudinal temperature increase has been observed in streams throughout the world. In Central African streams that originate from ice water on mountains over 4000 m in elevation, the temperature increases from near freezing to the high twenties (Celsius) over their length (Hynes, 1970). Several European researchers have shown that summertime stream temperatures increase in a downstream direction in such a way that the rise is more or less proportional to the logarithm of the distance from the watershed divide (Schmitz and Volkert, 1959, Schmitz, 1961, and Eckel, 1953 as cited in Hynes, 1970). The logarithmic relationship has also been observed in streams in United States (Vannote and Sweeney, 1979; Sullivan et al., 1990; Allan, 1995). Even in the tropics stream temperatures increase in a

downstream direction until they reach equilibrium with the air temperature. For instance, the Marowijne River in Surinam rises 22°C and reaches 31°C at its mouth (Geijskes, 1942 as cited in Hynes, 1970).

This simple picture of stream temperature change over downstream distance can be altered by local conditions. Riparian shading can vary along the length of a stream course due to natural or human-induced causes. Air temperature regimes can change from the headwaters to the mouth, not always in an increasing manner, as shown in Chapter 4. In Northern Coastal California air temperatures may decrease by as much as 15°C by the time a parcel of water reaches the ocean after its journey from the headwaters, due to oceanic control on air temperatures near the coast.

In this chapter we report that stream temperature was highly dependent upon watershed position, both in terms of watershed area and distance from the watershed divide. Each of the eighteen hydrologic units (HUC) that comprise the range of the coho salmon showed an increase in stream temperature with an increase in watershed area and distance from the watershed divide. The rate of downstream increase in stream temperature appeared to vary with HUC location, i.e., whether the HUC was completely coastal, partly coastal and partly interior, or completely interior. The mainstems of the Eel and Mad Rivers showed decreased water temperatures at their greatest distances from the watershed divide, most likely due to the cooling influence of marine air currents. Using Brown's mixing equation we demonstrated that tributaries can have a cooling or

FSP Regional Stream Temperature Assessment Report

warming influence on mainstem or receiving water temperatures, but that this influence was transient. The recipient of the cooler or warmer tributary water appeared to re-equilibrate with climatic and local riparian downstream conditions. Streams originating entirely inside the zone of coastal influence exhibited cooler temperatures than streams of similar size that originated outside the zone of coastal influence (ZCI). Streams that originated outside the ZCI showed a decrease in water temperature upon entry into the ZCI.

Watershed Area and Bankfull Width

Watershed area is a useful variable for grouping streams of similar size together, especially when bankfull width is not available for all sites. Watershed area was derived in GIS for all 1090 sites in the regional assessment area of interest. If

watershed area could be used as a surrogate for bankfull width, a larger number of sites could be used in the analyses.

Figure 7.1-A shows the relationship between log watershed area versus log bankfull width for the Upper Salmon River of Idaho (FISRWG, 1998). A similar plot is shown in Figure 7.1-B for 177 Forest Science Project sites monitored in 1998 that had non-null values for bankfull width. While the relationship may not be adequate for prediction purposes, it is deemed adequate for grouping streams of approximately the same size based on their watershed area.

Sullivan et al. (1990) used watershed area as a surrogate for stream flow. Watershed area calculated for FSP sites will be used in this chapter to derive relative stream-flow ratios for use in Brown's mixing equation (Brown, 1972).

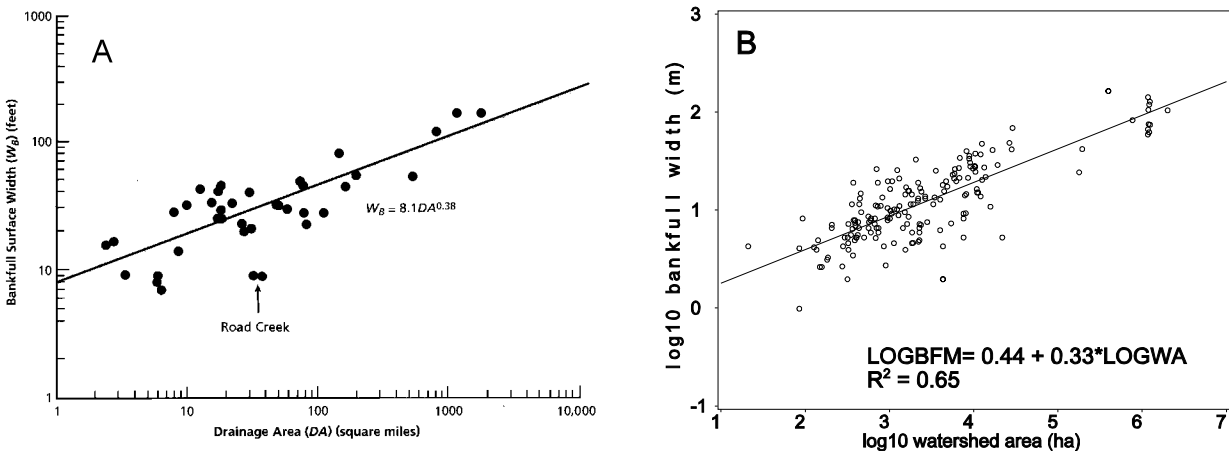


Figure 7.1. Relationship between watershed area and bankfull width. (A) Bankfull surface width versus drainage area - Upper Salmon River, Idaho. Taken from FISRWG, 1998. (B) Bankfull width (LOGBFM) versus watershed area (LOGWA) for 1998 Forest Science Project stream temperature monitoring sites (177 sites).

Distribution of Watershed Area and Distance from Watershed Divide Values

A characterization of the watershed position of stream temperature monitoring sites used in the regional stream temperature assessment was performed by examination of the frequency distribution of values for watershed area and distance from the watershed divide. Such an examination of frequency distributions showed whether most sites were closer to the headwaters or if more were located near the mouths. Since many cooperators did not provide the Forest Science Project with bankfull width values for each site, watershed area and distance from the watershed divide were the two most important variables that allowed us to aggregate sites by relative stream size. Both these variables were derived in GIS, based on point locations. Positional accuracy was thus critical for estimating these two variables (see Chapter 2).

Watershed Area Values

Watershed areas were calculated for all sites for years 1990 through 1998. The year with the most complete data set was 1998, so analyses will focus on data collected in that year. Figure 7.2-A shows the frequency distribution of watershed areas for stream temperature monitoring sites in 1998. The mean watershed area for 1998 sites was 58,299 ha with a median of 2404 ha and mode of 85 ha. The minimum was 21 ha and the maximum was 2,007,819 ha

Distance from Watershed Divide Values

Figure 7.2-B shows the frequency distribution of distance from watershed divide values for sites monitored in 1998. The mean divide distance for 1998 sites was 32 km, with a minimum of 1.3 km and a maximum of 331 km. The median was 9.9 km and the mode was 4.8 km.

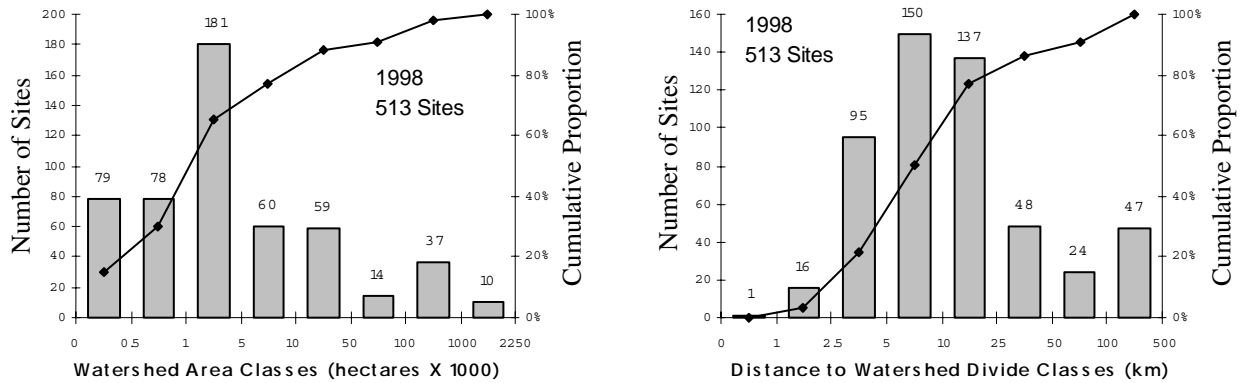


Figure 7.2. Frequency distribution of stream temperature monitoring sites by (A) watershed area classes and (B) distance from watershed divide classes. Plotted line is the cumulative proportion. Sites are those with complete data from July 21 to August 19.

Relationship Between Watershed Area and Distance From the Watershed Divide

One would expect a significant relationship between watershed area and distance from the watershed divide. Figure 7.3 shows that the two variables are highly correlated, with an R^2 value of 0.97 for the log transformed data. The relationship is based on 1087 unique site locations monitored in 1990 through 1998. If a point is located further down in the drainage it is expected that the area draining into the point will be greater. Distance from the watershed divide and watershed area can be easily calculated in a GIS, given a high-quality digital elevation model. Divide distance may be easier to acquire from topographic map. The equation in Figure 7.3 can be used to estimate the watershed area if distance from the watershed divide is known.

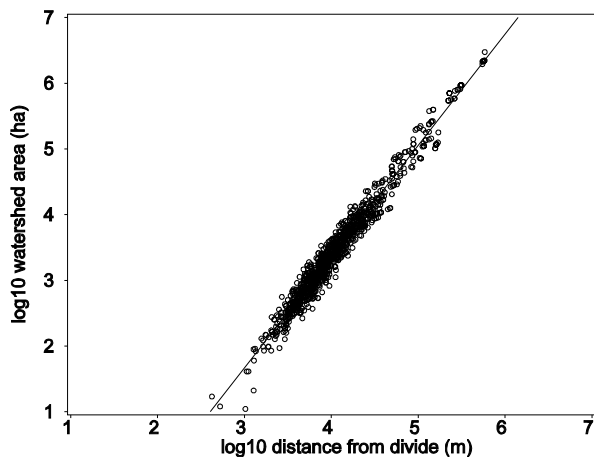


Figure 7.3. Relationship between watershed area and distance from the watershed divide. Linear regression line fit to the data has the equation: $\log_{10}(\text{watershed area}) = 1.693 * \log_{10}(\text{divide distance}) - 3.4135$, $R^2 = 0.97$, based on all sites and all years, 1087 sites.

Watershed Area and Stream Temperature Across the Region

The relationship between watershed area and five stream temperature metrics was investigated. The

five metrics were: the highest daily maximum (XY1DX), the highest seven-day moving average of the daily average (XYA7DA), the highest seven-day moving average of the daily maximum (XYA7DX), the lowest daily minimum (IY1DI), and the average diurnal fluctuation.

Daily Maximum and Watershed Area

Figure 7.4-A shows the relationship between \log_{10} watershed area and the highest daily maximum water temperature (XY1DX) for sites monitored in 1998. For the purposes of graphical presentation, watershed area was grouped into six classes: (1) 0 - 100 ha, (2) 101 - 1000 ha, (3) 1001 - 10,000 ha, (4) 10,001 - 100,000 ha, (5) 100,001 - 1,000,000 ha, and (6) greater than 1,000,001 ha (Figure 7.4-B). Each bar represents the average of the XY1DX for each watershed area class. The error bars represent ± 2 standard deviations.

There was an increase in XY1DX temperature with increasing watershed area. The average XY1DX ranged from 14.6°C for watershed areas between 0 and 100 ha to 26.4°C for watershed areas between 100,001 and 1,000,000 ha. It is interesting to note that the XY1DX in the greater-than-one-million-hectare class showed about a one degree Celsius decrease compared to the previous class. The water temperature decrease in the largest watershed area class is possibly due these sites being predominantly located on mainstem rivers near the coast. The decrease in the XY1DX temperature is most likely be due to the cooling effects of coastal air temperatures. Sites were poststratified by ecoprovince and are presented in Figure 7.5.

Figures 7.5-A and 7.5-B show that both ecoprovinces exhibited a slight decrease in the highest daily maximum temperature at the highest watershed area values. However, the CSP bar graph (Figure 7.5-C) does not reveal the decrease due to the grouping by watershed area classes. The sites showing the decrease in the highest daily maximum temperature for the CSP were just shy of one million hectares (~980,000 ha), and were grouped in watershed area class 5. Class 5 contained sites with watershed areas as low as 100,001 ha, thus the class average was not responsive to the minority of sites close to one

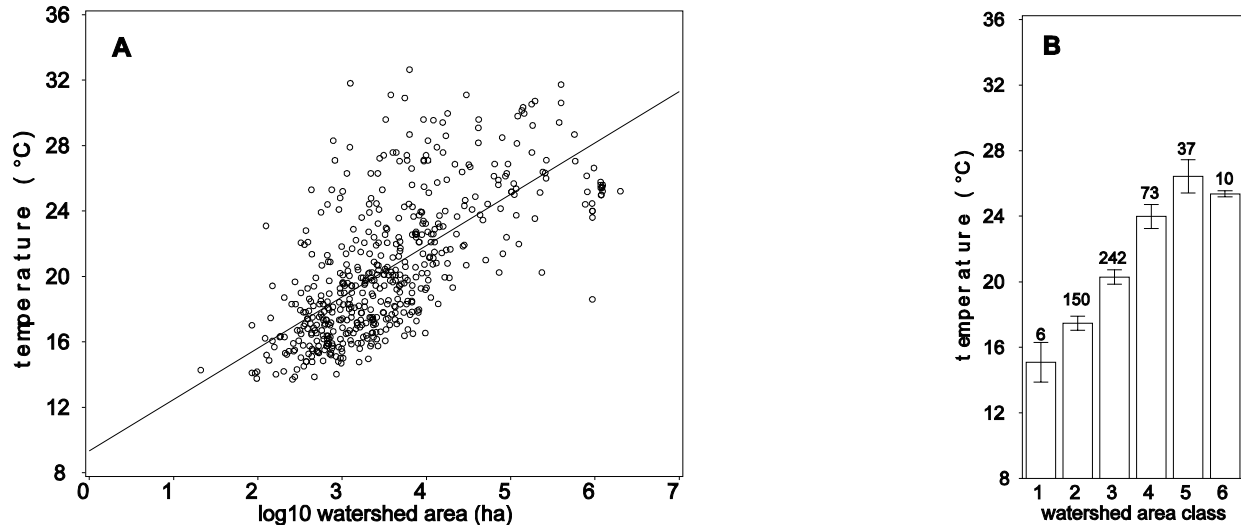
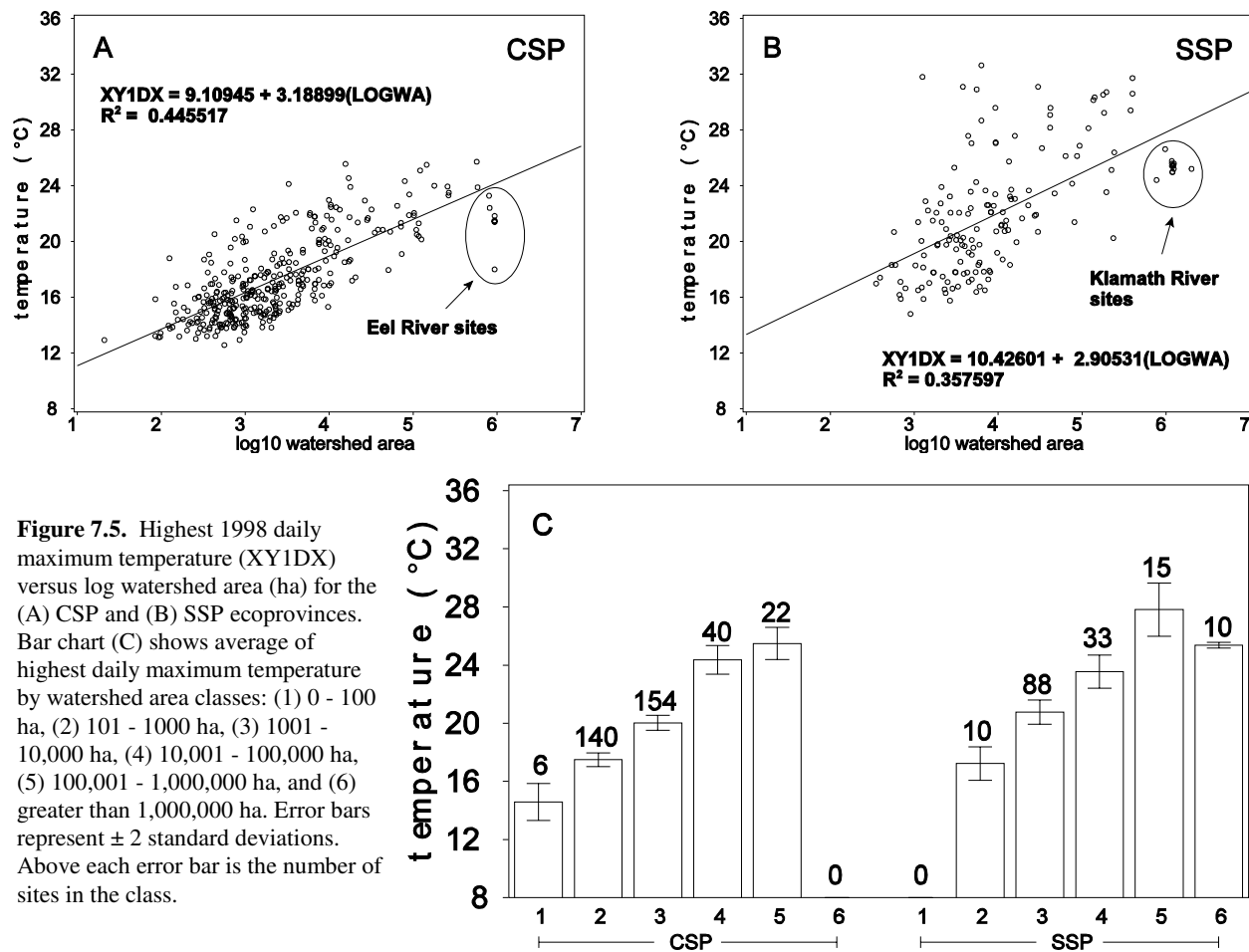


Figure 7.4. Relationship between the highest 1998 daily maximum stream temperature (XY1DX) and log watershed area (logwa). Scatter plot (A) with linear regression equation: $XY1DX = 9.344683 + 3.13764 \cdot \logwa$, $R^2 = 0.452726$. Bar chart (B) with watershed area classes: (1) 0 - 100 ha, (2) 101 - 1000 ha, (3) 1001 - 10,000 ha, (4) 10,001 - 100,000 ha, (5) 100,001 - 1,000,000 ha, and (6) greater than 1,000,000 ha. Error bars represent ± 2 standard deviations. Above each error bar is the number of sites in the class.

million hectares. Sites on the lower Eel River in the CSP represent the points in Figure 7.5-A exhibiting a decrease in temperature. Sites in the SSP that showed a decrease in temperature at over one million hectares were on the Klamath River (Figure 7.5-B). The sites on the Klamath River are approximately 80 km from the coast, placing them in the SSP. Air temperatures are nearly 15°C warmer in this area compared to coastal areas. What could account for the decrease in water temperature at large watershed areas in a warm interior portion of the SSP? Significant regulation of flow on the Klamath River began in 1962 when Iron Gate Dam went into operation (Blodgett, 1970). Water temperatures in the Klamath River may be influenced by dam releases from the impounded reservoir.

The distribution of XY1DX values in the CSP (Figure 7.5-A) are more closely clustered than SSP values (Figure 7.5-B). Also, the linear regression line is shifted down and has a lower y-intercept, indicating that, in general, the CSP XY1DX values are lower than the SSP values at similar watershed areas. The difference in water temperatures between the two ecoprovinces is supported by previous discussions of the differences in air temperature regimes in the two ecoprovinces (see Chapter 4). The cooler air temperatures along the coast seem to have a moderating influence on the daily maximum temperatures.

FSP Regional Stream Temperature Assessment Report



Seven-Day Moving Averages and Watershed Area

The relationship between the highest 1998 seven-day moving average of the daily average (XYA7DA) and the highest seven-day moving average of the daily maximum (XYA7DX) versus \log_{10} watershed area was investigated. The relationships were found to be similar to those observed for the XY1DX plots. For sake of brevity, graphs are shown in Appendix D and only linear regression equations are presented in Table 7.1.

The R^2 values for the XYA7DA-watershed area relationships were slightly higher than those observed for XYA7DX. Sullivan et al. (1990) believed that mean daily water temperatures were more responsive to air temperatures than the daily maxima, the latter

they postulated were more a function of solar radiation. This is supported by results of micro- and macroair temperature analyses presented in Chapter 5. Sullivan et al. (1990) found that the average water temperatures approached an equilibrium temperature that was close to the average air temperature for the basin. The slightly better correlation between XYA7DA (the average of the daily averages) and \log_{10} watershed area, rather the XYA7DX (the average of the daily maxima), would seem to reflect the greater association between average water temperature and air temperatures. The decrease in water temperature metrics (XY1DX, XYA7DA, and XYA7DX) at the highest watershed areas, i.e., nearest the coast, seems to further support the postulate that water temperatures tend to come into equilibrium with cooler coastal air temperatures at increasing watershed areas.

Table 7.1. Linear Regression Equations for Relationship between 1998 XYA7DA¹ and XYA7DX² versus Log₁₀ Watershed Area, Combined and by Ecoprovince.

Variable	Ecoprovince	No. of Sites	Slope	Intercept	R ²
XYA7DA	combined	518	2.81392	7.87853	0.58539
XYA7DX	combined	518	3.06196	8.92433	0.46575
XYA7DA	CSP	362	2.62661	8.44315	0.559684
XYA7DA	SSP	156	3.07022	6.99033	0.537656
XYA7DX	CSP	362	3.05958	8.83760	0.45668
XYA7DX	SSP	156	2.87608	9.89085	0.366816

¹XYA7DA = seven-day moving average of the daily average.

²XYA7DX = seven-day moving average of the daily maximum.

Daily Minimum and Watershed Area

The relationship between watershed position, as expressed in terms of watershed area, and the lowest 1998 daily minimum stream temperature (IY1DI) showed an increasing trend with increasing watershed area (Figure 7.6). The average IY1DI in the lowest watershed area class was 10.4°C, with a range from 9.0°C to 13.0°C.

There was a large scatter in IY1DI values at watershed areas less than approximately 31,600 ha (log₁₀ watershed area = 4.5) (Figure 7.6-A). The average IY1DI for watershed classes 2 and 3 was about 11°C, with ranges of 4.9°C to 14.4°C for class 2 and 3.1°C to 15.2°C for class 3, respectively (Figure 7.6-B).

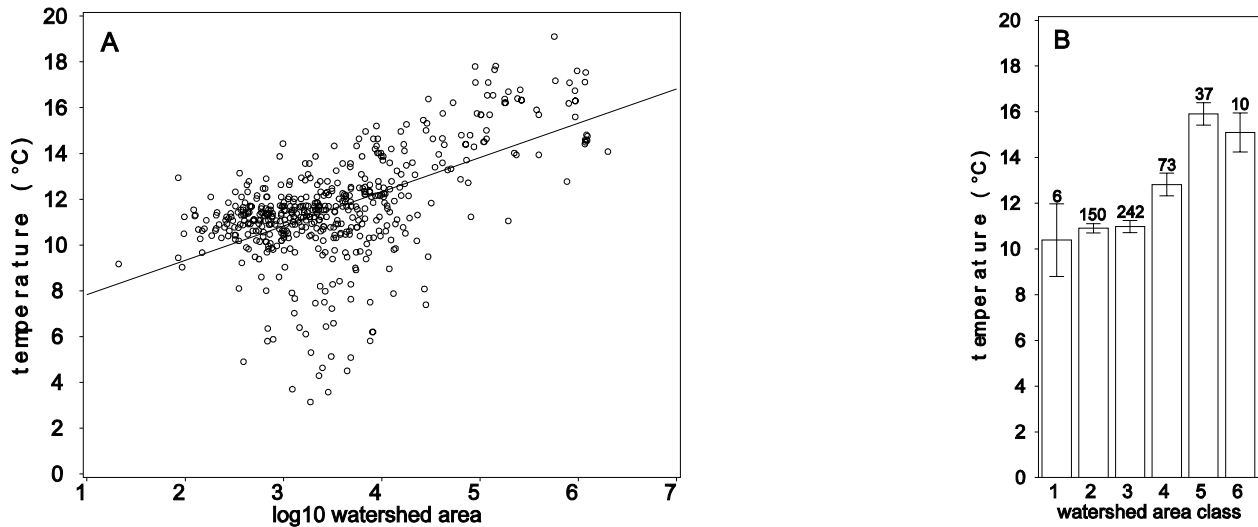


Figure 7.6. Relationship between the lowest 1998 daily minimum stream temperature (IY1DI) and log watershed area (ha) (LOGWA). Scatter plot (A) with linear regression equation: $IY1DI = 6.324127 + 1.499672 * LOGWA$, $R^2 = 0.331635$. Bar chart (B) with watershed area classes: (1) 0 - 100 ha, (2) 101 - 1000 ha, (3) 1001 - 10,000 ha, (4) 10,001 - 100,000 ha, (5) 100,001 - 1,000,000 ha, and (6) greater than 1,000,000 ha. Error bars represent ± 2 standard deviations. Number of sites in each class is shown above error bar.

FSP Regional Stream Temperature Assessment Report

Sites were poststratified by ecoprovince and the IY1DI versus log watershed area relationship was examined. Figures 7.7-A and 7.7-B reveal the source of scatter noted in Figure 7.6-A. The CSP showed a much tighter distribution of IY1DI values with log₁₀ watershed area (Figure 7.7-A) whereas the SSP

displayed much greater scatter (Figure 7.7-B). The moderating influence of coastal air currents on stream temperatures are believed to play a role in the reduced scatter of the lowest daily minimum temperatures at various positions in watersheds of Northern Coastal California.

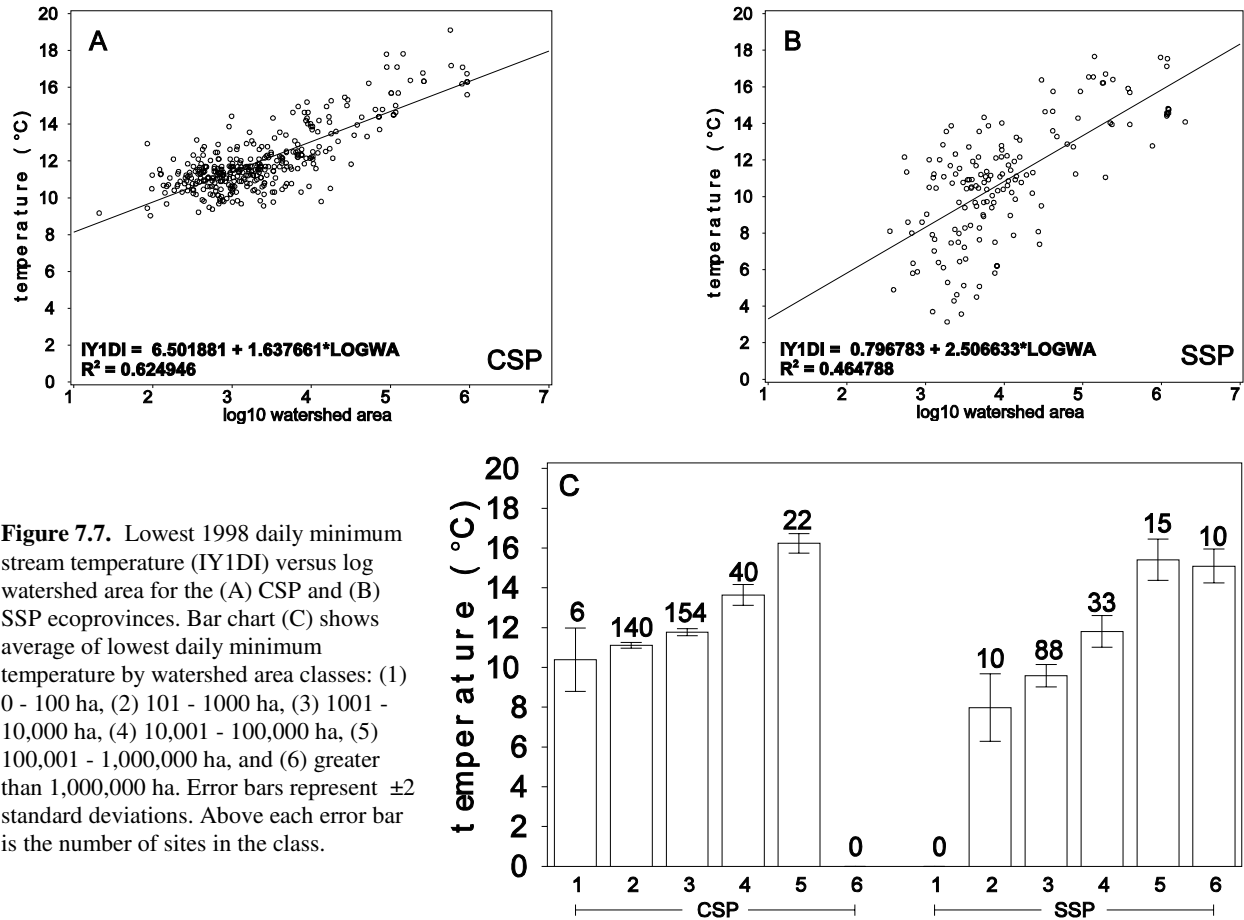


Figure 7.7. Lowest 1998 daily minimum stream temperature (IY1DI) versus log watershed area for the (A) CSP and (B) SSP ecoprovinces. Bar chart (C) shows average of lowest daily minimum temperature by watershed area classes: (1) 0 - 100 ha, (2) 101 - 1000 ha, (3) 1001 - 10,000 ha, (4) 10,001 - 100,000 ha, (5) 100,001 - 1,000,000 ha, and (6) greater than 1,000,000 ha. Error bars represent ±2 standard deviations. Above each error bar is the number of sites in the class.

Diurnal Fluctuation and Watershed Area

Diurnal fluctuation was calculated for each site and each day by subtracting the daily minimum stream temperature from the daily maximum. The average diurnal fluctuation was calculated using the PROC MEANS procedure in SAS (SAS, 1985). The restricted temporal window (July 21 to August 19) was imposed upon the 1998 daily stream temperature to calculate the average diurnal fluctuation for each day. Sites with complete records within this window were used in the calculations.

Figure 7.8-A shows the variation in diurnal fluctuation with log₁₀ watershed area. Great variability was observed in the diurnal fluctuation, with the lowest values near 0°C and the highest near 13°C. The general trend showed an increase in the diurnal fluctuation in the middle range of the watershed areas, followed by a decrease at the

highest watershed areas. The relationship between diurnal fluctuation and log₁₀ watershed area is not linear. The bell-shaped distribution in diurnal fluctuation becomes more apparent in the bar chart presented in Figure 7.8-B. Small tributaries near the headwaters have less variable stream temperatures because of groundwater influence and shading. Large rivers exhibit less diel temperature fluctuation because of their greater volume and thermal inertia (Allan, 1995). Vannote and Sweeney (1980) showed the relationship between maximum daily temperature range and stream order for streams in temperate climates (Figure 7.9). Our findings seem to coincide with those of Vannote and Sweeney (1980) rather than those of Sullivan et al. (1990) who hypothesized a continual decrease in diurnal temperature fluctuation with increasing distance from the watershed divide based on a smaller sample size.

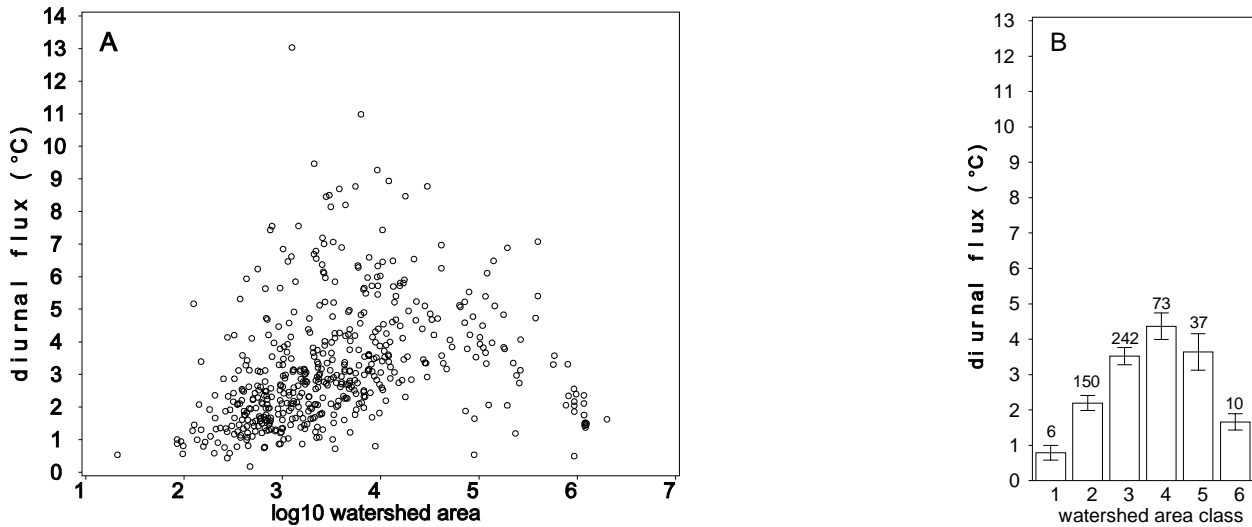


Figure 7.8. Relationship between the 1998 average diurnal stream temperature fluctuation (AFLUX) and log watershed area (LOGWA). Scatter plot (A) and bar chart (B) with watershed area classes: (1) 0 - 100 ha, (2) 101 - 1000 ha, (3) 1001 - 10,000 ha, (4) 10,001 - 100,000 ha, (5) 100,001 - 1,000,000 ha, and (6) greater than 1,000,000 ha. Error bars represent ± 2 standard deviations. Above each error bar is the number of sites in the class.

FSP Regional Stream Temperature Assessment Report

Sites were grouped by ecoprovince to discern differences in diurnal fluctuations between the two subregions. Figures 7.10-A and 7.10-B show the variation in diurnal temperature fluctuation with \log_{10} watershed area for each ecoprovince, CSP and SSP,

respectively. The linear regression line is shown on the graph to demonstrate that the relationship is clearly not linear. The shape in Figure 7.10-C is similar to Figure 7.9.

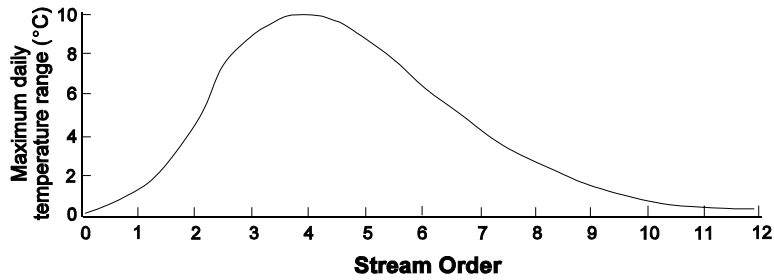


Figure 7.9. Maximum daily temperature range in relation to stream order in temperate streams. (From Vannote and Sweeney, 1980.)

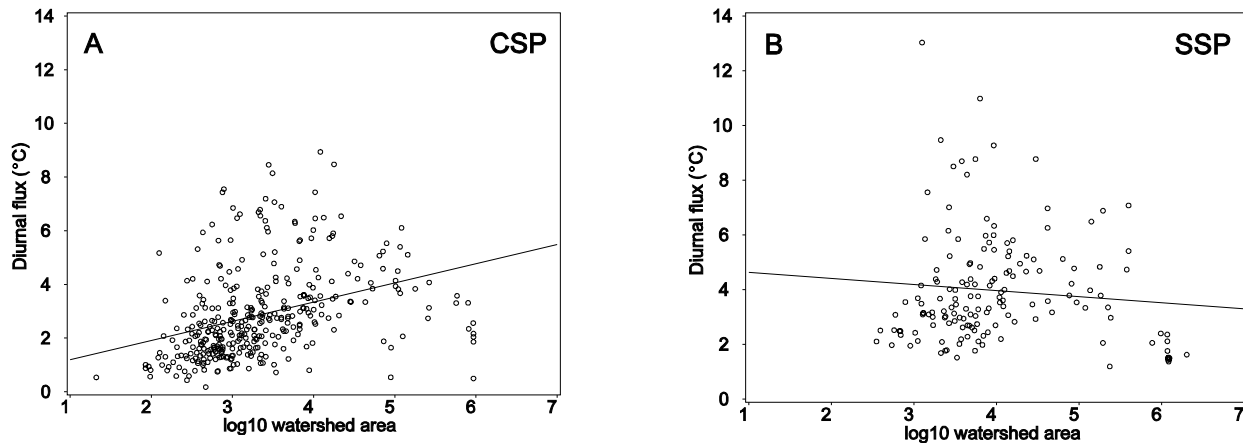


Figure 7.10. Average 1998 diurnal temperature fluctuation (AFLUX) versus log watershed area (LOGWA) for (A) CSP and (B) SSP ecoprovinces. Bar chart (C) shows mean of the average diurnal flux by watershed area classes: (1) 0 - 100 ha, (2) 101 - 1000 ha, (3) 1001 - 10,000 ha, (4) 10,001 - 100,000 ha, (5) 100,001 - 1,000,000 ha, and (6) greater than 1,000,000 ha. Error bars represent ± 2 standard deviations. Above each error bar is the number of sites in the class.

